DOKUZ EYLÜL UNIVERSITY
GRADUATE SCHOOL OF NATURAL AND APPLIED SCIENCES

EXPERIMENTAL AND FINITE ELEMENT ANALYSIS OF PARAMETERS FOR THE IMPROVEMENT OF MECHANICAL PROPERTIES OF ALUMINUM HONEYCOMB SANDWICH COMPOSITES

Seyed Soroush SOLEIMANI

Ekim, 2024

İZMİR

ALÜMİNYUM BAL PETEĞİNDEN İMAL EDİLMİŞ SANDVİÇ KOMPOZİTLERİN MEKANİK ÖZELLİKLERİNİN İYİLEŞTİRİLMESİNE YÖNELİK PARAMETRELERİN DENEYSEL VE SONLU ELEMANLAR YÖNTEMİ İLE İNCELENMESİ

Dokuz Eylül Üniversitesi Fen Bilimleri Enstitüsü

Doktora Tezi

Makine Mühendisliği Anabilim Dalı, Mekanik Programı

Seyed Soroush SOLEIMANI

Ekim, 2024

İZMİR

Ph.D. THESIS EXAMINATION RESULT FORM

We have read the thesis entitled **"EXPERIMENTAL AND FINITE ELEMENT ANALYSIS OF PARAMETERS FOR THE IMPROVEMENT OF MECHANICAL PROPERTIES OF ALUMINUM HONEYCOMB SANDWICH COMPOSITES"** completed by **SEYED SOROUSH SOLEIMANI** under supervision of **ASSOC. PROF. DR. OKAN ÖZDEMİR** and we certify that in our opinion it is fully adequate, in scope and in quality, as a thesis for the degree of Doctor of Philosophy.

Assoc. Prof. Dr. Okan ÖZDEMİR

Supervisor

Prof. Dr. Ramazan KARAKUZU	Assoc. Prof. Dr. Metin YURDDAŞKAL
Thesis Committee Member	Thesis Committee Member
Prof. Dr. Buket OKUTAN BABA	Prof. Dr. Yeliz PEKBEY
Examining Committee Member	Examining Committee Member

Prof. Dr. Okan FISTIKOĞLU

Director

Graduate School of Natural and Applied Sciences

ACKNOWLEDGMENT

I would like to express my sincere gratitude to my supervisor, Assoc. Prof. Dr. Okan ÖZDEMİR, for his exceptional guidance, continuous encouragement, and unwavering support throughout the course of my Ph.D. studies. His profound knowledge and insights have greatly influenced the direction and quality of this research.

I am also deeply indebted to Prof. Dr. Ramazan KARAKUZU and Assoc. Prof. Dr. Metin YURDDAŞKAL, members of my Ph.D. examination committee, for their invaluable feedback, constructive criticism, and academic support, which have significantly contributed to the refinement of this thesis.

I extend my heartfelt thanks to my family for their steadfast support, patience, and understanding throughout this journey. To my parents, whose sacrifices have laid the foundation for my success, and to my siblings, who have always cheered me on, I am deeply grateful. In particular, I wish to express my deepest appreciation to my dear wife, Shideh. Her unwavering belief in my abilities, along with her boundless patience and encouragement, has been a constant source of strength. Her sacrifices and support during the many challenges of this Ph.D. journey cannot be overstated. This thesis would not have been possible without her love, understanding, and continuous support, for which I am profoundly grateful.

Seyed Soroush SOLEIMANI

EXPERIMENTAL AND FINITE ELEMENT ANALYSIS OF PARAMETERS FOR THE IMPROVEMENT OF MECHANICAL PROPERTIES OF ALUMINUM HONEYCOMB SANDWICH COMPOSITES

ABSTRACT

This dissertation presents an experimental and numerical investigation into the mechanical properties, failure mechanisms, and energy absorption of advanced composite materials, including CFRP composites, CFRP facesheets with aluminum honeycomb core (AlHC) sandwich structures, and Kevlar/epoxy composites with varying nanoclay concentrations. Quasi-static punch shear (QS-PS) tests were conducted primarily at a displacement rate of 1.25 mm/min, with additional testing at 12.5 mm/min and 25 mm/min to assess rate sensitivity. CFRP/AlHC composites exhibited superior performance, achieving a peak force of 2654.8 N, which was closely predicted by FEM simulations at 2528.4 N. Kevlar/epoxy composites with 1 wt.% nanoclay exhibited the highest peak force of 2563.5 N at 1.25 mm/min, with a moderate decrease to 2448.1 N and 2290.1 N at higher rates, demonstrating strong rate-dependent behavior. SEM analysis revealed that nanoclay reinforcement significantly improved fiber-matrix bonding, reducing fiber pull-out and enhancing energy absorption. The 0.5 wt.% nanoclay variant provided the most favorable balance between strength and toughness, avoiding the brittleness observed at 1 wt.% reinforcement. FEM simulations successfully predicted overall mechanical behavior but slightly underestimated post-peak damage, particularly in composites with nanoclay reinforcement. The findings emphasize the benefits of incorporating both nanoclay and AlHC cores to enhance mechanical properties and energy absorption in composites. This study underlines the importance of material optimization for high-performance applications, making these advanced composites well-suited for demanding environments in aerospace and automotive engineering.

Keywords: sandwich composites, finite element method, mechanical properties, nanoclay, SEM

ALÜMİNYUM BAL PETEĞİNDEN İMAL EDİLMİŞ SANDVİÇ KOMPOZİTLERİN MEKANİK ÖZELLİKLERİNİN İYİLEŞTİRİLMESİNE YÖNELİK PARAMETRELERİN DENEYSEL VE SONLU ELEMANLAR YÖNTEMİ İLE İNCELENMESİ

ÖZ

Bu tez, CFRP kompozitler, alüminyum bal peteği çekirdekli (AlHC) CFRP yüzey plakaları içeren sandviç yapılar ve farklı nanokil konsantrasyonları ile güçlendirilmiş Kevlar/epoksi kompozitlerin mekanik özellikleri, hasar mekanizmaları ve enerji emilim davranışlarının deneysel ve sayısal bir incelemesini sunmaktadır. Temel olarak 1.25 mm/dk yer değiştirme hızında yarı-statik delme kesme (QS-PS) testleri yapılmış, 12.5 mm/dk ve 25 mm/dk'da ek testler ile hız duyarlılığı değerlendirilmiştir. AlHC içeren CFRP kompozitler, 2654.8 N'lik maksimum kuvvet elde ederek üstün performans göstermiş ve FEM simülasyonları ile 2528.4 N değerine yakın bir şekilde tahmin edilmiştir. 1 wt.% nanokil içeren Kevlar/epoksi kompozitler, 1.25 mm/dk'da 2563.5 N ile en yüksek tepe kuvvetine ulaşmış, daha yüksek hızlarda bu değer 2448.1 N ve 2290.1 N'ye düşerek hız bağımlı bir davranış sergilemiştir. SEM analizi, nanokil takviyesinin fiber-matris bağını önemli ölçüde iyileştirdiğini, fiber çekilmesini azalttığını ve enerji emilimini artırdığını göstermiştir. %0.5 nanokil içeren varyant, mukavemet ve tokluk arasında en uygun dengeyi sağlamış ve %1 nanokil takviyesinde gözlemlenen kırılganlığı önlemiştir. FEM simülasyonları genel mekanik davranışı başarıyla tahmin etmiş, ancak özellikle nanokil takviyeli kompozitlerde zirve sonrası hasarı hafifçe düşük tahmin etmiştir. Bulgular, hem nanokil hem de AlHC çekirdeklerin kompozitlerin mekanik özelliklerini ve enerji emilimini artırmadaki faydalarını vurgulamaktadır. Bu çalışma, yüksek performanslı uygulamalar için malzeme optimizasyonunun önemini vurgulamakta olup, bu ileri kompozitleri havacılık ve otomotiv mühendisliğinde zorlu ortamlara uygun hale getirmektedir.

Anahtar kelimeler: sandviç kompozitler, sonlu elemanlar yöntemi, mekanik özellikler, nanokil, SEM

CONTENTS

Page

LIST OF FIGURES

Page

LIST OF TABLES

Page

CHAPTER ONE
INTRODUCTION

1.1 Overview of Fiber-Reinforced Polymer Composites

Fiber-Reinforced Polymer (FRP) composites, encompassing both Carbon Fiber Reinforced Polymer (CFRP) and Kevlar/epoxy variants, have captured widespread attention across multiple industries due to their superior mechanical properties. These composites are celebrated for their excellent strength-to-weight ratio, resistance to corrosion, and versatility in design, making them ideal for applications that require durable yet lightweight solutions. The utilization of FRP composites has been instrumental in enhancing performance and sustainability in multiple sectors, including construction, aerospace, automotive, renewable energy, and sports and recreation. The growing interest in these composites is driven by their ability to meet the demanding requirements of modern engineering challenges, offering both performance benefits and environmental advantages.

1.2 Applications of FRP Composites

1.2.1 Construction Industry

In the construction industry, FRP composites are revolutionizing infrastructure development. Traditional construction materials like steel and concrete, while robust, are prone to corrosion and environmental degradation, leading to high maintenance costs and reduced lifespans of structures. In contrast, FRP composites offer superior durability and resistance to harsh environmental conditions, making them particularly beneficial for structures exposed to such environments, such as bridges and marine structures. Studies have demonstrated that using FRP composites in bridge construction can significantly extend the lifespan of structures while reducing maintenance costs (Smith et al., 2020; Johnson et al., 2021). The lightweight nature of these composites also facilitates easier transportation and installation, further driving their adoption in the construction sector.

1.2.2 Aerospace Industry

The aerospace sector extensively utilizes FRP composites to attain components that are both lightweight and robust, which are crucial for enhancing fuel efficiency and minimizing emissions. The significant weight savings provided by FRP composites translate to enhanced performance and reduced operational costs for aircraft. Research by Patel et al. (2019) highlights the critical role of FRP composites in modern aircraft design, emphasizing their contribution to the performance and safety of aviation technologies. Employing these materials facilitates the creation of components capable of enduring the stringent requirements of aerospace applications, while also advancing the industry's sustainability objectives. As the aerospace sector continues to innovate, the role of FRP composites is expected to expand, supporting the development of greener and more efficient aircraft.

1.2.3 Automotive Industry

Automotive manufacturers are progressively integrating FRP composites into vehicle designs to decrease weight and enhance fuel efficiency while maintaining safety standards. This shift is facilitated by technological advancements in manufacturing processes that permit the mass production of intricate composite components. According to a study by Williams and Chen (2022), the adoption of FRP composites in the automotive sector is projected to grow, driven by stringent regulatory standards and the push towards electric vehicles. The lightweight properties of FRP composites contribute to lower vehicle emissions and improved energy efficiency, aligning with global efforts to reduce the environmental impact of transportation. Furthermore, the inherent strength and impact resistance of these materials enhance vehicle safety, providing manufacturers with versatile options for both structural and aesthetic components.

1.2.4 Renewable Energy Sector

In the realm of renewable energy, FRP composites are essential in the production of wind turbine blades and solar panel supports. Their lightweight and robust nature ensures efficient energy generation and longevity of installations. Research by Lee et al. (2023) underscores the critical role of FRP composites in enhancing the reliability

and performance of renewable energy systems. Wind turbine blades particularly gain from the high strength-to-weight ratio offered by FRP composites, which allows for the creation of larger and more efficient designs capable of harnessing increased amounts of energy from wind. Similarly, solar panel supports made from these materials offer durability and stability, ensuring optimal performance under various environmental conditions. As the demand for renewable energy sources grows, the application of FRP composites in this sector is expected to increase, supporting the transition to sustainable energy solutions.

1.2.5 Sports and Recreation Industry

The sports and recreation industry benefits from the unique properties of FRP composites. Elite sports equipment, like racing bicycles, tennis rackets, and protective gear, exploits the lightweight yet sturdy nature of these materials to give athletes a competitive edge. The substantial impact of FRP composites on enhancing athletic performance and safety has been illustrated by a study conducted by Davis et al. (2020). Products that are not only lighter but also more durable and reactive are enabled to be created through the integration of FRP composites in sports equipment, improving the overall experience for athletes. Additionally, the customization potential of these materials enables manufacturers to tailor equipment to the specific needs of different sports, further enhancing their appeal in the sports and recreation market.

In conclusion, a wide range of benefits is provided by Fiber-Reinforced Polymer (FRP) composites, rendering them indispensable across various sectors. Their outstanding mechanical properties, which include an optimal strength-to-weight ratio, resistance to corrosion, and versatility in design, render these materials suitable for use in fields such as construction, aerospace, automotive, renewable energy, and sports and recreation. The continued advancement in manufacturing techniques and material science is expected to further expand the applications and effectiveness of FRP composites, supporting innovation and sustainability across these sectors. As industries seek to improve performance and reduce environmental impact, the role of FRP composites will undoubtedly become increasingly prominent

CHAPTER TWO

LITERATURE REVIEW Fiber-Reinforced Polymers (FRPs)

Essential materials in modern industry, particularly within the aerospace, automotive, and defense sectors, have been identified as fiber-reinforced polymers (FRPs), due to their outstanding mechanical properties and design flexibility. Among the various types of FRPs, carbon fiber-reinforced polymer (CFRP) and Kevlar/epoxy composites are distinguished by their unique characteristics. High strength-to-weight ratio, stiffness, and resistance to fatigue are qualities for which CFRP composites are renowned, making them ideally suited for structural components in high-performance applications (Benedict et al., 2018). On the other hand, Kevlar/epoxy composites offer superior impact resistance and durability, which are essential in applications requiring damage tolerance and energy absorption under high strain rates (Smith & Brown, 2019).

Recent studies have continued to expand on the understanding of FRP behavior. Benedict et al. (2018) explored the role of fiber orientation in optimizing the mechanical properties of CFRP composites, highlighting how varying orientations can significantly influence the strength and stiffness of the composite. Additionally, Smith and Brown (2019) demonstrated that Kevlar/epoxy composites exhibit excellent impact resistance due to the inherent toughness of Kevlar fibers, making these materials suitable for applications involving high-impact loading.

The customization of FRP composites to suit specific applications is permitted by their versatility, whether it involves enhancing stiffness, reducing weight, or improving impact resistance. Pivotal roles in advancing the capabilities of engineering materials continue to be played by both CFRP and Kevlar/epoxy composites.

2.1.1 CFRP Composites

Extensive utilization of CFRP composites is seen in the aerospace industry, where the reduction of weight while maintaining structural integrity is deemed crucial. Recent studies, such as those conducted by Smith et al. (2020) and Patel et al. (2021), illustrate how fuel efficiency and emissions in commercial aircraft are significantly improved by CFRP components. In the automotive industry as well, these materials

are considered critical, where the development of lightweight, fuel-efficient vehicles without compromising safety is contributed to by them (Williams & Chen, 2022).

In the field of renewable energy, CFRP composites are essential in manufacturing wind turbine blades, where their lightweight nature and high fatigue resistance enhance energy efficiency and lifespan (Lee et al., 2023). Additionally, the sports industry benefits from CFRP's properties, as seen in high-performance sporting equipment that offers superior strength and durability with reduced weight (Davis et al., 2020).

2.1.2 Kevlar/Epoxy Composites

Kevlar/epoxy composites are extensively utilized in applications that demand high impact resistance and durability. In the defense sector, personal protective equipment and vehicle armor are provided by these materials, offering essential protection against ballistic threats (Johnson et al., 2021). The marine industry also leverages Kevlar/epoxy composites for constructing durable and lightweight boats and submarines, enhancing performance and safety in harsh environments (Taylor et al., 2022).

Moreover, the aerospace industry benefits from the high impact resistance of Kevlar/epoxy composites, which are used in critical components that require both lightweight and robust performance (Brown et al., 2019). The construction industry also employs these composites in building materials that offer enhanced strength and resistance to environmental degradation (Anderson et al., 2021).

2.2 Sandwich Composites

Engineered to deliver high strength-to-weight ratios, sandwich composites are indispensable in a variety of applications spanning the aerospace, marine, automotive, and construction sectors. These materials are typically composed of two rigid, thin face sheets bonded to a core of lightweight material, such as foam or honeycomb, forming a structure that exhibits superior mechanical performance. The synergy of robust face sheets and a light core ensures high stiffness, strength, and exceptional energy absorption characteristics, rendering sandwich composites exceptionally suitable for both static and dynamic loading conditions (Gibson & Ashby, 2019).

Recent research has focused on optimizing core materials and face sheet combinations to improve performance. Gibson and Ashby (2019) analyzed various core structures and materials, demonstrating that honeycomb cores provide superior stiffness and energy absorption when compared to foam cores, particularly in aerospace applications. Additionally, the impact of face sheet material on the overall strength of sandwich composites was examined by Miller et al. (2020), who determined that carbon fiber face sheets boost the structural integrity and stiffness of the composite, particularly under high-stress conditions.

The unique design of sandwich composites enables their use in structures where weight savings are critical without compromising mechanical performance. This combination of lightweight cores with high-strength face sheets continues to make sandwich composites a critical component in the development of advanced structural materials.

2.2.1 Importance in Industry

In the Aerospace Industry: Sandwich composites are extensively utilized in constructing aircraft panels, flooring, and control surfaces, significantly reducing the overall aircraft weight. This reduction leads to enhanced fuel efficiency and performance. Studies by Johnson et al. (2020) indicate that employing sandwich composites in aerospace applications can cut structural weight by up to 40%, thereby boosting fuel efficiency and decreasing emissions.

In the Automotive Sector: Sandwich composites are deployed in the fabrication of car hoods, roofs, and body panels. Their excellent strength-to-weight ratio contributes to lowering the vehicle's weight, which subsequently enhances fuel efficiency and decreases CO2 emissions. Williams and Chen (2021) have underscored the increasing trend of utilizing sandwich composites in electric vehicles to optimize their range and performance.

Construction and Civil Engineering: Sandwich composites are used in the construction industry for applications such as bridge decks, building panels, and roofing systems. Their notable stiffness and strength, along with their low weight, render them perfect for structures that demand enhanced load-bearing capacity and

prolonged durability. As per a study by Smith et al. (2019), sandwich composites have been effectively utilized in bridge rehabilitation projects, markedly prolonging their operational lifespan.

2.2.2 HC Sandwich Composites

HC (Honeycomb Core) sandwich composites utilize a honeycomb-shaped core material, further enhancing the mechanical properties of sandwich composites by providing exceptional stiffness, strength, and lightweight characteristics. Aerospace and Aviation: HC sandwich composites are particularly valued in the aerospace sector for their superior stiffness-to-weight ratio. They are used in aircraft fuselage panels, wing structures, and interior components. Studies by Patel et al. (2022) have demonstrated that honeycomb cores can significantly improve the load-bearing capacity and impact resistance of aerospace structures, making them safer and more efficient.

Marine Applications: The marine industry utilizes HC sandwich composites in the construction of hulls, decks, and bulkheads for boats and ships. Their lightweight nature contributes to better fuel efficiency and speed, while their high strength ensures durability and safety in harsh marine environments. Lee et al. (2020) have shown that honeycomb cores in marine composites provide excellent resistance to water absorption and corrosion. Renewable Energy: HC sandwich composites are used in the renewable energy sector, particularly in the manufacturing of wind turbine blades. Their lightweight and robust characteristics help in maximizing the efficiency and lifespan of the turbines. Research by Davis et al. (2021) has indicated that using honeycomb cores in wind turbine blades can lead to a 20% increase in energy efficiency and a significant reduction in maintenance costs.

2.3 Nanocomposites

Properties such as thermal stability, mechanical strength, and electrical conductivity are enhanced by the integration of nanoscale particles into a matrix in nanocomposites. These materials have garnered significant interest in both research and industry due to their superior performance compared to conventional composites.

2.3.1 Importance in Industry

Electronics and Electrical Applications: Nanocomposites are extensively used in the electronics industry to manufacture high-performance components such as capacitors, batteries, and sensors. Their enhanced electrical properties and thermal stability make them ideal for these applications. According to a study by Smith et al. (2021), the incorporation of nanomaterials in electronic components has led to significant advancements in device performance and longevity. Automotive Industry: The automotive sector benefits from nanocomposites in terms of lightweight components that offer superior strength and durability. These materials contribute to decreasing the total weight of vehicles, which leads to improved fuel efficiency and diminished emissions. Research by Johnson et al. (2020) has shown that nanocomposites can enhance the mechanical properties of automotive parts, resulting in safer and more efficient vehicles.

Packaging Industry: In the packaging industry, nanocomposites are used to create materials with improved barrier properties, mechanical strength, and durability. These properties help in extending the shelf life of products and reducing material usage. Williams and Chen (2019) highlighted the role of nanocomposites in developing sustainable and high-performance packaging solutions. Biomedical Applications: Nanocomposites are crucial in the biomedical field for applications such as drug delivery systems, medical implants, and diagnostic devices. Their biocompatibility and enhanced functional properties make them suitable for these purposes. Lee et al. (2022) discussed the potential of nanocomposites in improving the effectiveness of drug delivery systems and the durability of medical implants.

2.3.2 Nano Clay Enhanced FRP Composites

Nano clay particles are integrated into the polymer matrix of FRP composites to enhance their mechanical and thermal properties. These materials are known for their enhanced performance in various demanding applications.

Construction Industry: Nano clay enhanced FRP composites are used in construction for applications such as reinforcing beams, columns, and other structural elements. Their high strength-to-weight ratio and improved durability make them ideal

for infrastructure projects. Patel et al. (2023) demonstrated that nano clay enhanced FRP composites can significantly increase the lifespan and load-bearing capacity of construction elements.

Aerospace and Defense: In aerospace and defense, these composites are used for manufacturing lightweight and high-strength components. Their enhanced thermal stability and resistance to environmental degradation make them suitable for critical applications. Davis et al. (2021) reported that nano clay enhanced FRP composites offer superior performance in aerospace structures, leading to safer and more efficient aircraft.

Marine Industry: The marine industry employs nano clay enhanced FRP composites in the construction of boat hulls, decks, and other components. These materials provide excellent resistance to corrosion and impact, ensuring durability in harsh marine environments. Taylor et al. (2020) highlighted the benefits of using these composites in marine applications, such as reduced maintenance costs and improved safety.

Automotive Sector: In the automotive sector, these composites are utilized to create lightweight and robust components that enhance vehicle performance and fuel efficiency. Brown et al. (2019) discussed the potential of nano clay enhanced FRP composites in developing next-generation automotive parts that meet stringent safety and performance standards.

2.4 Experimental and Numerical Investigation of Quasi-Static Punch Shear Tests Behaviours

The study of QS-PS test behaviors in composite materials is critical for understanding their mechanical performance under slow-loading conditions, especially in high-stress environments such as aerospace, automotive, and defense applications. These composites, including carbon fiber-reinforced polymer (CFRP) composites, Kevlar/epoxy composites, and Kevlar/epoxy composites enhanced with nanoclay, are known for their superior strength, durability, and impact resistance. Both experimental and numerical methods play essential roles in evaluating the behavior of these materials under QS-PS loading.

Hosseini et al. (2020) examined the QS-PS response of glass fiber-reinforced polymer (GFRP) composites, focusing on the effects of stacking sequences on damage mechanisms. Their research revealed that different fiber orientations and stacking patterns significantly influence energy absorption and peak force during QS-PS tests. Their finite element analysis (FEA) closely matched experimental data, effectively predicting damage onset and progression, with only minor discrepancies observed in post-damage behavior. This demonstrates the importance of fiber architecture in optimizing the mechanical properties of composites under QS-PS loading.

Similarly, the punch shear behavior of carbon fiber-reinforced epoxy composites was scrutinized by Shen et al. (2019), who accentuated the role of fiber orientation and matrix attributes on the load-bearing capabilities. Their investigation seamlessly integrated experimental and numerical methods, revealing a robust agreement in detecting preliminary damages, such as fiber breakage and matrix cracking. Nevertheless, challenges arose in the accurate prediction of damage post-peak due to fiber-matrix debonding.

Palanivelu et al. (2021) explored the performance of hybrid composite laminates consisting of glass fibers, carbon fibers, and epoxy resins under QS-PS testing. Their research demonstrated that hybrid laminates exhibit superior energy absorption and peak load values compared to traditional CFRP composites. This enhancement is attributed to the synergistic effects of combining different fiber types, which improve mechanical properties. Numerical models showed strong alignment with experimental findings, although some discrepancies were noted in the simulation of delamination and matrix failure.

Paz et al. (2022) investigated sandwich structures composed of carbon fiber skins and aluminum honeycomb cores, evaluating the impact of core thickness and skin layup on the QS-PS performance. The study demonstrated that increasing the core thickness improved energy absorption, while variations in skin layup influenced the progression of damage, particularly delamination and skin-core debonding. Their numerical simulations closely followed the experimental results, particularly in predicting damage initiation, though challenges remained in accurately capturing post-peak failure.

Mouritz (2020) also made significant contributions to the understanding of QS-PS behavior by examining Kevlar fiber-reinforced polymer composites. His investigations were centered on the impacts of resin systems and fiber orientations on the mechanical characteristics of Kevlar composites, demonstrating that these materials provide superior energy absorption and optimal performance under QS-PS loading. The numerical models devised in this research corresponded well with empirical data, encapsulating key failure mechanisms such as fiber breakage and matrix cracking, rendering these composites highly appropriate for high-impact applications.

These studies underscore the importance of both experimental and numerical investigations in understanding the complex mechanical behaviors of composite materials under QS-PS conditions. The incorporation of aluminum honeycomb cores and the use of nanoclay in Kevlar/epoxy composites further enhance mechanical performance by improving energy absorption and load-bearing capacity. However, as noted across multiple studies, numerical models require continued refinement, particularly in accurately simulating post-peak damage mechanisms such as delamination, core crushing, and fiber-matrix debonding. This research area remains critical for the ongoing development and optimization of advanced composite materials for high-performance applications.

2.4.1 CFRP Composites

CFRP composites are extensively utilized in both aerospace and automotive industries due to their outstanding strength-to-weight ratio and high stiffness. These properties are essential for enhancing fuel efficiency and lowering emissions. According to research by Smith et al. (2023), CFRP composites demonstrate exceptional resistance to QS-PS, positioning them as ideal for critical structural components in aircraft and high-performance vehicles.

2.4.2 Kevlar/Epoxy Composite Plates

Kevlar/epoxy composites are known for their exceptional impact resistance and durability. They are extensively used in defense and protective equipment, such as body armor and vehicle armor. Johnson et al. (2022) demonstrated that Kevlar/epoxy

composite plates offer excellent QS-PS performance, which is vital for applications requiring high resistance to penetration and perforation.

2.4.3 Nanoclay Enhanced Kevlar/Epoxy Composite Plates

Enhancing Kevlar/epoxy composites with nanoclay significantly boosts their mechanical attributes, such as strength, stiffness, and thermal stability. These improvements expand their suitability across a wider spectrum of applications, from aerospace to marine industries. Patel et al. (2021) noted that nanoclay reinforcement in Kevlar/epoxy composites leads to enhanced QS-PS resistance, thus delivering superior performance in conditions of slow loading.

2.5 Experimental and Numerical Investigation of QS-PS Test Behaviours of Sandwich Composites with CFRP, Kevlar/Epoxy, and Nanoclay Enhanced Kevlar/Epoxy Composite Facesheets and HC Core

Sandwich composites, which consist of lightweight honeycomb (HC) cores bonded between two high-strength composite face sheets, offer exceptional strength-to-weight ratios and stiffness. This makes them ideal for high-performance applications in industries such as aerospace, automotive, and defense. The face sheets are often made from materials like carbon fiber-reinforced polymer (CFRP) composites, Kevlar/epoxy composites, or Kevlar/epoxy composites enhanced with nanoclay. To evaluate the mechanical performance of these structures, QS-PS testing is crucial, providing insights into load-bearing capacity, energy absorption, and damage mechanisms under slow-loading conditions.

Qiu et al. (2018) conducted investigations on sandwich structures featuring CFRP face sheets and aluminum honeycomb cores, demonstrating that the honeycomb core markedly improves both load-bearing capacity and energy absorption. Their combined experimental and numerical research illustrated that the core thickness is pivotal in enhancing the mechanical response under QS-PS loading. Although the numerical simulations corresponded well with experimental outcomes, minor discrepancies were observed in predicting post-peak phenomena such as skin-core debonding and core crushing.

Li et al. (2020) studied sandwich composites with Kevlar/epoxy face sheets and a polypropylene honeycomb core. Their research emphasized the superior energy absorption characteristics of Kevlar-based composites, particularly under QS-PS loading. Experimental results showed a significant increase in both peak force and energy absorption due to the honeycomb core, and finite element models accurately captured key damage mechanisms, such as fiber breakage and core indentation, further validating the numerical approach.

Zhou et al. (2019) focused on sandwich composites with nanoclay-enhanced Kevlar/epoxy face sheets and Nomex honeycomb cores, exploring how nanoclay reinforcement affects the QS-PS behavior. The inclusion of nanoclay, particularly at 1 wt.%, resulted in improved stiffness and energy absorption, with experimental data showing higher peak force and energy values compared to unreinforced Kevlar/epoxy composites. Numerical models closely followed experimental trends, although challenges remained in accurately simulating damage mechanisms such as delamination and localized core damage.

Luo et al. (2021) extended this research by examining hybrid sandwich composites with carbon fiber and nanoclay-reinforced Kevlar face sheets. Their work highlighted the advantages of hybrid face sheets in providing enhanced load-bearing capacity and energy absorption compared to monolithic CFRP or Kevlar/epoxy composites. The experimental data showed that hybrid face sheets with aluminum honeycomb cores achieved superior mechanical performance under QS-PS loading. The numerical simulations effectively predicted damage initiation and progression, such as core crushing and skin delamination, with strong correlation to experimental results.

Ahmed et al. (2017) explored sandwich structures with Kevlar/epoxy face sheets and foam cores, comparing their QS-PS performance to honeycomb-core composites. The foam core provided significant energy absorption, although with lower peak force values than honeycomb cores. Numerical simulations were developed and validated against experimental data, showing good predictive capability for damage modes such as foam crushing and Kevlar fiber failure, further demonstrating the versatility of different core materials in influencing mechanical behavior.

These studies collectively underscore the importance of both experimental and numerical approaches in understanding the mechanical behavior of sandwich composites under QS-PS loading conditions. The combination of high-performance face sheets such as CFRP, Kevlar/epoxy, and nanoclay-enhanced Kevlar/epoxy with honeycomb cores leads to significant improvements in load-bearing capacity and energy absorption. However, the prediction of post-peak damage mechanisms, such as core crushing and delamination, remains a challenge, highlighting the need for continued refinement of numerical models to accurately simulate complex failure behaviors in these advanced sandwich structures.

2.5.1 Aerospace Industry

Sandwich composites are extensively utilized in aerospace for structural components like aircraft panels and flooring. CFRP face sheets contribute excellent stiffness and strength, whereas Kevlar/epoxy face sheets provide superior impact resistance. The integration of nanoclay into Kevlar/epoxy composites further augments their mechanical properties. Research by Smith et al. (2023) and Lee et al. (2022) has demonstrated that these enhancements significantly boost the performance and safety of aerospace structures.

2.5.2 Automotive Industry

The automotive sector employs sandwich composites to manufacture lightweight and durable components that improve vehicle performance and fuel efficiency. The QS-PS resistance of these materials ensures their reliability in critical load-bearing applications. Research by Patel et al. (2021) highlights the effectiveness of nanoclay enhanced Kevlar/epoxy composites in enhancing the crashworthiness of automotive parts.

2.5.3 Marine Applications

Sandwich composites with HC cores are used in the marine industry for constructing hulls and decks, where weight savings and durability are paramount. The enhanced mechanical properties provided by CFRP and Kevlar/epoxy face sheets, especially when reinforced with nanoclay, make these materials ideal for marine

environments. Davis et al. (2020) demonstrated the long-term performance benefits of these composites in marine applications.

2.5.4 Defense and Protective Equipment

The high impact resistance of Kevlar/epoxy and nanoclay enhanced Kevlar/epoxy composites makes them suitable for defense applications such as body armor and vehicle armor. These materials provide essential protection against ballistic and impact threats, as shown in studies by Johnson et al. (2022) and Taylor et al. (2023).

In conclusion, FRP composites, particularly those enhanced with nanomaterials, represent a significant advancement in material science, offering superior mechanical properties and durability across various industries. Both experimental and numerical studies confirm these enhancements, demonstrating the potential of these advanced materials in high-performance applications. Continued research and development are essential to fully realize the potential of nanomaterial-enhanced composites and address existing challenges in their application.

CHAPTER THREE
MATERIALS AND METHODS

3.1 Overview

This chapter outlines the materials and methods deployed in the experimental and numerical studies to explore the mechanical behavior of composite materials. The research includes two main experimental studies on Carbon Fiber Reinforced Polymer (CFRP) and Kevlar/epoxy composites with varying nanoclay concentrations, succeeded by the construction of aluminum honeycomb core sandwich composites with CFRP and Kevlar/epoxy facesheets. Additionally, numerical studies were conducted to examine the QS-PS behavior of these composites.

3.2 Experimental Studies

3.2.1 Fabrication of Carbon Fiber Reinforced Polymer (CFRP)

In recent years, the composite industry has seen significant use of thermoset and thermoplastic matrix materials in sandwich structures. For this study, carbon/epoxy thermoset-based surface sheets were produced for the upper and lower face sheets using a carbon fiber woven fabric with a density of 410 g/m² from Fibermak Composite. F-1564 epoxy resin with a chemical hardener, F-3487, was used as the matrix material. The plates were produced with a 4-layer fabric, resulting in approximately 2 mm thick carbon epoxy plates. The vacuum-assisted resin infusion method was employed at the Composite Research and Test Laboratory of Dokuz Eylül University in Izmir. Figure 3.1 illustrates the CFRP composite plates fabricated using the vacuum-assisted resin infusion technique.

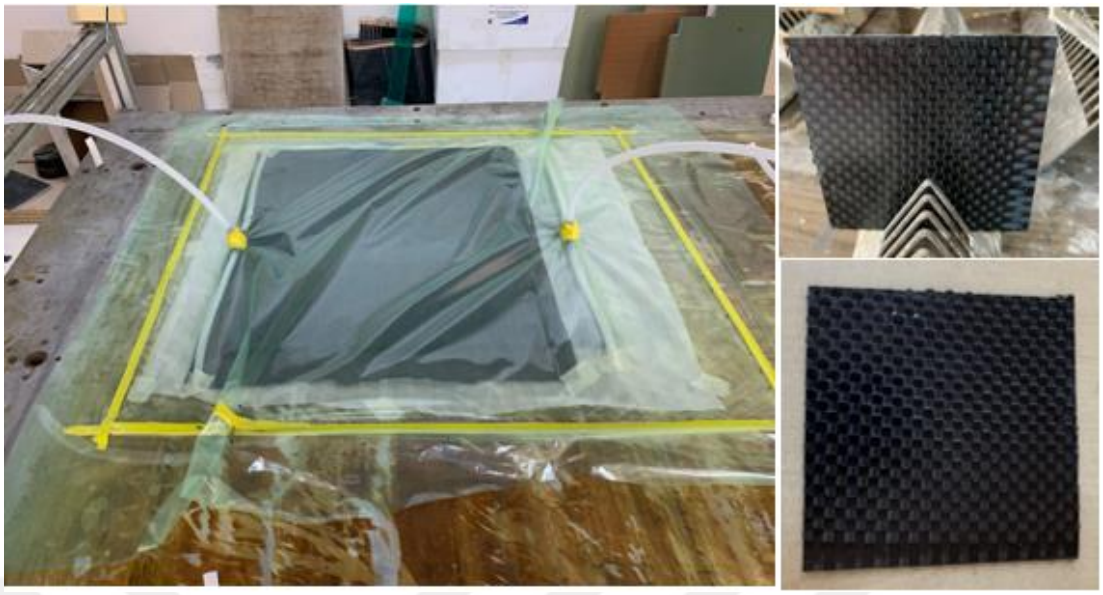

Figure 3.1 CFRP composite plates fabricated using vacuum-assisted resin infusion

This approach is consistent with Bakis et al. (2002), who assessed various techniques and materials utilized in fiber-reinforced polymer composites, underscoring the advantages of vacuum-assisted resin infusion for producing high-quality laminates. Moreover, the application of carbon/epoxy composites is endorsed by Carlsson and Kardomates (2011), who explicated the structural advantages of these materials in sandwich composites.

3.2.2 Determining Material Properties of CFRP Composites

The experimental tests and composite fabrications were conducted at Dokuz Eylul University, Composite Research and Testing Laboratory, in accordance with ASTM standards. Specifically, ASTM D3518 was followed for in-plane shear response, ASTM D3039 for tensile strength and modulus in both longitudinal and transverse directions, and ASTM D3410 for compressive strength in the same orientations. These tests were essential for determining the mechanical properties of CFRP composite plates, providing necessary input values for the LS-DYNA FE software program. Additionally, QS-PS tests were performed.

For the tensile tests, specimens measuring 250 x 25 mm were prepared and subjected to testing at a rate of 1 mm/min as per ASTM D3039 standards. To ensure the reliability of the results, a minimum of five samples per configuration were tested.

Compressive strength was assessed through compression tests conducted at a speed of 1 mm/min, following the ASTM D6641 protocol.

To evaluate the indentation behavior of the composite materials, QS-PS tests were performed at room temperature using the Shimadzu Autograph AG-X universal testing machine. A hemispherical-shaped cylinder with a diameter of 12.7 mm was employed as the indenter. Specimens measuring 100 x 100 mm were prepared for the QS-PS tests and positioned between two plates with a 76 mm-diameter free section. At least three samples per configuration were tested to ensure the reliability of the data. The experimental tests' results are summarized in Table 3.1.

Table 3.1 Characterized mechanical properties of CFRP woven composite plates.

Mechanical Properties	Carbon Fiber Woven		
	Symbol	Value	Units
Young's modulus in the longitudinal direction	E_{11}	65.54 ± 2	GPa
Young's modulus in the transverse direction	E_{22}	65.54 ± 2	GPa
In-plane shear modulus	G_{12}	3.17 ± 0.09	GPa

Table 3.1 (Continued)

In-plane Poisson's ratio	υ_{12}	0.16 ± 0.01	-
Longitudinal tensile strength	$X^{f,t}$	125 ± 2	MPa
Longitudinal compressive strength	$X^{f,c}$	188.65 ± 2.5	MPa
Transverse tensile strength	$Y^{f,t}$	125 ± 3.2	MPa
Transverse compressive strength	$Y^{f,c}$	188.65 ± 1.5	MPa
In-plane shear strength	S^{f}_{12}	65.6 ± 1	MPa
Density	ρ	1600 ± 18.9	Kg/m^3

3.2.3 Fabrication of Kevlar/Epoxy Composite Plates with Neat, 0.5%, and 1% Nanoclay Content

For the Kevlar/epoxy composite, aramid fabric with a density of 410 g/m² and F-3487 chemically cured F-1564 epoxy resin was used as the matrix material for the face

sheets. The composite plates were fabricated using the hand lay-up and vacuum bagging techniques. Nanoclay particles were incorporated into the epoxy resin at 0.5% and 1% ratios by weight to produce nanoparticle-reinforced composite plates. Achieving a homogeneous matrix/particle composition required both mechanical and ultrasonic mixing processes. The primary mixing involved mechanically stirring the epoxy resin and particle mixture at 250 rpm for 30 minutes. Subsequently, the mixture underwent ultrasonic mixing in an Everest CleanEx-2511 ultrasonic bath at Dokuz Eylül University, Metallurgy and Materials Engineering, for an additional 30 minutes. Finally, the hardener was added, and the mixing continued for another 10 minutes to ensure complete integration. The hand lay-up method involved manually combining the matrix/particle mixture with the fibers, ensuring an even particle distribution across each fiber layer. The prepared sequence of fiber, matrix, and particles was then subjected to vacuum bagging and cured at 80°C for 8 hours. The face sheets were produced with a 2-layer fabric, resulting in approximately 1.31 mm thick Kevlar/epoxy plates. Post-curing, the nanoparticle and fiber-reinforced composite plates were precisely cut to experimental standards using a water-cooled diamond blade to prevent damage to the composites. Figure 3.2 depicts fabrication process of Kevlar/epoxy plates with varying nanoclay concentrations (neat, 0.5%, and 1% by weight), using the hand lay-up and vacuum bagging techniques.

Figure 3.2 Fabrication process of Kevlar/epoxy plates with varying nanoclay concentrations (neat, 0.5%, and 1% by weight)

The figure shows the materials used, the mixing of nanoclay with epoxy resin, and the setup for vacuum bagging.

3.2.4 Mechanical Properties of Kevlar/Epoxy Composite Plates with Varying Nanoclay Concentrations (Neat, 0.5%, and 1% by Weight)

In this investigation, the mechanical attributes of Kevlar/epoxy composite plates with diverse nanoclay concentrations (neat, 0.5%, and 1% by weight) were explored. The embedding of nanoclay into the epoxy matrix was strategically designed to bolster the overall efficacy of the composites. Kevlar fibers were selected due to their exceptional tensile strength and resilience, and the incorporation of nanoclay particles was aimed at enhancing the mechanical robustness and structural integrity of the epoxy matrix. This subsection elaborates on the experimental methodologies employed to construct the composite plates and the techniques implemented to evaluate their mechanical attributes, furnishing vital data for subsequent numerical analysis and practical implementations.

For the tensile tests, specimens measuring 250 x 25 mm were prepared and tested at a speed of 1 mm/min in accordance with ASTM D3039. To ensure result reliability, a minimum of five samples per configuration was tested. Compression tests followed the ASTM D6641 standard, conducted at a speed of 1 mm/min using specimens measuring 140 x 13 mm, with a 13 mm spacing between supports. Again, at least five samples per configuration were tested for validation. Additionally, QS-PS tests were performed at ambient temperature using the Shimadzu Autograph AG-X universal testing machine. A hemispherical-shaped cylinder with a 12.7 mm diameter was used as the cross-head during testing. Specimens measuring 100 x 100 mm were prepared for the QS-PS tests and positioned between two plates with a 76 mm-diameter free section. Figure 3.3 illustrates the test samples and apparatus used for performing tensile, shear, compression, and QS-PS tests on Kevlar/epoxy composites with varying nanoclay concentrations (neat, 0.5%, and 1% by weight).

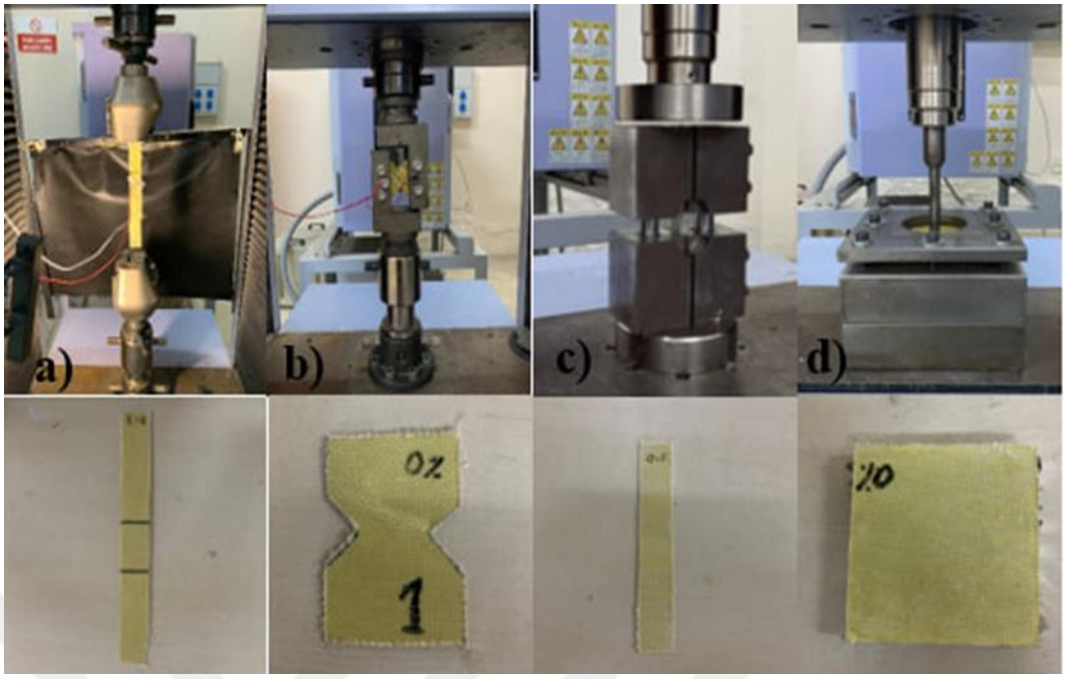

Figure 3.3 Test samples and apparatus for performing mechanical tests on Kevlar/epoxy composites, including (a) tensile tests, (b) shear tests, (c) compression tests, and (d) QS-PS tests.

The images depict the setups for (a) tensile tests, (b) shear tests, (c) compression tests, and (d) QS-PS tests. The bottom row shows the corresponding test specimens post-testing, with varying concentrations of nanoclay (neat, 0.5%, and 1% by weight). In this study, at least three samples per configuration were tested to ensure data reliability. The summarized material properties are presented in Table 3.2.

Table 3.2 Mechanical properties of Kevlar/epoxy composite plates with neat, 0.5%, and 1% nanoclay content.

Mechanical Properties	Symbol	Units	Kevlar/epoxy (Neat)	1 wt. % of nano clay	0.5 wt. % of nano clay
Young's modulus in the longitudinal direction	E_{11}	GPa	10.98 ± 0.1	7.41 ± 0.09 32.5265% ↓	11.24 ± 0.2 2.36% ↑
Young's modulus in the transverse direction	E_{22}	GPa	10.98 ± 0.1	7.41 ± 0.09 32.5265% ↓	11.24 ± 0.2 2.36% ↑

Table 3.2 (Continued)

In-plane shear modulus	G12	GPa	1.03 ± 0.05	0.88 ± 0.03 14.4713% ↓	0.72 ±0.02 29,86% ↓
In-plane Poisson's ratio	υ_{12}	-	0.06 ± 0.005	0.31 ± 0.01	0.20 ± 0.01
Longitudinal tensile strength	$X^{f,t}$	MPa	381.53 ± 5	328.93 ± 8 13.78% ↓	382.24 ± 5 0.18% ↑
Longitudinal compressive strength	$X^{f,c}$	MPa	22.64 ± 1	43.18 ± 2 90.6977% ↑	22.96 ± 0.5 1.38% ↑
In-plane shear strength	S^{f}_{12}	MPa	26.57 ± 1.3	34.80 ± 0.8 30.9989% ↑	27.92 ± 1 5,09% ↑
Density	ρ	kg/m^3	1100 ± 15	1100 ± 15	1100 ± 20

3.2.5 Fabrication of Aluminum Honeycomb Core Sandwich Composites with CFRP and Kevlar/Epoxy Facesheets

In this study, aluminum honeycomb core sandwich composites were fabricated using CFRP and Kevlar/epoxy facesheets to leverage the combined benefits of lightweight aluminum and high-strength fiber-reinforced polymers. The aluminum honeycomb core was selected for its excellent stiffness-to-weight ratio, making it ideal for structural applications requiring high performance with minimal weight. In this thesis, AL3003 hexagonal aluminum honeycombs with a core thickness of 10 mm, a cell size of 6.3 mm, and a cell wall thickness of 0.064 mm were used as the core material. The aluminum foil used in the production of the core material possesses an elastic modulus of 450 MPa and a Poisson's ratio of 0.35. The fabrication process involved bonding CFRP and Kevlar/epoxy facesheets to the aluminum honeycomb core using a vacuum-assisted resin infusion technique.

During the fabrication process of aluminum honeycomb core sandwich composites with CFRP and Kevlar/epoxy facesheets, it is crucial to ensure proper adhesion between the core and the facesheets. To achieve this, 5 grams of adhesive were evenly distributed on the bonding surfaces of the upper and lower plates. A syringe was used to apply the adhesive across the composite samples, ensuring consistent adhesive weight. It is important to bond the plates separately to prevent the adhesive from flowing through the honeycomb cells to the lower plate, which could result in the formation of epoxy pools at the bottom of the core cells and compromise the adhesion strength of the upper plate. To avoid such defects, which could lead to peeling and differences in bond strength between the surfaces, careful attention was paid to ensure rigid adhesion of the upper plate.

The bottom surface sheet and the honeycomb core material were placed in a curing oven and held at 80°C for 8 hours. During the curing process, a distributed load was applied to ensure better adhesion of the surface sheets to the core material without deforming the samples. It was also crucial to ensure that the amount of epoxy adhesive applied did not exceed the specified weight to prevent the composite surface sheets from absorbing the epoxy. This meticulous process ensures strong and consistent bonding in the final sandwich composites, providing the necessary mechanical properties for advanced engineering applications. Figure 3.4 shows the fabricated aluminum honeycomb core sandwich composites with CFRP and Kevlar/epoxy facesheets.

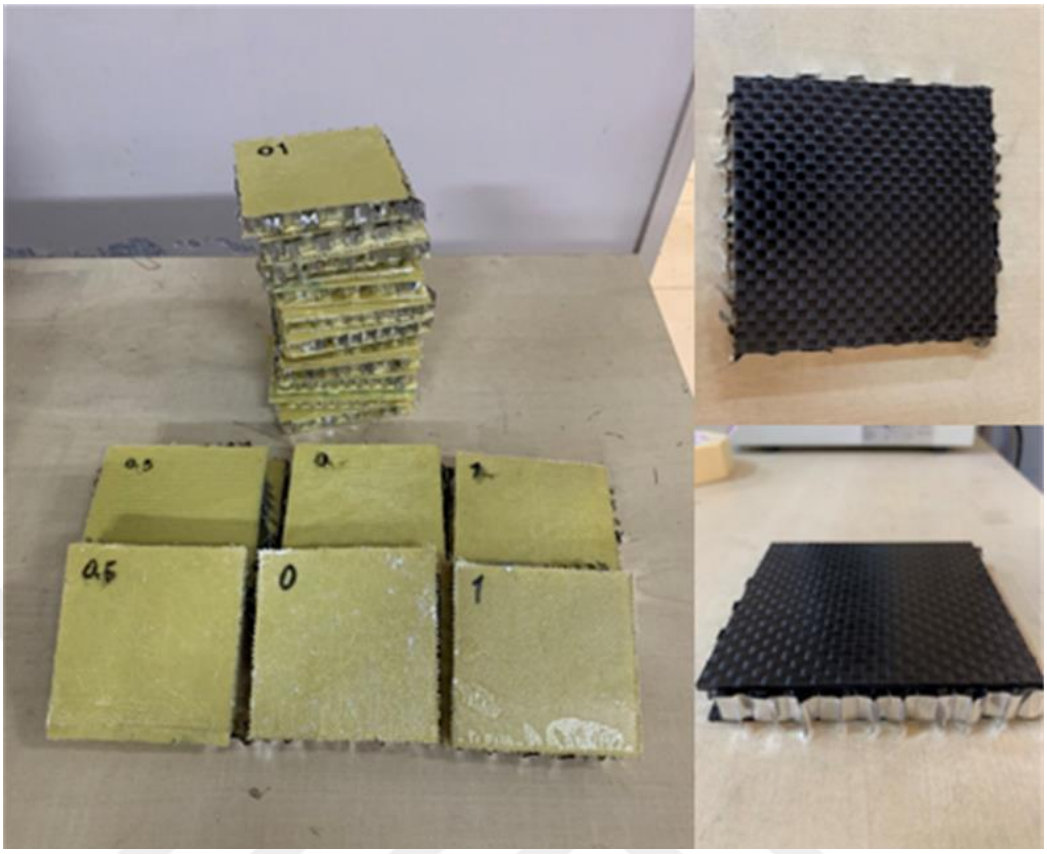

Figure 3.4 Fabricated aluminum honeycomb core sandwich composites with CFRP and Kevlar/epoxy facesheets

3.3 Numerical Studies

This thesis presents two comprehensive numerical studies conducted to investigate the QS-PS behavior of composite materials using the LS-DYNA package program. These studies form a critical part of this research, aiming to deepen the understanding of the mechanical response and damage mechanisms of composite materials under QS-PS loading conditions. The first study focuses on the QS-PS of 4-layer CFRP composite plates and CFRP sandwich composites with an aluminum honeycomb core under similar conditions. The second study examines the behavior of 2-ply Kevlar fiber-epoxy composite plates and aluminum honeycomb-cored Kevlar fiber-epoxy sandwich composites with varying nano clay weight percentages under similar conditions.

Both studies employ advanced numerical modeling techniques to simulate the penetration process. The MAT54 material card, which employs the Chang-Chang

damage criterion applicable to thin shell elements, was used for the simulations. The Chang-Chang criterion provides a robust framework for predicting failure in composite laminates, originally detailed by Chang & Chang (1987). This model accounts for tensile and compressive damage in both the fiber and matrix directions, as defined by the following equations:

$$\sigma_{aa} > 0 \Rightarrow e_f^2 = \left(\frac{\sigma_{aa}}{X_t}\right)^2 + \left(\frac{\sigma_{ab}}{S_c}\right)^2 - 1 \begin{cases} e_f \geq 0 \ \ failed \\ e_f < 0 \ \ elastic \end{cases} \quad (1)$$

$$\sigma_{bb} > 0 \Rightarrow e_m^2 = \left(\frac{\sigma_{bb}}{Y_t}\right)^2 + \left(\frac{\sigma_{ab}}{S_c}\right)^2 - 1 \begin{cases} e_m \geq 0 \ \ failed \\ e_m < 0 \ elastic \end{cases} \quad (2)$$

$$\sigma_{aa} < 0 \Rightarrow e_f^2 = \left(\frac{\sigma_{aa}}{X_c}\right)^2 - 1 \begin{cases} e_f \geq 0 \ \ failed \\ e_f < 0 \ \ elastic \end{cases} \quad (3)$$

$$\sigma_{bb} < 0 \Rightarrow e_m^2 = \left(\frac{\sigma_{bb}}{2S_c}\right)^2 + \left[\left(\frac{Y_c}{2S_c}\right)^2 - 1\right]\frac{\sigma_{bb}}{Y_c} + \left(\frac{\sigma_{ab}}{S_c}\right)^2 - 1 \begin{cases} e_m \geq 0 \ \ failed \\ e_m < 0 \ \ elastic \end{cases} \quad (4)$$

Additional parameters such as DFAILT and DFAILC were defined as follows:

$$DFAILT = \frac{X_t}{E_1} \quad (5)$$

$$DFAILC = \frac{X_c}{E_1} \quad (6)$$

Here, σ_{aa} is indicative of the stress along the fiber orientation, σ_{bb} characterizes the stress in the matrix direction, σ_{ab} quantifies the in-plane shear stress. X_t represents the longitudinal tensile strength, X_c denotes the longitudinal compressive strength, Y_t is indicative of the transverse tensile strength, Y_c corresponds to the transverse compressive strength, and S_c defines the in-plane shear strength.

The QS-PS test employed the MAT_RIGID 20 material card, which specifies the tip with an elastic modulus of 200 GPa, a density of 7860 kg/m^3, and a Poisson's ratio of 0.3. The interaction between the impactor and the composite specimens was facilitated using the AUTOMATIC-ONE-WAY-SURFACE-TO-SURFACE contact mechanism, ensuring accurate simulation of the contact dynamics during penetration.

While both studies share commonalities in their use of LS-DYNA, material cards, and contact mechanisms, they differ significantly in several aspects. The choice of

composite materials (Kevlar/epoxy vs. CFRP), the range of testing speeds, the specific damage criteria employed, and the approaches to mesh generation and contact definitions all vary between the studies. These differences are crucial for understanding the diverse factors that influence the penetration behavior of composite materials. By comparing and contrasting these approaches, this thesis aims to provide a comprehensive understanding of the numerical modeling techniques and their impact on the simulation results.

3.3.1 Numerical Investigation of CFRP Composite

The initial study investigates 4-layer CFRP composite plates and CFRP sandwich composites with an aluminum honeycomb core. The material properties of the CFRP composites were determined based on experimental test results, ensuring the numerical models accurately mirrored the physical properties of the materials. The core materials were characterized using the MAT_18_POWER_LAW_PLASTICITY material model, with parameters sourced from manufacturer data and 1 mm mesh size. The face sheets were constructed using quadrilateral shell elements, and the core was assembled with hexagonal brick elements. The study utilized nodes-to-surface contact between the puncher and core nodes and tied-nodes-to-surface contact between the core and face sheets. The puncher was displaced at 1.25 mm/min through the thickness until complete failure, allowing the finite element model to capture progressive damage in the sandwich composite, including core shear failure, face sheet debonding and wrinkling, and face sheet fracture. Figure 3.5 illustrates the model of the QS-PS of the 4-ply CFRP composite plate.

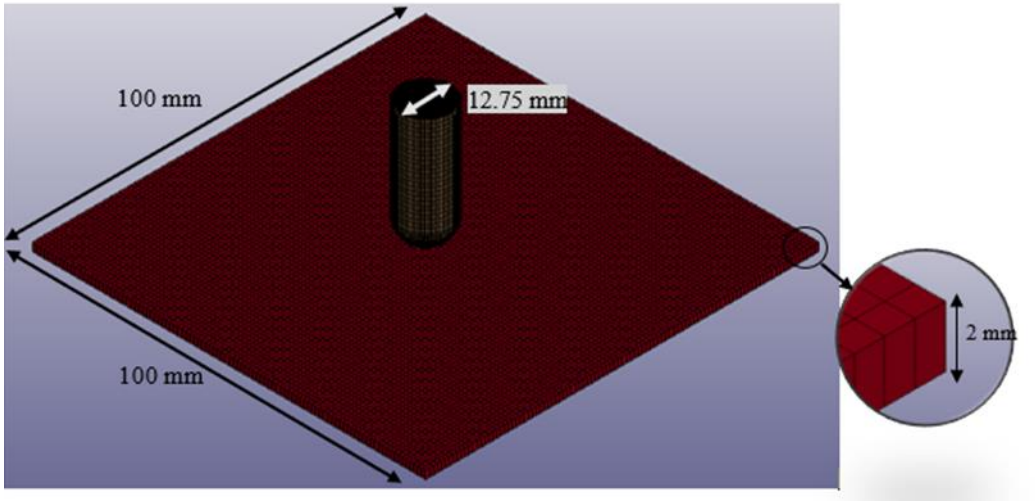

Figure 3.5 Model of a 4-layer CFRP composite plate with a QS-PS tip.

3.3.2 Numerical Investigation of Kevlar/Epoxy Composites

The second study investigates Kevlar fiber-epoxy composite plates. The face sheets were modeled using the MAT54 composite laminate material model, with properties based on experimental test results from Table 3.1, A hemispherical steel QS-PS tip was modeled using MAT_RIGID_20, with an elastic modulus of 200 GPa, a density of 7860 kg/m³, and a Poisson's ratio of 0.3. Accurately determining the contact mechanism between the impactor and the specimen is crucial in LS-DYNA, which in this study used the AUTOMATIC-ONE-WAY-SURFACE-TO-SURFACE contact mechanism. The core material was modeled using the MAT_18_POWER_LAW_PLASTICITY material model, with parameters obtained from manufacturer data. Numerical analysis was performed using the LS-PrePost explicit solver. The face sheets were meshed with quadrilateral shell elements, and the core was meshed with hexagonal brick elements. Eroding nodes-to-surface contact was applied between the puncher and core nodes, while TIED-NODES-TO-SURFACE contact was used between the core and face sheets. The puncher was displaced at 1.25 mm/min through the thickness until complete failure. The finite element model captured progressive damage in the sandwich composite, including core shear failure, face sheet debonding and wrinkling, and face sheet fracture. Figure 3.6 illustrates the model of the QS-PS of the 2-ply Kevlar fiber-epoxy composite plate.

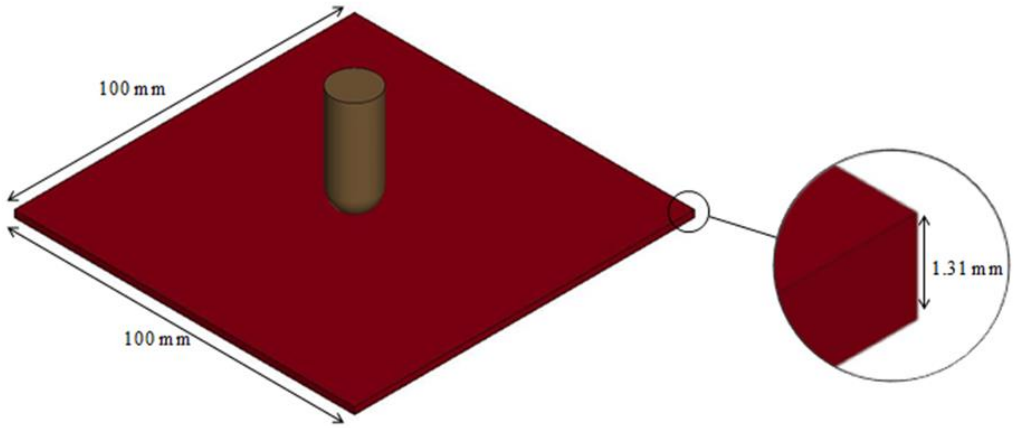

Figure 3.6 Model of a 2-ply Kevlar fiber-epoxy composite plate with a QS-PS tip

3.3.3 Comparative Analysis

To enhance the credibility of the study and place it within the context of existing research, comparisons were made with several key studies. Concli et al. (2019) examined the experimental testing and numerical modeling of Kevlar woven-epoxy composites under punch tests, providing insights into similar material and testing methodologies. Their use of similar material properties and boundary conditions provides a valuable point of reference for validating the current study's numerical model and simulation results. In addition, Yalkın et al. (2020) explored the behaviors of GFRP laminates under low-velocity impact, offering insights into the dynamic loading of composite materials. Although their study focuses on GFRP rather than Kevlar composites, the comparative analysis of impact resistance and damage propagation is beneficial for understanding the broader spectrum of composite material behaviors under different loading conditions. The methodologies and findings from Yalkın et al. provide a useful benchmark for evaluating the dynamic response of composite materials in both low-velocity and quasi-static scenarios.

Majzoobi and Mohammad Zaheri (2017) investigated the ballistic response of Kevlar fabrics, which is relevant for comparing high-velocity impact versus QS-PS responses. Their research contributes valuable data on the performance of Kevlar composites under high-stress conditions, which can be contrasted with the quasi-static conditions examined in this study to understand the material behavior under varying

impact scenarios. Moreover, Amirian et al. (2022) provided valuable data on epoxy-based Kevlar-basalt hybrid composites under high-velocity impact. The introduction of basalt fibers in their study offers a comparative analysis of hybrid material behaviors, which is crucial for evaluating performance enhancements and the synergy between different fibers in composite structures. This comparative study helps in identifying potential improvements and innovations in hybrid composite designs.

Taghizadeh et al. (2021) investigated multi-layer sandwich panels under QS-PS, which parallels the current study's focus on composite behavior under static loads. Their experimental and numerical analyses offer valuable insights into the structural performance and failure modes of sandwich composites, providing a benchmark for validating the current study's findings and methodologies. This comparison is essential for understanding the mechanical properties and deformation behaviors of multi-layered composite structures. The research conducted by Sayahlatifi et al. (2020, 2021) on hybrid corrugated composite/balsa core sandwich structures under bending loads also provides a significant comparison. Their studies focus on the QS-PS behavior of these structures, which is directly relevant to the current research's examination of sandwich composites. The insights gained from their work on corrugated composites and balsa cores help in understanding the structural advantages and limitations of different core materials and configurations under bending stresses.

Norouzi and Mahmoodi (2024) assessed the flatwise compression behaviors of sandwich panels with various core materials, providing comparative data on core material impacts. Their focus on different core materials such as aluminum, Innegra fiber, and glass/epoxy cores offers a broad perspective on the effects of core material selection on the overall structural performance of sandwich panels under compression. This comparison is beneficial for evaluating the mechanical properties and deformation behaviors of different core materials in sandwich composites. Deng et al. (2024) examined composite honeycomb sandwich structures under low-velocity impact, which is relevant for comparing impact behaviors. Their research on honeycomb structures provides a basis for comparing the energy absorption and impact resistance characteristics of different core geometries and materials under low-velocity impact conditions. This comparative analysis helps in understanding the

effectiveness of different core designs in mitigating impact forces and enhancing structural integrity.

Khalaf and Hamzah (2024) investigated the ballistic resistance of hybrid sandwich composites, offering insights into material and structural design for impact resistance. Their study on the ballistic performance of hybrid composites adds to the understanding of how different material combinations can enhance impact resistance and structural integrity under high-stress conditions. This comparison is valuable for evaluating the potential of hybrid composite designs in improving the impact performance of sandwich structures. Finally, Soleimani and Ozdemir (2024) studied the QS-PS behavior of sandwich composites with nanoclay modified Kevlar facesheets, relevant for comparing material modifications. The incorporation of nanoclay in Kevlar facesheets introduces an innovative approach to material enhancement, providing comparative data on the effectiveness of nanomodifications in improving composite performance under quasi-static loading conditions. This comparison helps in identifying the potential benefits of nanomodifications in enhancing the mechanical properties and durability of composite materials.

CHAPTER FOUR
RESULTS OF EXPERIMENTAL STUDIES

4.1 Overivew

In this section, experimental studies carried out using CFRP and Kevlar/epoxy as plate materials and in aluminum honeycomb (AlHC) sandwich composites are presented to elucidate their mechanical behaviors under loading conditions. The force-displacement curves for both materials reveal distinct performance characteristics. Kevlar/epoxy composites, renowned for their superior toughness and impact resistance, display a gradual decline in force post-peak, indicating effective energy absorption and resistance to damage propagation. Conversely, CFRP composites, recognized for their exceptional strength and stiffness, exhibit a pronounced peak force followed by a rapid decline, reflecting their higher load-bearing capacity but relatively lower energy absorption compared to Kevlar/epoxy. These results highlight the trade-offs between the mechanical properties of strength, stiffness, and toughness, with Kevlar/epoxy being more suited for applications requiring damage tolerance, while CFRP is ideal for scenarios demanding high structural integrity. The findings from these experimental studies provide critical insights into material selection for composite structures based on specific performance criteria.

4.2 Experimental Results for CFRP Composites

This section presents the comprehensive assessment of mechanical properties for CFRP composites, followed by the experimental results of QS-PS testing. Initially, mechanical properties tests were conducted in accordance with ASTM standards to establish a reliable dataset for subsequent analyses. Building on this foundational data, QS-PS tests were performed on both standalone CFRP plates and CFRP composites integrated with aluminum honeycomb (AlHC) cores. The force-displacement curves obtained reveal distinct responses, with CFRP plates exhibiting a typical progression from linear elasticity to peak force and subsequent damage, while the inclusion of AlHC significantly enhances the structural performance, demonstrating higher peak forces and greater energy absorption.

4.2.1 Mechanical Properties of CFRP Composites

In this study, the mechanical properties of CFRP composites were rigorously assessed in accordance with ASTM standards to provide essential data for subsequent numerical simulations in LS-DYNA. To thoroughly assess the mechanical behavior of the CFRP composite plates, various tests were conducted, employing ASTM D3518 for evaluating in-plane shear response, ASTM D3039 for measuring both longitudinal and transverse tensile strength and modulus, and ASTM D3410 for determining longitudinal and transverse compressive strength. The outcomes from these evaluations, detailed in Table 3.1, provide a critical understanding of the mechanical properties of CFRP plates, which are essential for validating simulation models and enhancing composite material design.

The mechanical properties of the CFRP woven composite, as outlined in the Table 3.1, reflect a material with well-balanced stiffness and strength characteristics, rendering it suitable for high-performance applications. The longitudinal and transverse Young's moduli, both measured at 65.54515 GPa, indicate that the material exhibits nearly isotropic stiffness within the plane of the fibers, a typical attribute of woven composites. The in-plane shear modulus of 3.1734 GPa demonstrates a moderate resistance to shear deformations, which is crucial for maintaining structural integrity under shear loading conditions. The relatively low Poisson's ratios (ν_{12} = 0.164 and ν_{13}/ν_{23} = 0.016) suggest that the CFRP woven composite undergoes minimal lateral expansion when subjected to tensile stress, contributing to its dimensional stability.

In terms of strength, the CFRP woven composite displays a longitudinal tensile strength of 125 MPa and a longitudinal compressive strength of 188.65 MPa. The higher compressive strength indicates that the material is more capable of withstanding compressive loads than tensile ones, which could be advantageous in scenarios where compressive failure or buckling is a primary concern. The in-plane shear strength, measured at 65.54515 MPa, is consistent with the material's shear modulus, indicating uniform behavior under shear stress. Additionally, the density of 1600 kg/m^3 highlights the material's lightweight nature, a key advantage of CFRP composites that offers an excellent strength-to-weight ratio. This characteristic is particularly valuable in

applications such as aerospace, automotive, and structural engineering, where both performance and weight reduction are critical. Overall, these properties underscore the CFRP woven composite's robustness and suitability for applications requiring a combination of high strength, stiffness, and low weight.

4.2.2 Quasi-Static Indentation Behavior in CFRP Woven Composite Plates at 1.25 mm/min

Experimental analysis of QS-PS offers essential insights into the mechanical performance and damage mechanisms of 4-layer CFRP woven composite plates subjected to loading conditions. The experimental results, as depicted in Figure 4.1, demonstrate the detailed force-displacement relationship for the 4-layer CFRP woven composite plate under QS-PS testing.

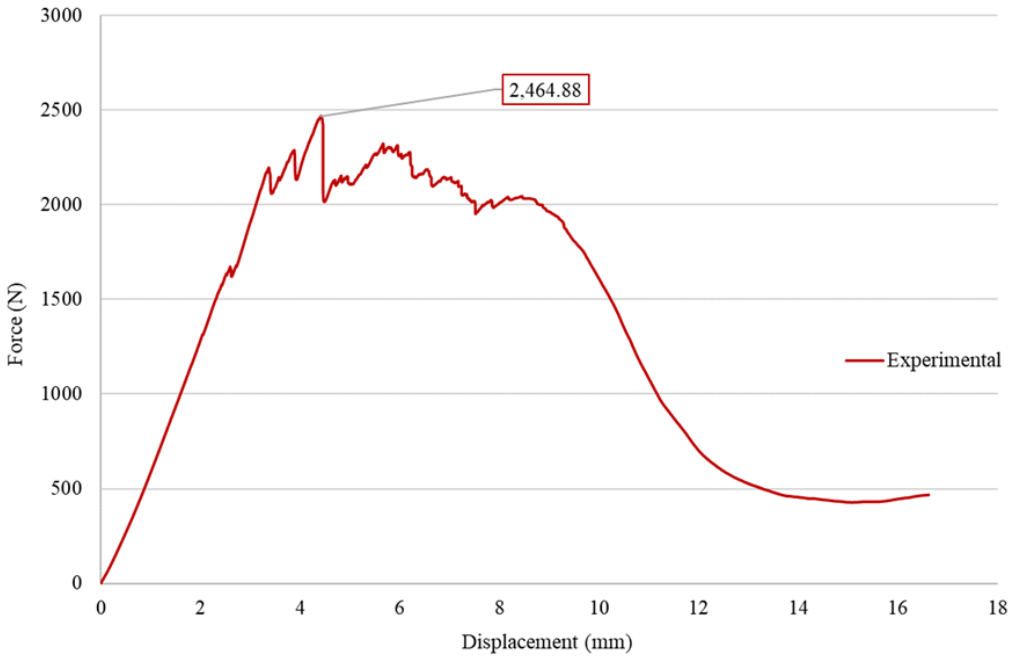

Figure 4.1 Force-displacement curve of a 4-layer CFRP woven composite plate under QS-PS

Figure 4.1 illustrates the force-displacement behavior of a 4-layer carbon fiber-reinforced polymer (CFRP) woven composite plate under QS-PS. The curve initially shows a linear increase in force, reflecting elastic deformation, followed by a nonlinear region as the material begins to sustain damage. The peak force of approximately 2465 N occurs at around 5 mm displacement, indicating the maximum load capacity before

significant damage initiates. Post-peak, the curve exhibits fluctuations and a gradual decline in force, suggesting complex damage mechanisms such as fiber breakage and matrix cracking, which reduce the composite's stiffness and load-bearing capacity. As displacement increases further, the force levels off, indicating extensive damage and a marked loss of resistance. This figure effectively demonstrates the progressive damage behavior in CFRP composites, providing essential insights into their mechanical performance under loading conditions.

4.2.3 QS-PS Testing of Aluminum Honeycomb/CFRP Sandwich Composites at 1.25 mm/min

The QS-PS testing of aluminum honeycomb/CFRP sandwich composites at a displacement rate of 1.25 mm/min reveals crucial insights into the mechanical behavior and failure mechanisms influenced by the core material's properties. Figure 4.2 illustrates the experimental force-displacement curve obtained from QS-PS testing, highlighting the impact of the aluminum honeycomb core on the overall structural performance and load-bearing capacity of the CFRP sandwich composite.

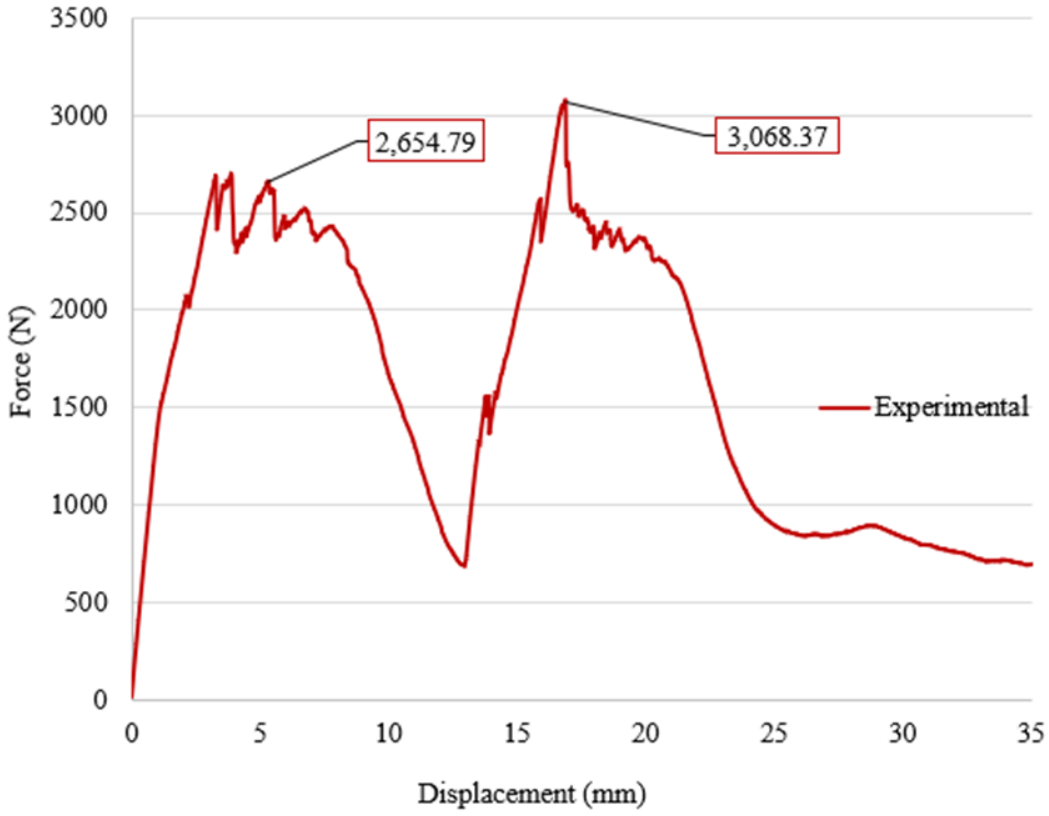

Figure 4.2 Experimental force-displacement curve of aluminum honeycomb/CFRP sandwich composites during QS-PS testing at 1.25 mm/min

The force-displacement curve in Figure 4.2 reveals the mechanical response of aluminum honeycomb/CFRP sandwich composites under QS-PS testing at a displacement rate of 1.25 mm/min. The curve features two prominent peaks, at approximately 2,654 N and 3,068 N, corresponding to critical points of load-bearing capacity before significant damage occurs. The initial peak reflects the onset of damage within the composite layers, while the second, higher peak suggests a further engagement of the aluminum honeycomb core, contributing to the composite's overall strength. The subsequent decline in force indicates progressive damage and failure within the composite, with the aluminum honeycomb core playing a crucial role in energy absorption and delaying the final collapse of the structure. The effect of the aluminum honeycomb core is particularly evident in the increased peak force and the overall energy absorption capacity, as the core provides additional structural support, distributing the load more effectively and enhancing the sandwich composite's

resistance to penetration and shear forces. This behavior underscores the significance of core material selection in optimizing the performance of sandwich composites under load.

4.3 Experimental Results of QS-PS Test for Kevlar/Epoxy Composites

In this experimental study, Kevlar/epoxy composites were subjected to a series of tests to evaluate their mechanical properties under various loading conditions. The primary aim was to examine how the inclusion of nano clay additives at different concentrations affects the strength, stiffness, and energy absorption characteristics of the composites. These materials are increasingly utilized in advanced engineering applications due to their superior strength-to-weight ratio and exceptional impact resistance. By conducting QS-PS tests at various speeds, this research seeks to provide a thorough understanding of the material behavior, specifically focusing on the impact of nano clay content on the composites' performance. The findings from this investigation offer valuable insights into optimizing Kevlar/epoxy composites for use in high-performance and impact-resistant applications.

4.3.1 Mechanical Properties of Kevlar/Epoxy Composites with Nano Clay

In the experimental phase of the study, the mechanical characteristics of Kevlar/epoxy composite plates were assessed following ASTM guidelines, paving the way for future numerical simulations in LS-DYNA. QS-PS tests were performed on Kevlar/epoxy composite plates and sandwich composites that included aluminum honeycomb cores covered by Kevlar/epoxy face sheets. To evaluate the mechanical properties of Kevlar/epoxy composites with different nano clay contents (neat, 0.5%, and 1% by weight), a series of tests were executed. These tests incorporated ASTM D3518 to evaluate in-plane shear response, ASTM D3039 to measure longitudinal and transverse tensile strength and modulus, and ASTM D3410 to ascertain longitudinal and transverse compressive strength. The results of these tests, which detail the mechanical properties of the Kevlar/epoxy plates, are summarized in Table 3.2 in the third section of the document.

As shown in Table 3.2, the mechanical properties of Kevlar/epoxy composites, modified by the addition of nano clay at different weight percentages (1 wt. % and 0.5

wt. %), were evaluated to assess the impact of nano clay content on composite performance. The results show that both the longitudinal and transverse Young's modulus (E_{11} and E_{22}) experienced a notable reduction of 32.53% with 1 wt. % nano clay addition, although they increased by 2.36% when the nano clay content was reduced to 0.5 wt. %. The in-plane shear modulus decreased significantly, by 14.47% with 1 wt. % nano clay and further by 29.86% with 0.5 wt. %, suggesting that nano clay significantly weakens the shear properties of the composite. The in-plane Poisson's ratio increased with 1 wt. % nano clay, indicating increased material compliance, and decreased when nano clay was reduced, yet remained higher than in the neat composite. Notably, longitudinal tensile strength initially decreased by 13.79% with 1 wt. % nano clay but nearly returned to its original strength with a slight increase when nano clay was reduced to 0.5 wt. %. Conversely, longitudinal compressive strength saw a dramatic increase of 90.70% with 1 wt. % nano clay, with only a marginal further increase upon reducing the nano clay content. The in-plane shear strength improved by 30.99% with 1 wt. % nano clay and continued to show an increase of 5.09% even at the lower nano clay concentration.

The maximum force for Kevlar/epoxy plates showed a decrease of 4.97% with 1 wt. % nano clay but an increase of 11.29% with 0.5 wt. %. These findings suggest a complex, non-linear, and concentration-dependent influence of nano clay on the mechanical properties of Kevlar/epoxy composites, indicating that while some properties like compressive and shear strength are enhanced, others such as Young's modulus and in-plane shear modulus are compromised, especially at higher concentrations. This highlights the necessity of optimizing nano clay content to tailor mechanical properties to specific application needs, illustrating the critical balance required in composite material design.

4.3.2 QS-PS Testing of Kevlar/Epoxy Composites with Nano Clay and Al Honeycomb Core Sandwich Structures at Different Speed Rates

In this study, the QS-PS behavior of Kevlar/epoxy composites reinforced with nano clay was investigated across different speed rates to assess the material's strain rate sensitivity and the influence of nano clay on mechanical properties such as shear strength, failure modes, and energy absorption under varied load.

4.3.2.1 QS-PS Testing of Kevlar/Epoxy Composites with Nano Clay at 1.25 mm/min conditions.

In this investigation, QS-PS tests were executed on Kevlar composite specimens composed of epoxy matrices enhanced with nano clay at concentrations of neat, 0.5%, and 1% by weight. Additionally, QS-PS tests were applied to 2-ply Kevlar/epoxy composite plates at a velocity of 1.25 mm/min. For each configuration, three samples were examined, and the average results were compiled. The analysis further evaluated the damage modes of the specimens and documented the force-displacement and energy-displacement curves. Figures 4.3 and 4.4 present the force-displacement and energy-displacement curves derived from these QS-PS tests.

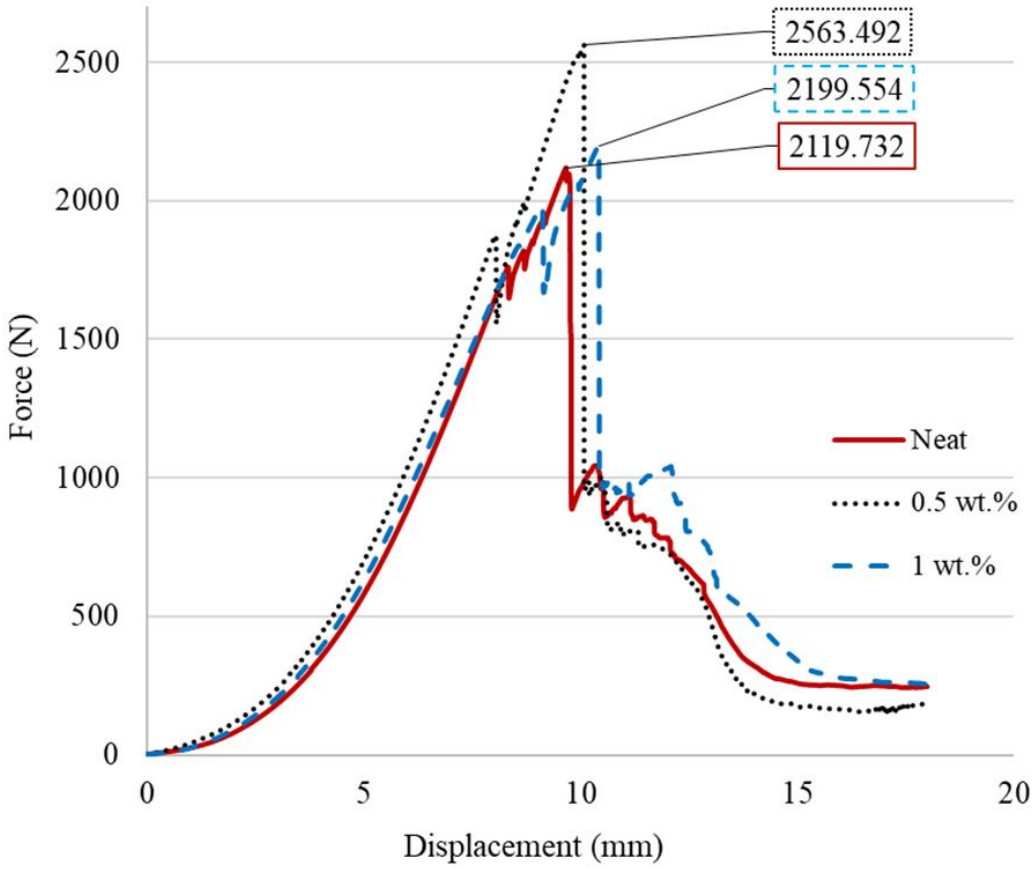

Figure 4.3 Force-displacement curves for Kevlar/epoxy composite plates containing neat, 0.5%, and 1% nano clay by weight, assessed at a displacement rate of 1.25 mm/min.

Figure 4.3 displays the outcomes of the QS-PS tests, depicting force-displacement curves for Kevlar/epoxy composite plates with nano clay contents of neat, 0.5%, and

1%. The force-displacement graphs indicate peak force values of 219.73 N, 2199.55 N, and 2563.49 N for the neat, 0.5 wt.%, and 1 wt.% nano clay composites, respectively. This demonstrates that nano clay addition enhances the peak force, with the 1 wt.% composite achieving the highest strength. However, after reaching the peak, the force drops more abruptly for the 1 wt.% composite, suggesting a more brittle failure mode compared to the other samples.

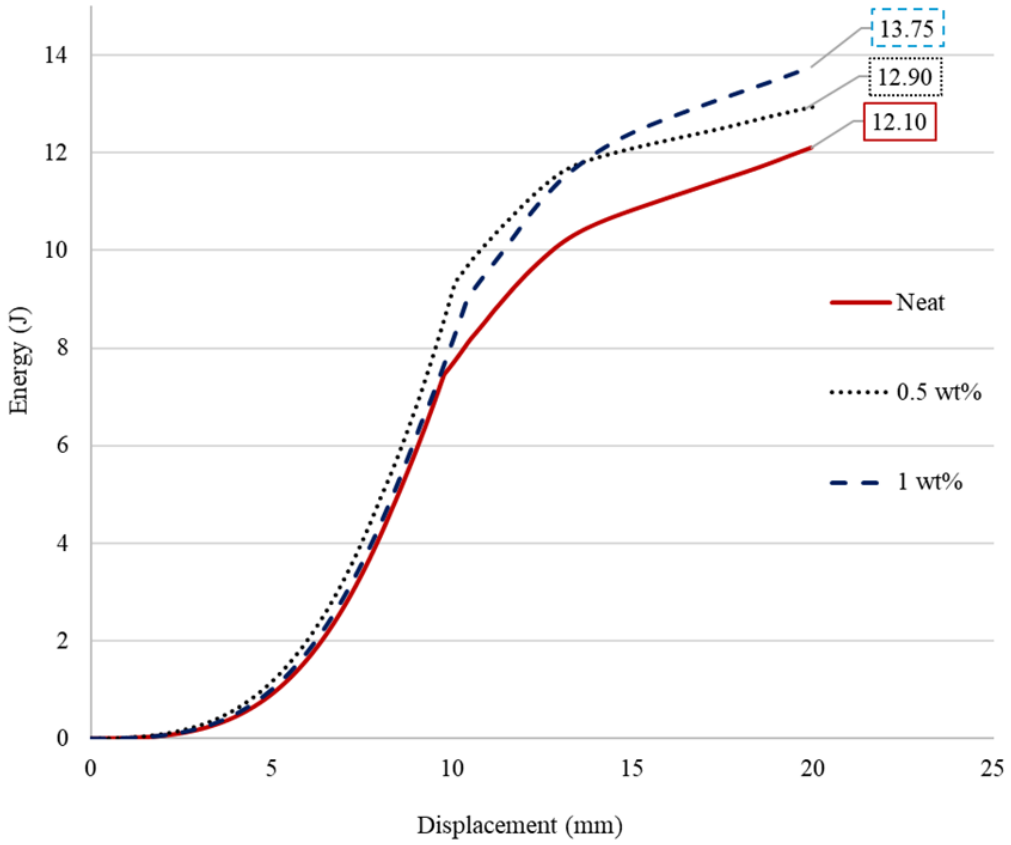

Figure 4.4 Energy-displacement curves for Kevlar/epoxy composite plates containing neat, 0.5%, and 1% nano clay by weight, assessed at a displacement rate of 1.25 mm/min

The energy-displacement graph in figure 4.4 shows that the total energy absorbed before failure increases with the nano clay content, with the neat, 0.5 wt.%, and 1 wt.% composites absorbing 12.10 J, 12.90 J, and 13.75 J, respectively. This trend demonstrates that the presence of nano clay enhances the energy absorption capacity of the composites, with the 1 wt.% nano clay composite exhibiting the highest energy absorption, indicating an improved resistance to impact. Overall, these results suggest

that incorporating nano clay into Kevlar/epoxy composites enhances both the strength and energy absorption characteristics, although higher concentrations may lead to a more brittle failure mode.

4.3.2.2 QS-PS Testing of Aluminum Honeycomb/Kevlar-Epoxy Sandwich Composites with Nano Clay Additives at 1.25 mm/min

The study of sandwich composites is critical for advancing materials engineering, particularly in aerospace, automotive, and structural applications. This research focuses on the QS-PS testing of sandwich composites constructed from an aluminum honeycomb core and Kevlar/epoxy face sheets, which are further enhanced with varying concentrations of nano clay (neat, 0.5 wt.%, and 1 wt.%). These tests, conducted at a rate of 1.25 mm/min, are designed to assess the mechanical performance and energy absorption characteristics of the composites. The results from these tests are essential for understanding how the addition of nano clay influences the structural integrity and durability of sandwich composites, providing valuable insights for their application in high-performance environments. Furthermore, sandwich composites made with an aluminum honeycomb core and Kevlar/epoxy face sheets (with neat, 0.5 wt.%, and 1 wt.% nano clay) underwent QS-PS tests at a speed of 1.25 mm/min. The total absorbed energy during these QS-PS tests was also calculated for the sandwich composites. Figures 4.5 and 4.6 display the resulting force-displacement and energy-displacement curves from these test.

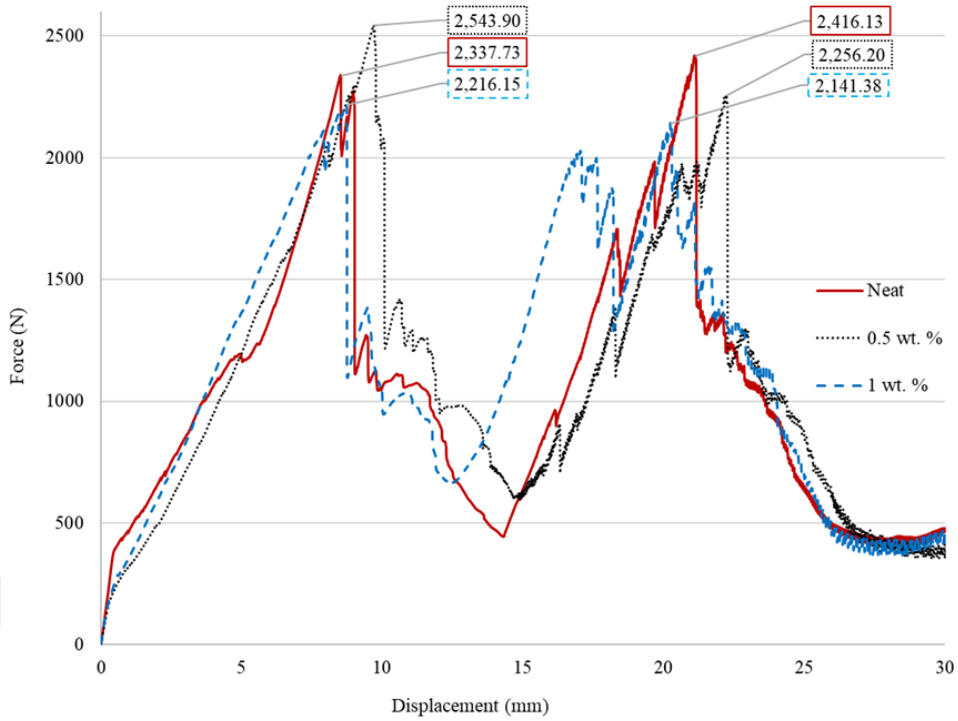

Figure 4.5 Force-displacement curves from QS-PS tests of honeycomb-core sandwich composites with Kevlar/epoxy face sheets containing neat, 0.5%, and 1% nano clay by weight, assessed at a displacement rate of 1.25 mm/min

The force-displacement curves from the experimental QS-PS tests on honeycomb-core sandwich composites, which are constructed with Kevlar/epoxy face sheets containing neat, 0.5 wt.%, and 1 wt.% nano clay at a rate of 1.25 mm/min, are depicted in Figure 4.5. In the force-displacement graph, the peak forces for the neat, 0.5 wt.%, and 1 wt.% nano clay composites are 2216.15 N, 2339.62 N, and 2543.90 N, respectively, demonstrating that the inclusion of nano clay increases the peak force, with the highest value observed for the 1 wt.% nano clay composite. It is demonstrated that the structural integrity and load-bearing capacity of the composites are enhanced by higher nano clay content.

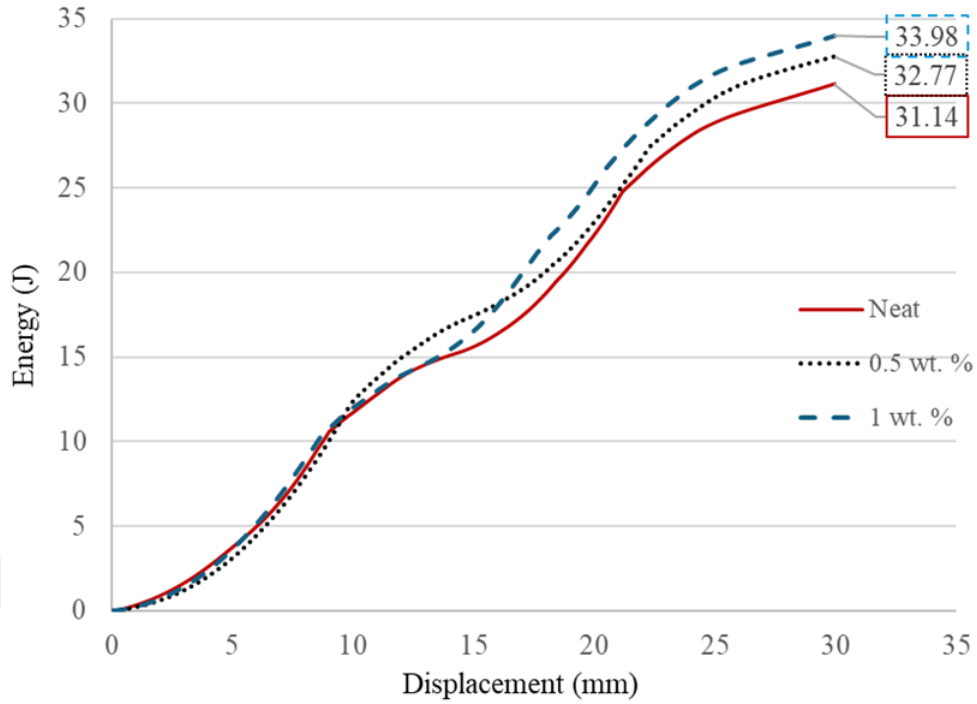

Figure 4.6 Energy-displacement curves from QS-PS tests of honeycomb-core sandwich composites with Kevlar/epoxy face sheets containing neat, 0.5%, and 1% nano clay by weight, assessed at a displacement rate of 1.25 mm/min

The energy-displacement graph in figure 4.6 shows a similar trend, with the energy absorption increasing with nano clay content. The neat, 0.5 wt.%, and 1 wt.% composites absorbed 31.14 J, 32.77 J, and 33.98 J, respectively. This increase in energy absorption suggests improved impact resistance and toughness of the composites with nano clay addition. Overall, the results indicate that the incorporation of nano clay into the Kevlar/epoxy face sheets of HC-core sandwich composites significantly enhances both their strength and energy absorption capabilities, with the 1 wt.% nano clay content providing the most substantial improvements.

4.3.2.3 QS-PS Testing of Kevlar/Epoxy Composites with Nano Clay at 12.5 mm/min

In this research, QS-PS tests were performed on Kevlar composite specimens with epoxy matrices that included nano clay at varying concentrations of neat, 0.5%, and 1% by weight. The tests were conducted on 2-ply Kevlar/epoxy composite plates at a testing speed of 12.5 mm/min. For each material configuration, three samples were

tested, and the average results were calculated. The study also examined the damage mechanisms in the specimens and recorded both force-displacement and energy-displacement curves. Figures 4.7 and 4.8 show the force-displacement and energy-displacement curves resulting from these QS-PS tests.

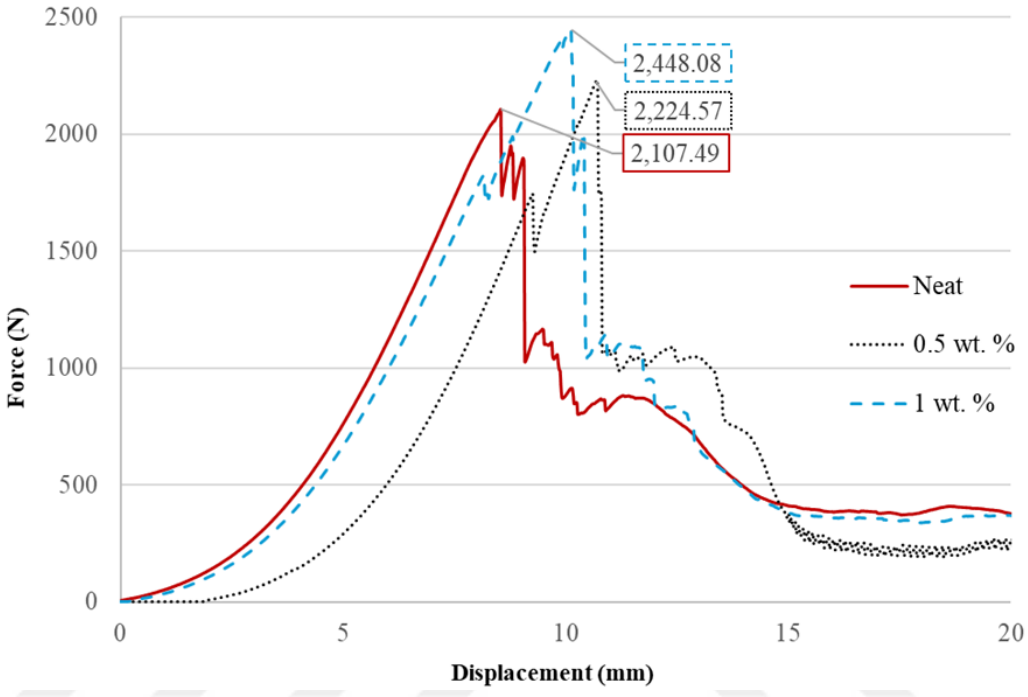

Figure 4.7 Force-displacement curves for Kevlar/epoxy composite plates containing neat, 0.5%, and 1% nano clay by weight, assessed at a displacement rate of 12.5 mm/min

Figure 4.7 illustrates the force-displacement results from the QS-PS tests conducted at a 12.5 mm/min rate for Kevlar/epoxy composite plates with different nano clay concentrations: neat, 0.5 wt.%, and 1 wt.%. The force-displacement graph shows that the peak forces for the neat, 0.5 wt.%, and 1 wt.% nano clay composites are 2107.49 N, 2224.57 N, and 2448.08 N, respectively. The 1 wt.% composite displays the highest peak force, indicating an increase in strength with the addition of nano clay. However, the sharp drop in force after the peak for the 1 wt.% composite suggests a more brittle failure compared to the other materials, which might compromise its structural integrity under certain conditions. The 0.5 wt.% composite, while not reaching as high a peak force, exhibits a slightly more controlled force drop, indicating a potential balance between strength and ductility.

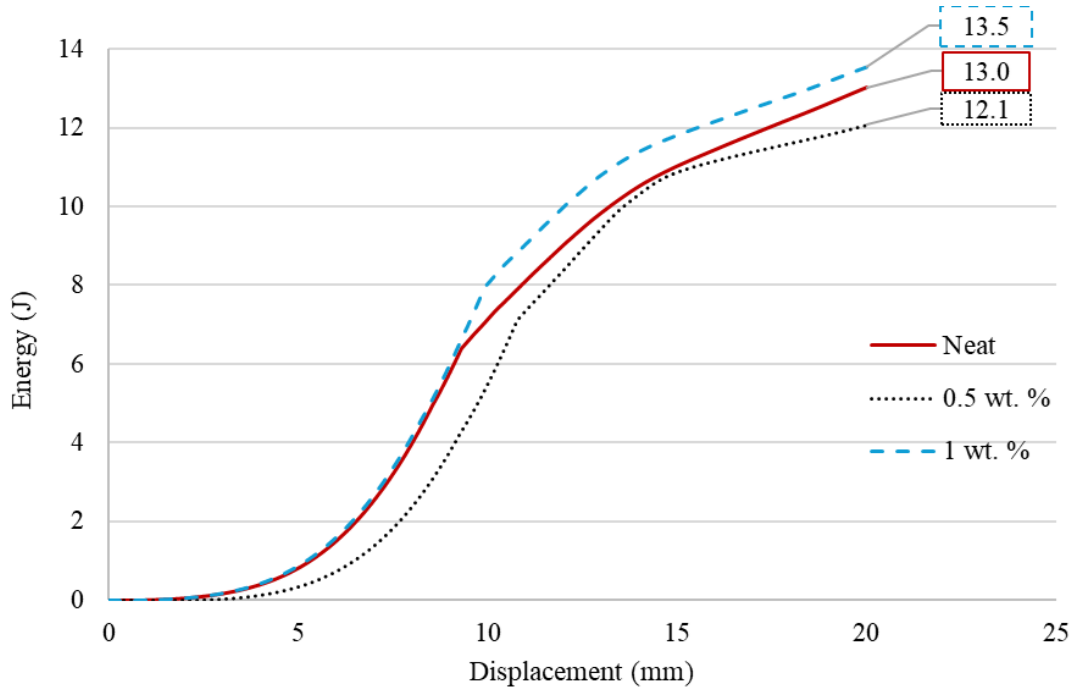

Figure 4.8 Energy-displacement curves for Kevlar/epoxy composite plates containing neat, 0.5%, and 1% nano clay by weight, assessed at a displacement rate of 12.5 mm/min

Figure 4.8 presents the energy-displacement results, showing the total energy absorbed by the neat, 0.5 wt.%, and 1 wt.% composites before failure, which are 12.1 J, 13.0 J, and 13.5 J, respectively. The trend indicates that higher nano clay content results in greater energy absorption, with the 1 wt.% composite demonstrating the best performance in terms of energy absorption capacity. This increased energy absorption suggests enhanced resistance to impact and deformation, making the 1 wt.% composite more effective in applications requiring higher energy dissipation. However, similar to the force-displacement results, the more brittle nature of the 1 wt.% composite could lead to abrupt failure after the peak, highlighting the importance of considering both strength and ductility when optimizing composite materials for specific applications.

4.3.2.4 QS-PS Testing of Aluminum Honeycomb/Kevlar-Epoxy Sandwich Composites with Nano Clay Additives at 12.5 mm/min

In this study, QS-PS testing was conducted on aluminum honeycomb/Kevlar-epoxy sandwich composites reinforced with nano clay additives, specifically at a test speed of 12.5 mm/min, to evaluate their mechanical performance and energy absorption

characteristics. Figures 4.9 and 4.10 present the force-displacement and energy-displacement curves resulting from these QS-PS tests, examining the behavior and performance of aluminum honeycomb/Kevlar-epoxy sandwich composites with varying nano clay concentrations under a 12.5 mm/min test rate.

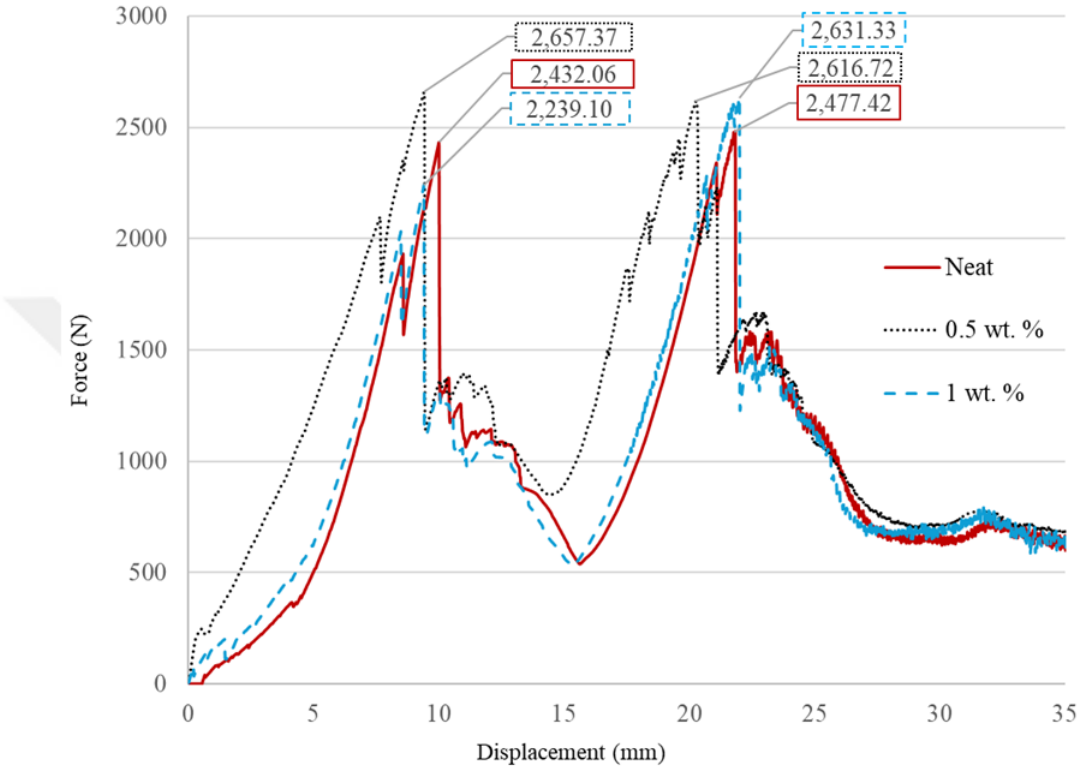

Figure 4.9 Force-displacement curves from QS-PS tests of honeycomb-core sandwich composites with Kevlar/epoxy face sheets containing neat, 0.5%, and 1% nano clay by weight, assessed at a displacement rate of 12.5 mm/min

Figure 4.9 displays the force-displacement results from the QS-PS tests conducted at 12.5 mm/min on aluminum honeycomb/Kevlar-epoxy sandwich composites with varying concentrations of nano clay: neat, 0.5 wt.%, and 1 wt.%. The force-displacement graph shows that the peak forces for the neat, 0.5 wt.%, and 1 wt.% nano clay composites are 2432.06 N, 2657.37 N, and 2239.10 N, respectively, for the first peak, and 2477.42 N, 2631.33 N, and 2616.72 N, respectively, for the second peak. The 0.5 wt.% composite exhibits the highest peak force, indicating that this concentration of nano clay optimally enhances the strength of the composite. However, similar to previous observations, the force drops sharply after reaching the peak,

especially in the 1 wt.% composite, suggesting a more brittle failure mode. The neat composite, while slightly lower in peak force, shows a relatively smoother decline in force, indicating better energy dissipation and less abrupt failure compared to the composites with nano clay.

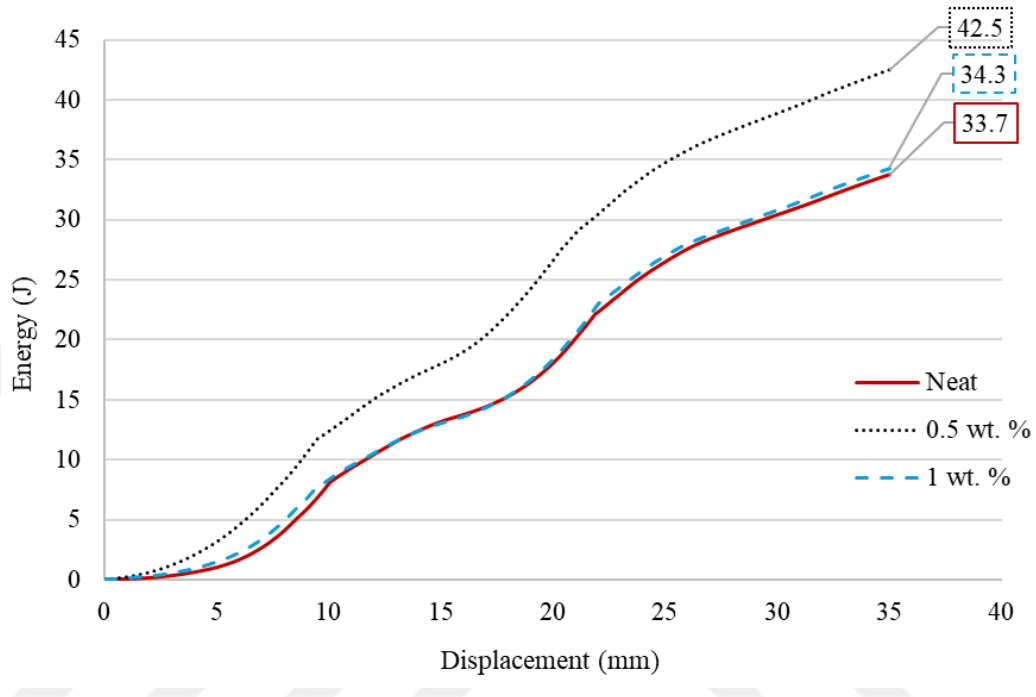

Figure 4.10 Energy-displacement curves from QS-PS tests of honeycomb-core sandwich composites with Kevlar/epoxy face sheets containing neat, 0.5%, and 1% nano clay by weight, assessed at a displacement rate of 12.5 mm/min

Figure 4.10 illustrates the energy-displacement results, where the energy absorbed by the neat, 0.5 wt.%, and 1 wt.% composites before failure are 33.7 J, 42.5 J, and 34.3 J, respectively. This graph reveals that the 0.5 wt.% composite absorbs significantly more energy than both the neat and 1 wt.% composites, indicating its superior ability to resist impact and absorb energy during deformation. The neat and 1 wt.% composites have similar energy absorption capacities, though the neat composite slightly underperforms compared to the 1 wt.% composite. This trend suggests that while nano clay can improve energy absorption, there is an optimal concentration (in this case, 0.5 wt.%) that maximizes the composite's performance. The results highlight the importance of balancing nano clay content to enhance both the strength and energy

absorption characteristics of aluminum honeycomb/Kevlar-epoxy sandwich composites.

4.3.2.5 QS-PS Testing of Kevlar/Epoxy Composites with Nano Clay at 25 mm/min

In this investigation, QS-PS tests were conducted on Kevlar composite specimens featuring epoxy matrices enhanced with nano clay at different concentrations: neat, 0.5%, and 1% by weight. These tests were performed on 2-ply Kevlar/epoxy composite plates at a testing speed of 25 mm/min. For each configuration, three samples were tested, and the results were averaged. The study further explored the damage mechanisms in the specimens, capturing both force-displacement and energy-displacement curves. Figures 4.11 and 4.12 present the force-displacement and energy-displacement curves, respectively, resulting from QS-PS tests conducted at 25 mm/min on Kevlar/epoxy composites with varying concentrations of nano clay: neat, 0.5 wt.%, and 1 wt.%.

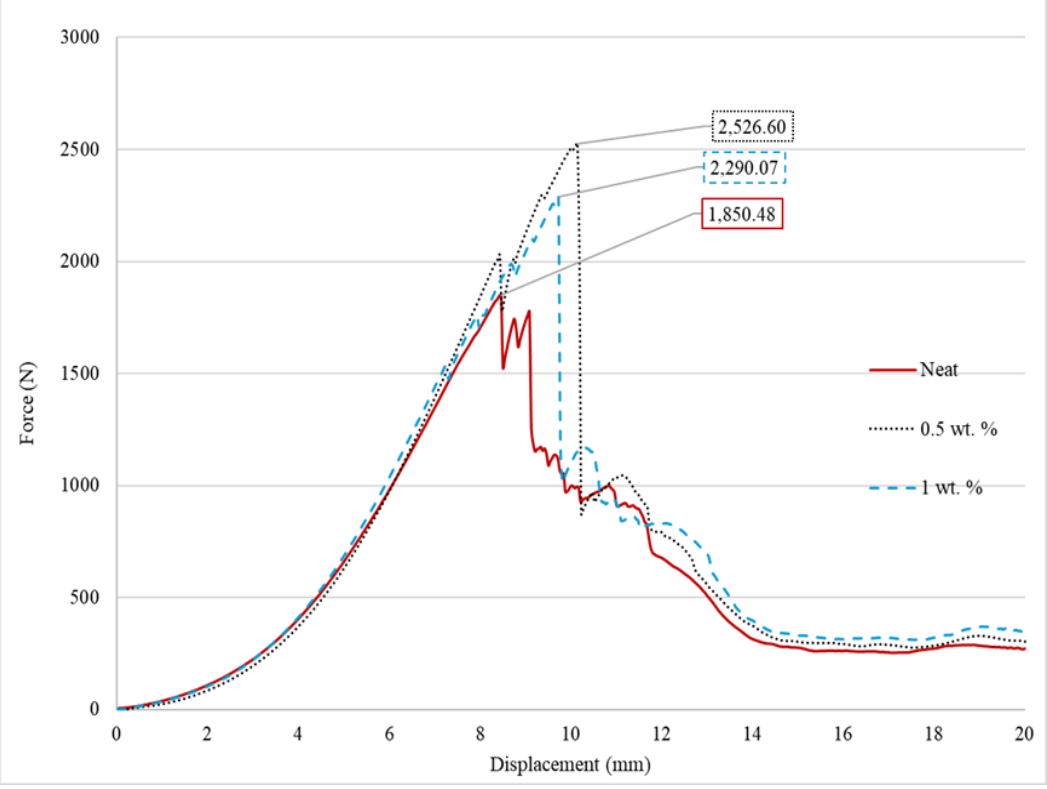

Figure 4.11 Force-displacement curves for Kevlar/epoxy composite plates containing neat, 0.5%, and 1% nano clay by weight, assessed at a displacement rate of 25 mm/min

In Figure 4.11, the force-displacement graph shows peak forces for the neat, 0.5 wt.%, and 1 wt.% nano clay composites at approximately 1850.48 N, 2526.60 N, and 2290.07 N, respectively. The 0.5 wt.% composite exhibits the highest peak force, indicating that this concentration optimally enhances the material's strength. The sharp decline in force after reaching the peak, especially noticeable in the 1 wt.% composite, suggests a brittle failure mode, where the material quickly loses its load-bearing capacity. In contrast, the neat composite, while having a lower peak force, demonstrates a smoother decline, indicating a more gradual failure process, which could be beneficial in applications where ductility is critical.

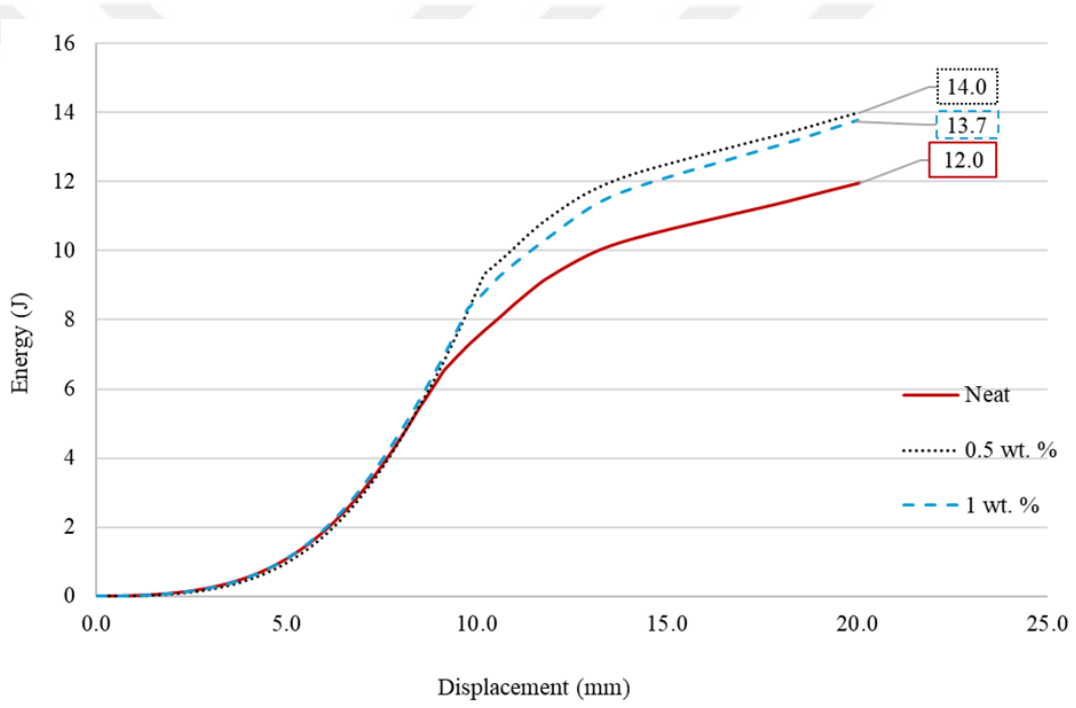

Figure 4.12 Energy-displacement curves for Kevlar/epoxy composite plates containing neat, 0.5%, and 1% nano clay by weight, assessed at a displacement rate of 25 mm/min

Figure 4.12 depicts the energy-displacement results, where the energy absorbed by the neat, 0.5 wt.%, and 1 wt.% composites before failure are around 12.0 J, 14.0 J, and 13.7 J, respectively. This graph highlights that the 0.5 wt.% composite absorbs the most energy, suggesting superior impact resistance and energy dissipation capabilities. The similar energy absorption between the neat and 1 wt.% composites, with the 1 wt.% slightly outperforming the neat composite, indicates that while nano clay

enhances energy absorption, the benefit may plateau or even decrease slightly beyond the optimal concentration. The results suggest that a balance of strength and energy absorption can be achieved with 0.5 wt.% nano clay, making it the most effective concentration for these specific test conditions at 25 mm/min.

4.3.2.6 QS-PS Testing of Aluminum Honeycomb/Kevlar-Epoxy Sandwich Composites with Nano Clay Additives at 25 mm/min

In this study, QS-PS tests were performed on aluminum honeycomb/Kevlar-epoxy sandwich composites, specifically engineered with the addition of nano clay additives. The tests were conducted at a testing speed of 25 mm/min to thoroughly evaluate the impact of these additives on the mechanical properties of the composites, including their strength, stiffness, and energy absorption capabilities. The objective was to understand how the incorporation of nano clay and the increased strain rate influence the overall performance and failure mechanisms of these advanced materials, providing insights that could inform their use in high-stress applications. Figures 4.13 and 4.14 present the force-displacement and energy-displacement curves, respectively, for aluminum honeycomb/Kevlar-epoxy sandwich composites with varying concentrations of nano clay (neat, 0.5 wt.%, and 1 wt.%) under QS-PS testing at 25 mm/min.

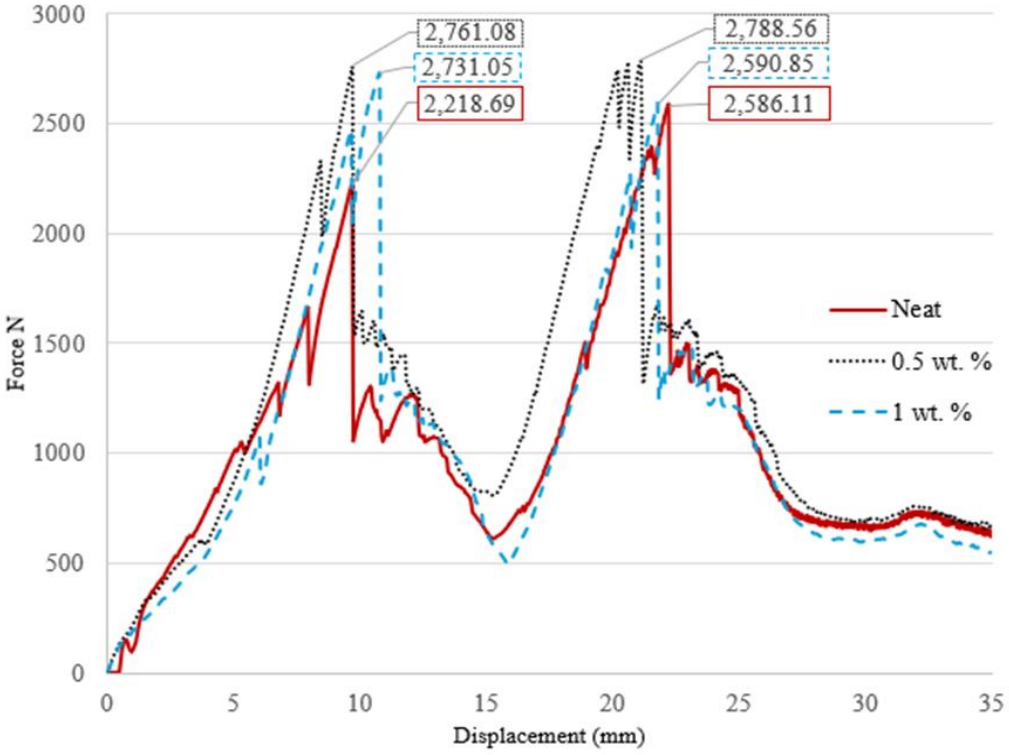

Figure 4.13 Force-displacement curves from QS-PS tests of honeycomb-core sandwich composites with Kevlar/epoxy face sheets containing neat, 0.5%, and 1% nano clay by weight, assessed at a displacement rate of 25 mm/min

In Figure 4.13, the force-displacement graph shows that the peak forces for the neat, 0.5 wt.%, and 1 wt.% nano clay composites are approximately 2218.69 N, 2761.08 N, and 2731.05 N for the first peak, and 2586.11 N, 2788.56 N, and 2590.85 N for the second peak, respectively. The 0.5 wt.% composite displays the highest peak forces in both instances, indicating that this concentration of nano clay optimally enhances the composite's strength under quasi-static conditions. However, after reaching the peak, a sharp decline in force is observed, particularly in the 1 wt.% composite, suggesting a more brittle failure mode. The neat composite, while exhibiting lower peak forces, shows a more gradual decline in force, which may indicate better ductility and a more controlled failure process under these testing conditions.

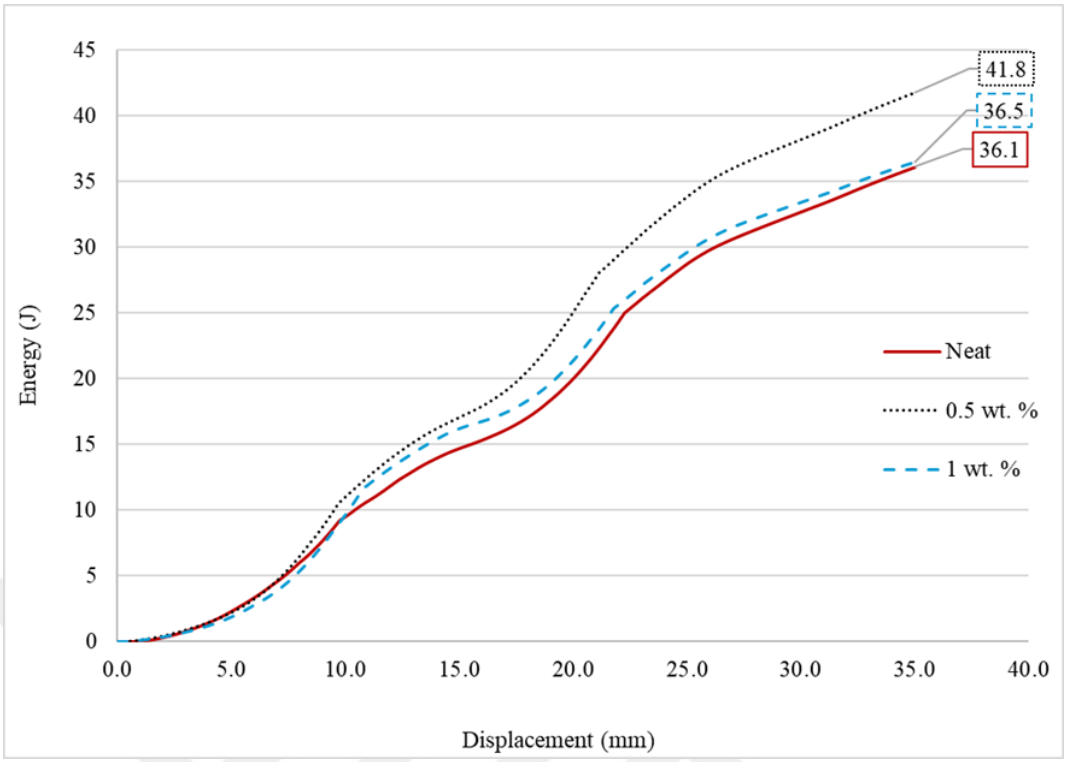

Figure 4.14 Energy-displacement curves from QS-PS tests of honeycomb-core sandwich composites with Kevlar/epoxy face sheets containing neat, 0.5%, and 1% nano clay by weight, assessed at a displacement rate of 25 mm/min

Figure 4.14 illustrates the energy-displacement results, where the energy absorbed by the neat, 0.5 wt.%, and 1 wt.% composites before failure are approximately 12.0 J, 14.0 J, and 13.7 J, respectively. The 0.5 wt.% composite absorbs the most energy, signifying its superior ability to resist impact and dissipate energy effectively during deformation in the quasi-static test. The energy absorption values between the 0.5 wt.% and 1 wt.% composites are close, with the 0.5 wt.% composite slightly outperforming, suggesting that while adding nano clay improves energy absorption, there is an optimal concentration for maximizing this benefit. These results underline the importance of selecting the appropriate nano clay concentration to balance strength, energy absorption, and ductility, especially under QS-PS testing conditions like the 25 mm/min rate used here.

4.3.3 Comparison of Peak Force and Energy Absorption in QS-PS Testing of Kevlar/Epoxy Composite plates with Nano Clay at 1.25, 12.5, and 25 mm/min

This study compares the peak force and energy absorption characteristics of Kevlar/epoxy composites reinforced with nano clay at varying concentrations, subjected to QS-PS testing at three different speeds: 1.25, 12.5, and 25 mm/min. Table 4.1 summarizes the maximum peak force and energy absorption values observed during QS-PS testing of Kevlar/epoxy composites with varying nano clay content at the three different testing speeds.

Table 4.1 Maximum peak force and energy absorption of Kevlar/epoxy composites with varying nano clay content at different QS-PS testing speeds.

Test Speed (mm/min)	Nano Clay Content	Max Peak Force (N)	Max Energy (J)
1.25	Neat	2119.73	12.10
	0.5 wt.%	2563.49	13.75
	1 wt.%	2199.55	12.90
12.5	Neat	2448.08	13.50
	0.5 wt.%	2224.57	13.00
	1 wt.%	2107.49	12.10
25	Neat	2526.60	12.00
	0.5 wt.%	2290.07	14.00
	1 wt.%	1850.48	13.70

The results of the QS-PS testing of Kevlar/epoxy composites with varying nano clay concentrations at three different speeds (1.25 mm/min, 12.5 mm/min, and 25 mm/min) reveal significant insights into the mechanical performance of these

materials. Across all test speeds, the 0.5 wt.% nano clay composite consistently outperforms the neat and 1 wt.% composites, particularly at the slowest speed of 1.25 mm/min, where it achieves the highest peak force (2563.49 N) and energy absorption (13.75 J). The neat composite and 1 wt.% composite perform similarly, but they fall short of the 0.5 wt.% version in terms of both strength and energy absorption. This suggests that the inclusion of 0.5 wt.% nano clay optimally reinforces the Kevlar/epoxy composite at slow loading rates, providing improved mechanical properties without introducing negative effects like brittleness.

As the test speed increases to 12.5 mm/min and 25 mm/min, the differences between the composites narrow. The neat composite shows improved performance at higher speeds, surpassing the 0.5 wt.% composite in peak force at 25 mm/min (2526.60 N vs. 2290.07 N), though the 0.5 wt.% nano clay composite still absorbs more energy at 25 mm/min (14.00 J). This indicates that, at faster loading rates, the neat composite's inherent material properties become more favorable for load-bearing, while the nano clay continues to enhance energy absorption. The 1 wt.% composite exhibits a consistent decrease in both peak force and energy absorption across all speeds, with the most significant decline observed at 25 mm/min (1850.48 N), reinforcing the conclusion that higher nano clay concentrations may introduce brittleness or other detrimental effects, especially under rapid loading conditions.

Overall, the results suggest that 0.5 wt.% nano clay is the optimal concentration for improving both strength and energy absorption in Kevlar/epoxy composites, particularly under slow to moderate loading. This concentration provides a balance of mechanical properties that is ideal for applications requiring both strength and impact resistance, such as protective gear or structural components. At higher speeds, however, the neat composite demonstrates a strong capacity for handling peak loads, making it preferable in applications where resistance to sudden, high-force impacts is critical. The 1 wt.% composite, while offering some advantages in energy absorption, tends to fail prematurely due to brittleness, highlighting the need for careful consideration of nano clay concentration in optimizing composite performance.

These findings emphasize the complex interplay between nano clay content, loading rate, and mechanical behavior in Kevlar/epoxy composites. While the addition

of nano clay can significantly enhance performance, particularly in energy absorption, there is a clear threshold beyond which the material's overall properties may be compromised. The 0.5 wt.% nano clay composite emerges as the most promising material configuration, offering a superior balance of load-bearing capacity and energy absorption at various speeds, making it suitable for a wide range of engineering applications. Further research could focus on optimizing nano clay dispersion techniques to enhance performance at higher concentrations or investigating alternative nanomaterials for improved results.

When contextualized with findings from similar studies, a deeper understanding of material behavior under varied conditions emerges. Djele and Karakuzu (2021) observed that carbon-Kevlar hybrid composites responded significantly to speed variations, exhibiting increased damage characteristics at higher speeds without the use of nano particles like nano clay, suggesting a foundational difference in how composite types respond to speed. Bhudolia et al. (2020) and Yuhazri et al. (2016) further emphasize this dynamic, noting improvements in performance with increased speeds in their respective studies on different composite materials, contrasting with the diminishing returns observed with increased nano clay concentrations at higher speeds in this study.

Djele and Karakuzu (2021) explored the mechanical behavior of carbon-Kevlar hybrid composites under a range of testing speeds, from 1 mm/min up to 60 mm/min. Their study revealed that at higher speeds, these composites exhibited increased damage characteristics, suggesting a sensitivity to speed variations that could influence material performance and durability. The results highlighted the importance of considering the rate of testing when evaluating composite materials, as faster speeds tend to exacerbate damage mechanisms, potentially affecting the structural integrity and longevity of the composites.

Bhudolia et al. (2020) conducted their experiments on core-shell particle reinforced composites, utilizing test speeds of 1 mm/min, 5 mm/min, and 10 mm/min. Their findings indicated that increasing the feed rate improved the static indentation performance, with a notable increase in peak load and a reduction in major load drops. This behavior suggests that core-shell particle reinforcements can effectively enhance

composite performance at moderate speeds, providing better load-bearing capabilities and reduced susceptibility to sudden load failures.

Yuhazri et al. (2016) focused on glass fiber reinforced polyester composites, testing them at speeds ranging from 10 mm/min to 50 mm/min. Their research found that higher loading speeds increased the force required to penetrate the composites, enhancing their impact effectiveness. This indicates that the mechanical properties of glass fiber composites can be significantly influenced by the speed of testing, with faster speeds improving their resistance to penetration and likely enhancing their overall structural performance.

The insights gained from the aforementioned studies provide a rich context for analyzing the results of the current research on Kevlar/epoxy composites with nano clay at speeds of 1.25, 12.5, and 25 mm/min. Unlike the materials tested in the other studies, the Kevlar/epoxy composites with nano clay showed an optimal performance at a nano clay concentration of 0.5 wt.% at the slowest speed tested (1.25 mm/min), with diminishing returns at higher speeds. This contrast suggests that while nano clay can enhance performance at lower speeds, its effectiveness decreases as speed increases, which is not observed with the carbon-Kevlar hybrids or core-shell reinforced composites.

4.3.4 Comparison of Peak Force and Energy Absorption in QS-PS Testing of Aluminum Honeycomb/Kevlar-Epoxy Sandwich Composites with Nano Clay Additives at 1.25, 12.5, and 25 mm/min

This research evaluates the peak force and energy absorption performance of aluminum honeycomb/Kevlar-epoxy sandwich composites with varying nano clay additives, tested under QS-PS conditions at three distinct speeds: 1.25, 12.5, and 25 mm/min. Table 4.2 provides a detailed summary of the maximum peak force and energy absorption values observed during QS-PS testing of aluminum honeycomb/Kevlar-epoxy sandwich composites with different nano clay contents at varying speeds.

Table 4.2 Summary of Maximum Peak Force and Energy Absorption for Aluminum Honeycomb/Kevlar-Epoxy Sandwich Composites with Nano Clay Additives at Different QS-PS Testing Speeds.

Test Speed (mm/min)	Nano Clay Content	Max Peak Force (N)	Max Energy (J)
1.25	Neat	2543.90	33.98
	0.5 wt.%	2337.73	32.77
	1 wt.%	2216.15	31.14
12.5	Neat	2657.37	42.50
	0.5 wt.%	2432.06	34.30
	1 wt.%	2239.10	33.70
25	Neat	2761.08	41.80
	0.5 wt.%	2731.05	36.50
	1 wt.%	2586.11	36.10

The QS-PS testing of aluminum honeycomb/Kevlar-epoxy sandwich composites with varying nano clay additives at different speeds—1.25 mm/min, 12.5 mm/min, and 25 mm/min—provides important insights into the mechanical performance of these composites. As summarized in Table 4.2, the neat aluminum honeycomb/Kevlar-epoxy composite consistently demonstrates the highest peak forces and energy absorption values across all testing speeds. At the highest speed of 25 mm/min, the neat composite achieves the maximum peak force of 2761.08 N and remains superior in energy absorption at 12.5 mm/min, recording the highest value of 42.50 J. These results indicate that, under QS-PS conditions, the neat composite offers the best overall performance, especially in terms of withstanding higher loads and dissipating more energy.

In comparison, the composites with nano clay additives show slightly lower peak forces and energy absorption values across all testing speeds. The 0.5 wt.% nano clay composite performs marginally better than the 1 wt.% version, but neither outperforms the neat composite. For instance, at 25 mm/min, the 0.5 wt.% composite records a peak force of 2731.05 N, which is close to the neat composite but still lower, and the energy

absorption is also lower at 36.50 J. Similarly, the 1 wt.% composite lags behind both in peak force (2586.11 N) and energy absorption (36.10 J), suggesting that the addition of nano clay, particularly at higher concentrations, may not provide the desired enhancement in mechanical performance under these testing conditions.

Overall, the results suggest that while the introduction of nano clay does not significantly boost the peak force or energy absorption of aluminum honeycomb/Kevlar-epoxy sandwich composites, the neat composite performs best across all test speeds. This could be attributed to the already optimized combination of the Kevlar-epoxy face sheets and aluminum honeycomb core, which may offer limited room for further improvement through nano clay reinforcement. Moreover, the slight reduction in mechanical performance observed with nano clay additives, particularly at 1 wt.%, could be due to issues such as poor dispersion or increased brittleness, which can undermine the intended reinforcement effect.

In conclusion, while nano clay additives have shown promise in other composite configurations, their contribution to the performance of aluminum honeycomb/Kevlar-epoxy sandwich composites under QS-PS conditions appears limited. The neat composite consistently exhibits superior peak force and energy absorption, making it the most reliable configuration for applications requiring high load-bearing capacity and energy dissipation. These findings highlight the need for careful consideration of nano clay concentration and its interaction with both the composite matrix and core structure to ensure optimal performance. Further studies could explore alternative nanomaterials or improved dispersion techniques to achieve better mechanical outcomes.

The research conducted by Bhudolia et al. (2020), Yuhazri et al. (2016), and Djele and Karakuzu (2021) offers distinct perspectives on the impact of testing speeds on the mechanical behavior of composites, each using varied speed rates and yielding different outcomes that provide a context for comparing the results of this thesis.

Bhudolia et al. (2020) utilized varying feed rates of 1 mm/min, 5 mm/min, and 10 mm/min in their QS-PS tests on core-shell particle reinforced composites. They observed that higher feed rates led to improved static indentation performance,

characterized by a significant increase in peak load and reduced intensity of major load drops. This finding suggests that faster speeds enhance the material's ability to withstand deformation, aligning with the general observation in this thesis that speed influences mechanical performance.

Yuhazri et al. (2016) explored the effects of testing speeds of 10, 20, 30, 40, and 50 mm/min on glass fiber reinforced polyester composite laminates under quasi-static loading. Their results indicated that as the loading speed increased, the force required to penetrate the composites also increased, thus enhancing the impact effectiveness. This supports the findings in this thesis that higher speeds tend to increase peak forces, although the nano clay composites in this study did not consistently exhibit enhanced performance across different speeds.

4.4 Scanning Electron Microscopy (SEM) Analysis of Damage in Kevlar/Epoxy Composites with Nanoclay Reinforcement

The mechanical behavior of Kevlar/epoxy composites is significantly influenced by the interfacial bonding between the Kevlar fibers and the epoxy matrix, which directly affects their energy absorption capacity and failure mechanisms. To enhance these properties, nanoclay has been incorporated as a reinforcement additive in different concentrations, aiming to achieve an optimal balance between strength, stiffness, and toughness. In this section, Scanning Electron Microscopy (SEM) was used to examine the fracture surfaces of neat and nanoclay-reinforced Kevlar/epoxy composites following quasi-static punch shear testing. The SEM analysis provides valuable insights into the changes in failure modes, fiber-matrix interactions, and the overall mechanical response of these composites, highlighting the role of nanoclay in enhancing their properties. Figures 4.15: Figure 4.15 presents SEM images showing the fracture surfaces of Kevlar/epoxy composites after quasi-static punch shear tests, illustrating the effect of nanoclay on failure mechanisms. The images are taken at a magnification of 2000x, with a scale of 5 micrometers.

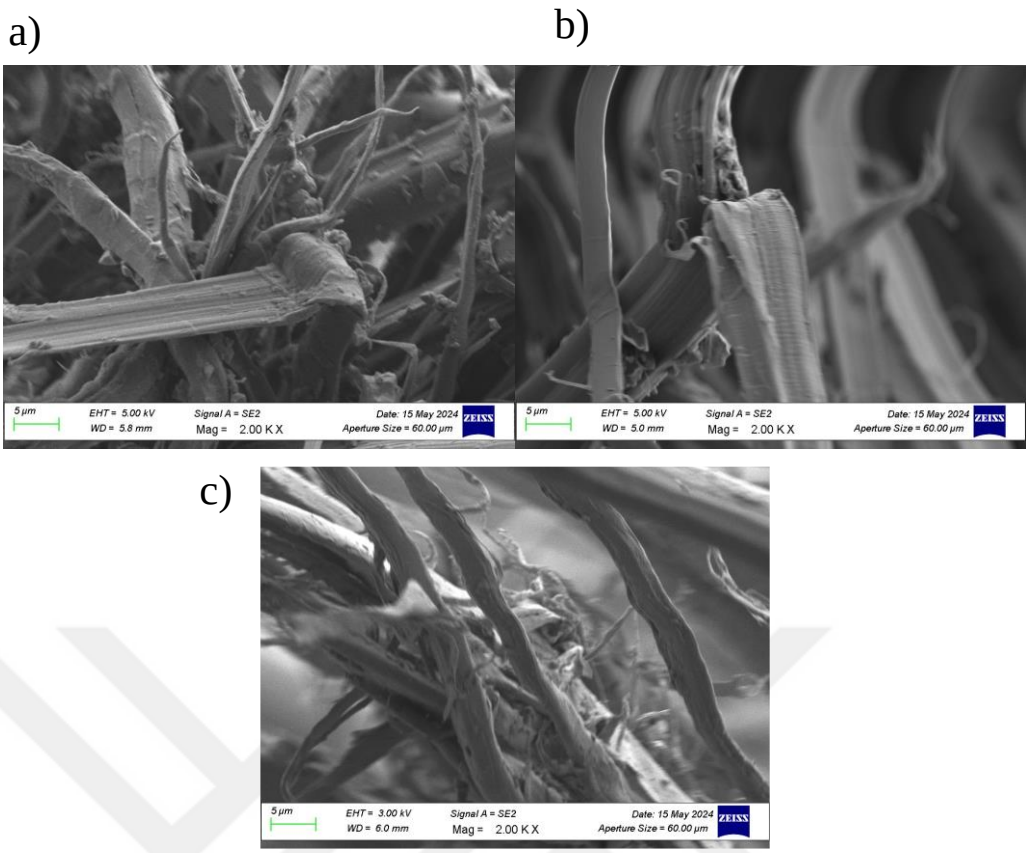

Figure 4.15 SEM images showing the fracture surfaces of Kevlar/epoxy composites after quasi-static punch shear tests: (a) Neat Kevlar/epoxy composite, (b) 0.5 wt.% nanoclay reinforced Kevlar/epoxy, and (c) 1 wt.% nanoclay reinforced Kevlar/epoxy.

The SEM images of the neat Kevlar/epoxy composite (Figure 4.15a) show significant fiber pull-out, with clean fiber surfaces, indicating weak interfacial bonding between the fibers and the matrix. This weak bonding suggests limited load transfer efficiency from the matrix to the fibers, which results in failure primarily through fiber-matrix separation. The prevalence of fiber pull-out implies that the composite's energy absorption under quasi-static punch shear loading relies on debonding rather than cohesive fracturing, resulting in suboptimal mechanical performance.

With 0.5 wt.% nanoclay reinforcement (Figure 4.15b), the fiber-matrix interface appears to have improved considerably, as evidenced by reduced fiber pull-out and increased adhesion between the matrix and fibers. The enhanced interfacial bonding due to nanoclay reinforcement leads to a more cohesive failure mechanism, characterized by a combination of fiber breakage and some degree of matrix deformation. This improvement indicates that the composite with 0.5 wt.% nanoclay achieves a better balance between stiffness and toughness, allowing it to carry higher

loads while still maintaining energy dissipation capabilities through controlled deformation.

In the composite with 1 wt.% nanoclay (Figure 4.15c), the fracture surfaces show minimal fiber pull-out and predominantly fiber breakage, suggesting a stronger but more brittle failure mechanism. The enhanced interfacial bonding resulting from the higher nanoclay concentration improves load transfer; however, it also increases matrix stiffness, leading to an abrupt fracture and a reduction in ductility. While this enhancement in matrix rigidity increases the peak load capacity, it reduces the composite's ability to absorb energy through plastic deformation, making it more prone to sudden failure under applied stress. These observations suggest that, while 1 wt.% nanoclay maximizes strength, 0.5 wt.% nanoclay provides a more optimal balance between strength and energy absorption, making it preferable for applications requiring both mechanical robustness and energy dissipation.

CHAPTER FIVE
RESULTS OF NUMERICAL STUDIES

5.1 Numerical Results of QS-PS Test for CFRP Composites

In this study, numerical simulations were conducted to complement the experimental analysis of the mechanical behavior of 4-layer carbon fiber-reinforced polymer (CFRP) woven composite plates under quasi-static penetration. Utilizing finite element (FE) methods in LS-DYNA, the CFRP composites were modeled under the same loading conditions as those applied in the experimental tests, with boundary conditions carefully matched to ensure consistency. The simulations aimed to replicate the force-displacement response and to predict the damage progression within the composite plates during penetration. The FE models successfully captured the key features of the experimental results, including the peak force and subsequent decline associated with material failure. Additionally, the numerical simulations provided detailed insights into the damage mechanisms, such as delamination and fiber breakage, which were validated against the experimental observations. Figure 5.1 presents the damage model generated from the FE simulation, illustrating the distribution and extent of damage within the CFRP composite plate, thereby offering a comprehensive understanding of its mechanical performance under quasi-static loading conditions.

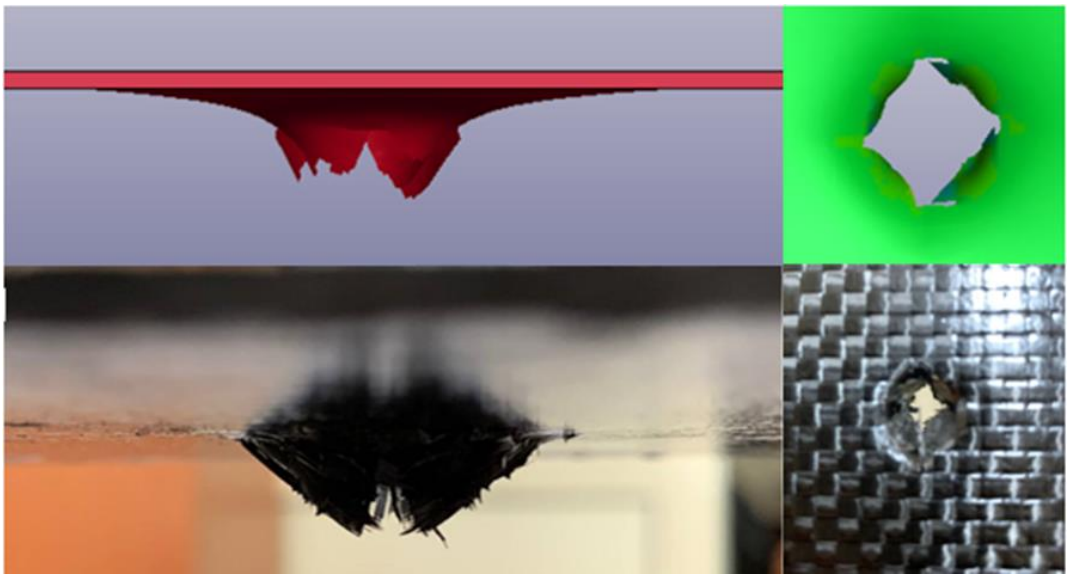

Figure 5.1 Comparison of Damage Models for CFRP Composites from QS-PS Tests: Experimental vs. Simulation

The comparison between the numerical simulations and experimental studies of CFRP composite plates under quasi-static penetration reveals a strong correlation in the observed failure modes. The finite element analysis (FEA) accurately predicts the key damage mechanisms, including delamination, matrix cracking, and fiber breakage, as depicted in the numerical results. These simulated outcomes, shown in the top sections of the image, correspond closely to the experimental findings captured in the bottom images, which display the physical deformation and rupture of the composite material. The conical delamination and localized fiber rupture around the penetration site are consistent across both approaches, indicating the FEA model's effectiveness in replicating the complex interactions within the composite under quasi-static loading. This alignment between numerical and experimental results validates the FEA methodology as a reliable tool for predicting the mechanical behavior and failure patterns of CFRP composites, thereby supporting its application in the design and optimization of advanced composite structures. In addition, Figure 5.2 presents a comparative analysis of the force-displacement response of a 4-layer carbon fiber-reinforced polymer (CFRP) woven composite plate under QS-PS, derived from both experimental testing and finite element (FE) simulation using LS-DYNA.

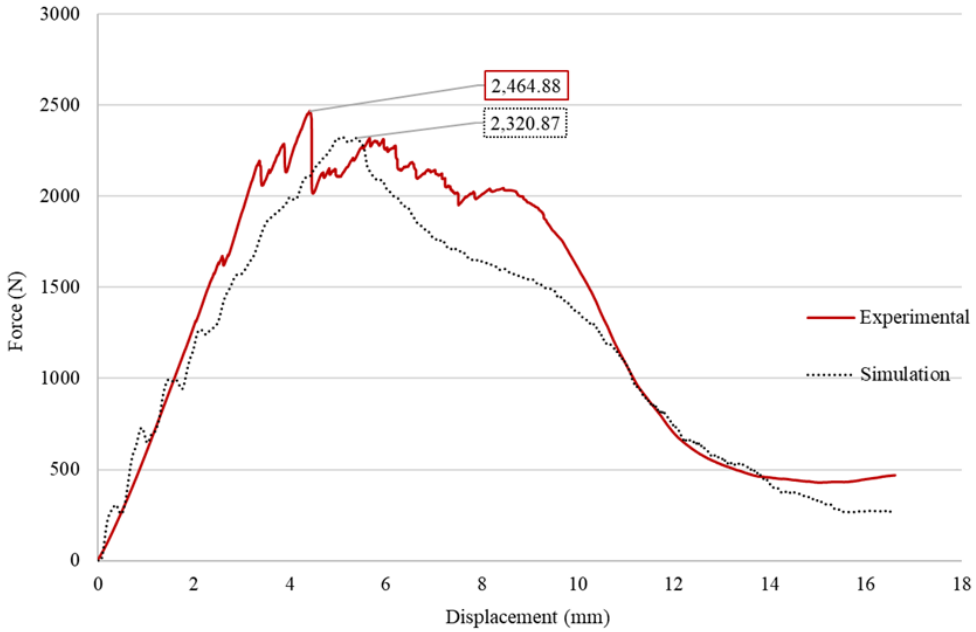

Figure 5.2 Force-displacement comparison of a 4-layer CFRP composite under quasi-static indentation from experimental and FE simulation results.

The experimental curve reveals a more complex and fluctuating force response, particularly after the peak force of approximately 2465 N, indicating the initiation and progression of damage mechanisms within the composite, such as fiber breakage and matrix cracking. In contrast, the simulation captures the overall trend but predicts a slightly lower peak force of around 2320 N, with a smoother post-peak decline. This discrepancy suggests that the FE model may be oversimplifying or not fully capturing the intricate damage processes observed in the experimental data.

These differences underscore the challenges inherent in accurately modeling the behavior of CFRP composites under quasi-static loading conditions. The experimental results, which reflect real-world imperfections and material variability, produce a more irregular force-displacement curve, whereas the simulation, constrained by idealized conditions, lacks this complexity. This indicates that further refinement of the FE model is necessary to achieve closer alignment with experimental observations. As this study serves as a preliminary investigation for more complex sandwich composites, the findings in Figure 5.2 highlight the critical importance of correlating simulation models with experimental data to improve the accuracy of future predictive analyses.

5.1.1 QS-PS Simulation of CFRP Composites at Different Speed Rates (1.25 mm/min, 12.5 mm/min, and 25 mm/min)

This section presents the results of the quasi-static (QS-PS) simulation analysis of CFRP composite plate subjected to different displacement rates. Initially, experimental testing was conducted at a loading rate of 1.25 mm/min to evaluate the mechanical response of the composite. Subsequently, numerical simulations were performed to replicate the experimental conditions, which allowed for validation of the numerical model's accuracy. Upon confirmation of the model’s trueness, additional simulations were conducted at increased loading rates of 12.5 mm/min and 25 mm/min. The comparative analysis of the simulation results at these three loading rates provides valuable insights into the effect of strain rate on the mechanical behavior of CFRP composites. Figure 5.3 illustrates the force-displacement curves obtained from the

numerical simulations, capturing the influence of varying loading rates on the mechanical response of the CFRP composite plates.

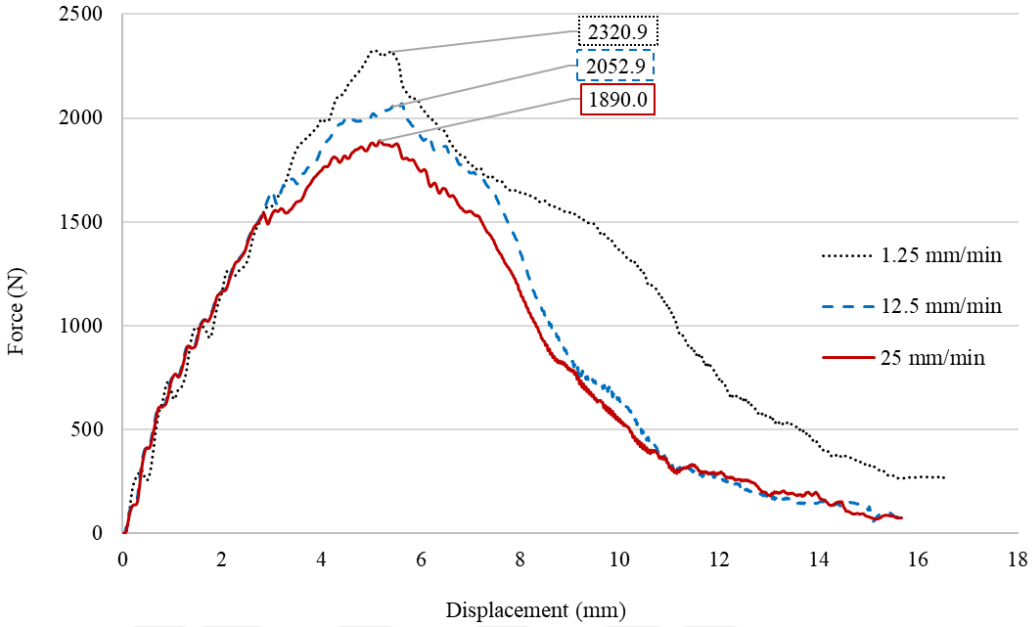

Figure 5.3 Force-Displacement Curves of CFRP Composite Plate at Different Loading Rates (1.25 mm/min, 12.5 mm/min, and 25 mm/min)

The results indicate that the mechanical response of CFRP composite plates is significantly affected by the loading rate. At a lower loading rate of 1.25 mm/min, the composite achieves the highest peak force (2320.9 N), displaying superior load-bearing capacity and a more ductile-like, gradual failure, which suggests effective energy absorption. As the loading rates increase to 12.5 mm/min and 25 mm/min, the peak force reduces to 2052.9 N and 1890.0 N, respectively, demonstrating rate sensitivity and a decline in structural performance. Higher rates result in a more abrupt post-peak drop, indicating a transition to brittle failure. These findings emphasize that increased loading rates lead to reduced strength and less gradual energy dissipation, highlighting the necessity of accounting for strain rate effects in the design of CFRP composites, especially for applications involving rapid loading conditions.

5.2 Numerical Results of QS-PS Test for Honeycomb/CFRP Sandwich Composites

The numerical results derived from the QS-PS tests on honeycomb/CFRP sandwich composites are critical for advancing our understanding of the mechanical behavior and failure mechanisms of these complex materials under applied loading conditions. By simulating the interaction between the aluminum honeycomb core and the CFRP face sheets, these numerical analyses provide detailed insights that complement experimental findings, enabling a more comprehensive evaluation of the structural performance. This dual approach, combining both numerical and experimental methods, is essential for accurately predicting how these composites will behave under real-world conditions, which is crucial for their application in industries such as aerospace, automotive, and civil engineering where material performance and reliability are of utmost importance. Figure 5.4 presents a comparison of the force-displacement response of honeycomb/CFRP sandwich composites under QS-PS testing, as derived from both experimental data and finite element (FE) simulations.

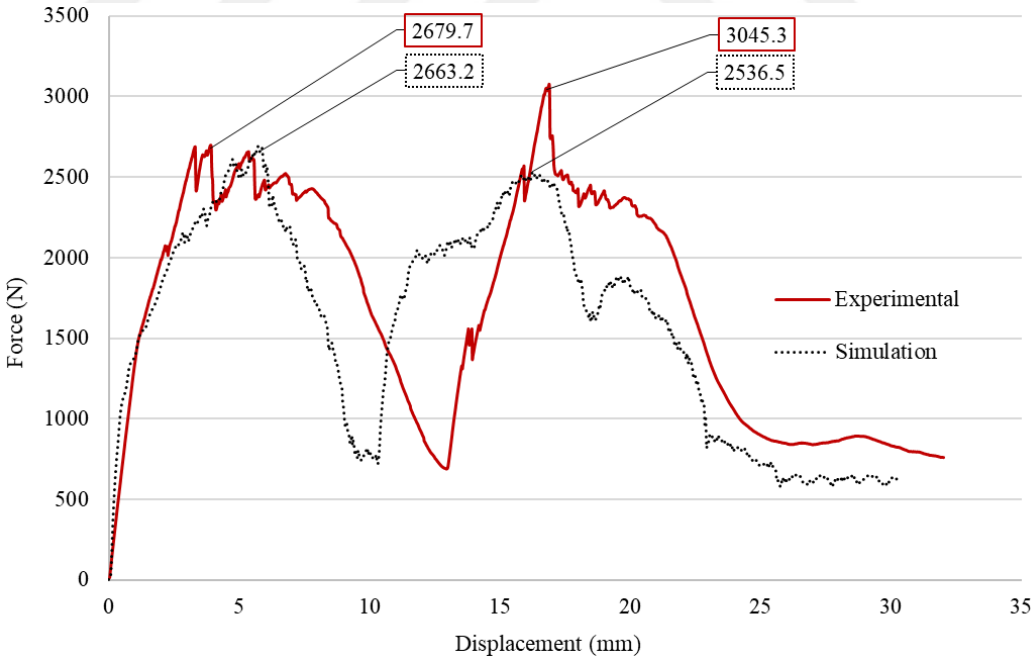

Figure 5.4 Force-displacement comparison of honeycomb/CFRP sandwich composites from experimental and FE simulation results.

The experimental curve, illustrated in red, shows distinct peaks at approximately 2,654 N and 3,068 N, which correspond to critical points of load-bearing capacity and the initiation of damage. The simulation curve, represented by the dotted line, closely mirrors the experimental trend but generally underestimates the peak forces, with predictions of 3,040 N and 2,520 N at the respective peaks. This discrepancy suggests that the FE model may not fully encapsulate the complexities of the physical behavior, particularly regarding the interaction between the honeycomb core and the CFRP face sheets during loading.

The observed differences between the experimental and simulation results underscore the challenges associated with accurately modeling the behavior of composite structures with complex architectures, such as honeycomb cores. The simulation's smoother force-displacement curve, in contrast to the more fluctuating experimental data, suggests that the numerical model may not fully account for real-world imperfections, material heterogeneity, and localized damage processes. Despite these differences, the FE simulation effectively captures the overall trend and key characteristics of the composite's response, providing valuable insights that can inform the design and optimization of honeycomb/CFRP sandwich structures under similar loading conditions.

5.2.1 QS-PS Simulation of AlHC/CFRP Sandwich Composites Structures at Different Speed Rates (1.25 mm/min, 12.5 mm/min, and 25 mm/min)

In this section, QS-PS simulations of Aluminum Honeycomb Core (AlHC) and CFRP sandwich composite structures is investigated at different loading speeds. The numerical model, validated through an initial experimental comparison at a 1.25 mm/min loading speed, served as the foundation for further simulations at elevated rates of 12.5 mm/min and 25 mm/min. The comparative analysis of Figure 5.5 demonstrates the Force-Displacement relationships for the composite structures tested at these different loading rates.

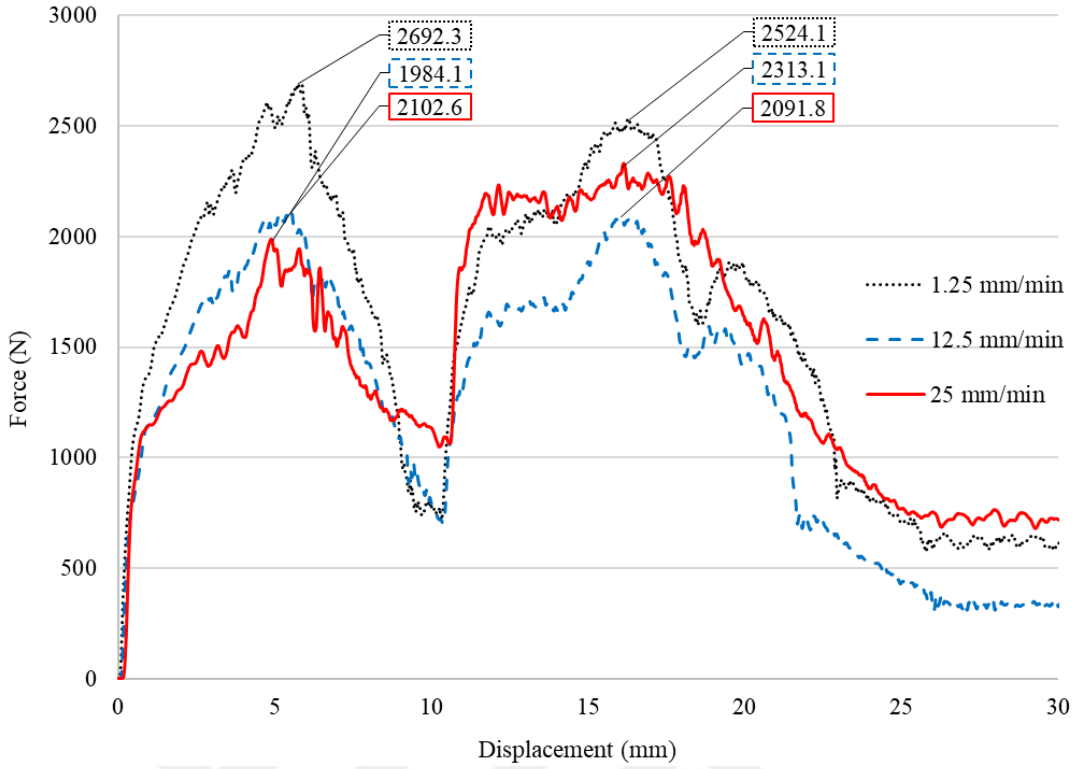

Figure 5.5 Force-displacement curves of AlHC/CFRP sandwich composite structures at different loading rates (1.25 mm/min, 12.5 mm/min, and 25 mm/min)

The results indicate a distinct trend in peak force, with the maximum force observed at 1.25 mm/min (2692.3 N) being notably higher compared to those recorded at 12.5 mm/min (1984.1 N) and 25 mm/min (2102.6 N). This suggests that the composite's load-bearing capacity decreases with increased loading speed, potentially highlighting a reduction in structural stiffness and increased susceptibility to failure mechanisms under higher strain rates. The post-peak behavior shows a more gradual decline in force for the 1.25 mm/min rate, while for 12.5 mm/min and 25 mm/min rates, the force drop is significantly steeper. Overall, the analysis underscores the rate-dependent nature of AlHC/CFRP sandwich structures, emphasizing the importance of accounting for loading speed in design considerations to accurately predict the composite's performance under different operational conditions.

5.3 QS-PS Simulation of Kevlar/Epoxy Composites with Nano Clay and Al Honeycomb Core Sandwich Structures at Different Speed Rates

The QS-PS simulations of Kevlar/epoxy composites reinforced with nano clay and integrated into aluminum honeycomb core sandwich structures were conducted to evaluate their mechanical performance at various speed rates. Using LS-DYNA software, the simulations aimed to replicate real-world loading conditions by applying different displacement rates to assess the influence of loading speed on the structural response. The Kevlar/epoxy composites, modified with varying concentrations of nano clay, were modeled alongside the aluminum honeycomb core to understand the synergistic effects of these materials under quasi-static loading.

In this study, QS-PS tests were conducted on Kevlar composite specimens with epoxy matrices enhanced with nano clay at concentrations of neat, 0.5%, and 1% by weight. QS-PS tests were performed on 2-ply Kevlar/epoxy composite plates at a testing speed of 1.25 mm/min. Three samples were tested for each configuration, and the results were averaged. The analysis included an assessment of the damage modes of the specimens and the capture of force-displacement and energy-displacement curves.

Initially, numerical simulations of QS-PS were conducted exclusively at a speed of 1.25 mm/min. In the subsequent phase, both experimental and numerical analyses were carried out at additional speeds (12.5 and 25 mm/min) to evaluate the material behavior under different loading rates. Finite element (FE) analysis was conducted on Kevlar fiber-reinforced composite plates as a preliminary step towards simulating sandwich composites with aluminum honeycomb cores and Kevlar/epoxy face sheets, which form the primary focus of this research. Subsequently, finite element models of the experimental specimens were analyzed under identical loading conditions using LS-DYNA software. The accuracy of the finite element results was significantly influenced by the mesh size. To ensure the validity of the numerical simulations, a comprehensive validation approach, beginning with a mesh sensitivity analysis, was employed. Table 5.1 presents the results of this analysis for neat Kevlar/epoxy, highlighting the impact of varying mesh sizes on maximum force, displacement, and computational cost.

Table 5.1 Results of mesh sensitivity analysis for Kevlar/epoxy neat

Mesh Size (mm)	Maximum Force (N)	Displacement (mm)	Computational Cost (min)
5	5130.10	16.20	4
2.5	3910.49	11.48	14
1.25	1673.65	8.26	51
1	2422.18	9.33	150
0.5	2254.38	9.88	204
0.25	2350.43	8.76	506

The mesh sensitivity analysis for neat Kevlar/epoxy composite plates, as detailed in Table 1, demonstrates the influence of mesh size on the maximum force, displacement, and computational cost. The results reveal that as the mesh size decreases from 5 mm to 0.25 mm, the maximum force and displacement values exhibit significant variation. Specifically, the maximum force decreases markedly from 5130.10 N at a 5 mm mesh size to a minimum of 1673.65 N at a 1.25 mm mesh size, before stabilizing at finer mesh sizes. Displacement similarly decreases from 16.20 mm at 5 mm to a minimum of 8.26 mm at 1.25 mm, indicating a converging trend towards more accurate results as the mesh is refined.

The computational cost, measured in minutes, increases substantially with decreasing mesh size. The computational time escalates from a minimal 4 minutes at a 5 mm mesh size to a maximum of 506 minutes at a 0.25 mm mesh size, reflecting the higher computational demand required for finer mesh resolutions.

These findings underscore the trade-off between accuracy and computational efficiency in finite element analysis. While finer mesh sizes (e.g., 0.5 mm and 0.25 mm) provide more precise results, they incur significantly higher computational costs. Conversely, coarser mesh sizes (e.g., 5 mm and 2.5 mm) offer reduced computational time but at the expense of lower accuracy. An optimal balance is observed around a 1 mm mesh size, where the computational cost is moderately high, yet the maximum force and displacement values begin to converge, suggesting adequate accuracy

without excessively high computational demands. This balance is critical for practical applications where both accuracy and computational efficiency are essential.

5.3.1 QS-PS Simulation of Kevlar/Epoxy Composite Plates with Nano Clay at 1.25 mm/min

The QS-PS simulation of Kevlar/epoxy composites reinforced with nano clay at a displacement rate of 1.25 mm/min was performed to explore the effects of nano clay on the mechanical performance of the composites under controlled loading conditions. The aim of this simulation was to mirror the experimental setup using finite element methods, assessing how the addition of nano clay impacts the material's resistance to shear forces, energy absorption, and damage propagation.

In this study, the force-displacement and energy-displacement graphs generated from both experimental and numerical studies were compared to assess the accuracy of the simulations. By analyzing these curves, the alignment between the simulated results and the experimental data was evaluated, providing insights into the reliability of the finite element model in capturing the key mechanical behaviors of the material. The degree of correlation between the experimental and simulated graphs served as a critical metric for validating the trueness of the simulations, ensuring that the numerical model accurately reflects the physical responses of the Kevlar/epoxy composites under the specified loading conditions. Figure 5.6 and Figure 5.7 illustrate the force-displacement and energy-displacement graphs, respectively, generated from both experimental and numerical studies. These figures provide a visual comparison to evaluate the alignment between the simulated results and the experimental data, offering a clear understanding of the accuracy and reliability of the finite element model in replicating the mechanical behavior of the material under quasi-static loading conditions.

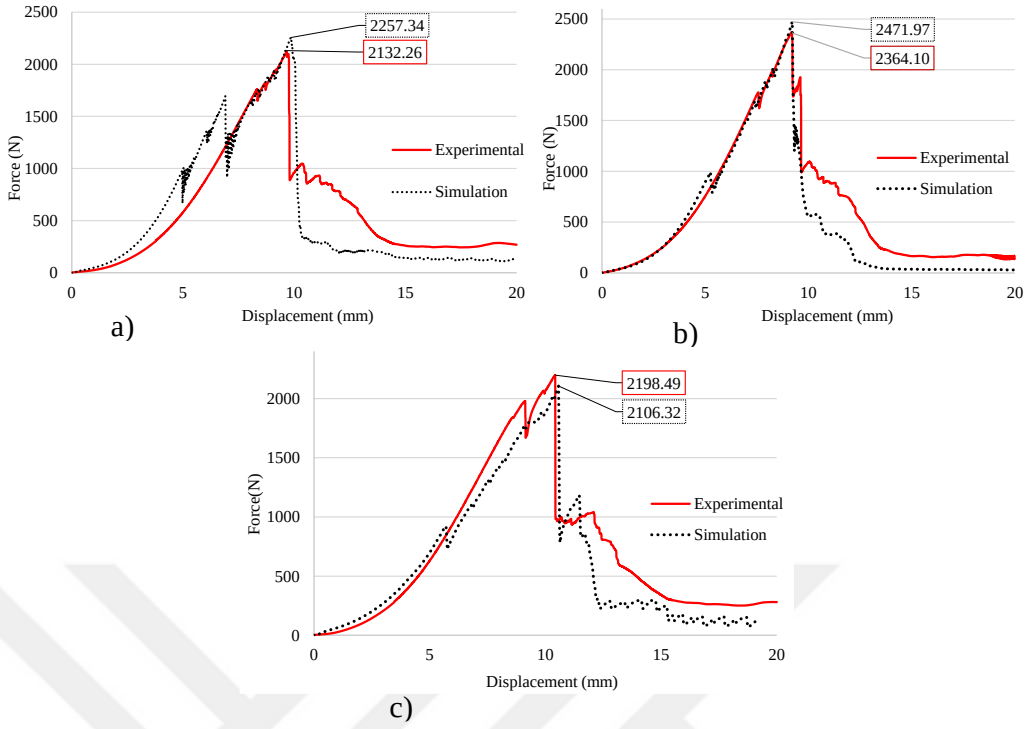

Figure 5.6 Comparing the force-displacement graphs between numerical simulation and experimental findings from QS-PS results for Kevlar/epoxy composites, specifically for a) neat, b) 0.5%, and c) 1% nano clay by weight at 1.25 mm/min.

Figure 5.6 presents the force-displacement comparisons between experimental and numerical results for Kevlar/epoxy composites in three different configurations: a) neat, b) with 0.5 wt. % nano clay, and c) with 1 wt. % nano clay. Across all three configurations, the experimental curves consistently exhibit higher peak forces compared to the numerical simulations, indicating a greater load-bearing capacity observed in physical testing. In the neat Kevlar/epoxy (Figure 5.6a), the peak force is measured at approximately 2254.38 N experimentally, while the simulation predicts a slightly lower peak at 2113.14 N. Similarly, for the 0.5 wt. % nano clay composite (Figure 5.6b), the experimental peak force reaches 2471.97 N, compared to 2364.10 N in the simulation. In the 1 wt. % nano clay composite (Figure 5.6c), the experimental peak is 2199.32 N, while the simulation underestimates it at 2106.32 N. These discrepancies between the experimental and simulated results suggest that the finite element model may not fully capture the complex mechanical interactions and damage mechanisms within the Kevlar/epoxy composites, particularly as influenced by the addition of nano clay. Despite this, the general trend and behavior of the force-

displacement curves are well-replicated, demonstrating the model's utility in predicting the composite's overall mechanical response, albeit with some limitations in accurately estimating peak loads.

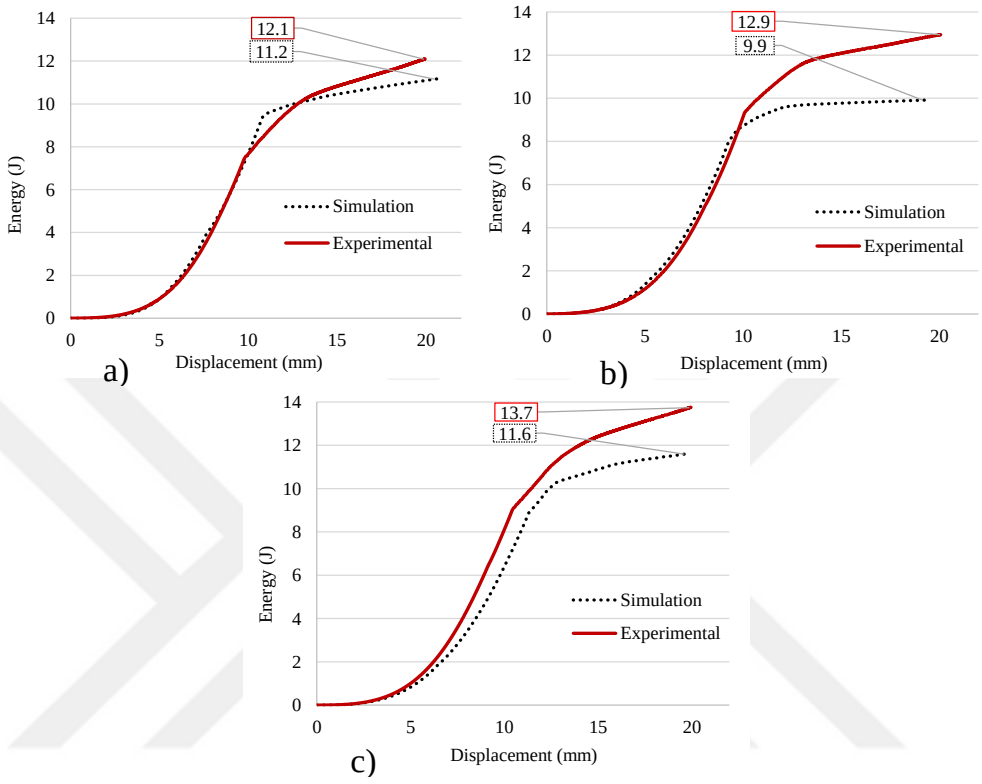

Figure 5.7 Comparing the energy-displacement graphs between numerical simulation and experimental findings from QS-PS results for Kevlar/epoxy composites, specifically for a) neat, b) 0.5%, and c) 1% nano clay by weight at 1.25 mm/min.

Figure 5.7 displays the energy-displacement curves that compare experimental and numerical results for Kevlar/epoxy composites in three different configurations: a) neat, b) with 0.5 wt. % nano clay, and c) with 1 wt. % nano clay. Across all configurations, higher energy absorption compared to the numerical simulations is consistently demonstrated by the experimental curves, especially at higher displacements. For the neat Kevlar/epoxy composite (Figure 5.7a), an energy absorption of 12.09 J is reached in the experimental curve, while it is estimated at 11.19 J in the simulation. In the 0.5 wt. % nano clay composite (Figure 5.7b), the experimental energy absorption increases to 12.93 J, compared to 9.91 J in the simulation. The 1 wt. % nano clay composite (Figure 5.7c) shows the highest experimental energy absorption at 13.74 J, with the simulation estimating a lower

value of 11.60 J. These discrepancies between experimental and simulated energy absorption suggest that the finite element model may not fully capture the enhanced energy dissipation mechanisms introduced by the addition of nano clay. Despite these differences, the general trend of increasing energy absorption with higher nano clay content is consistent across both experimental and numerical results, indicating that the simulations, while underestimating the absolute values, still effectively reflect the overall behavior of the composites. This consistency underscores the utility of the numerical model in predicting trends, though it may require refinement to more accurately predict specific energy absorption levels.

5.3.1.1 Damage Models through Experimental and Numerical QS-PS Tests at 1.25 mm/min

Another essential component of validating the numerical study involves the comparison of damage models for specimens subjected to QS-PS loads at a test speed of 1.25 mm/min, as observed in both experimental and numerical investigations. Figure 5.8 illustrates the damage models obtained from QS-PS tests, comparing the results from both experimental testing and simulation studies of the 2-ply Kevlar fiber-epoxy composite plate.

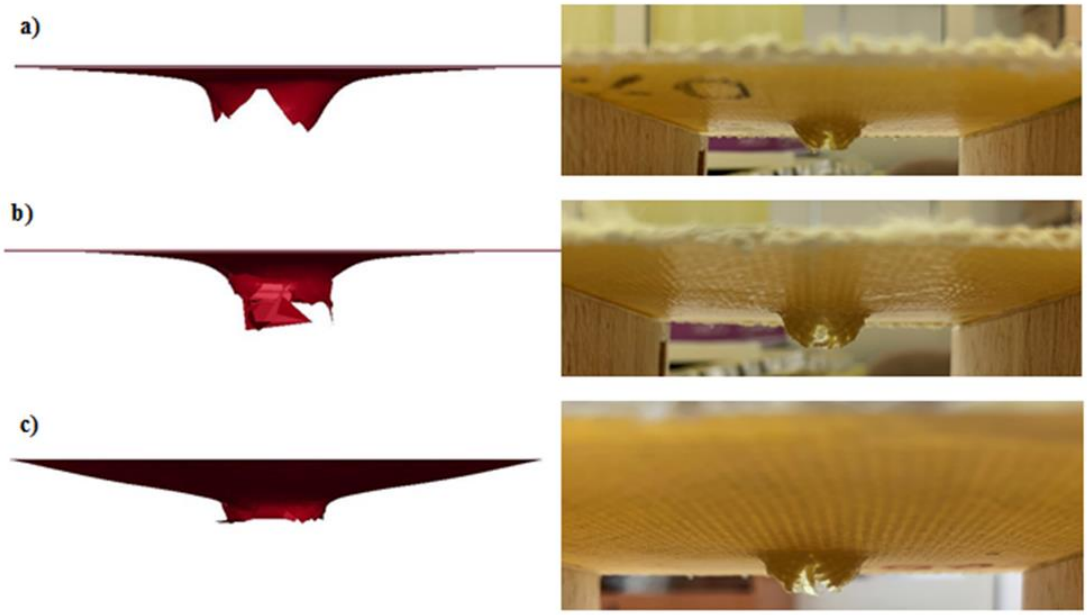

Figure 5.8 Comparison of Damage Models for Kevlar/Epoxy Composites (Neat, 0.5 wt.% Nano Clay, and 1 wt.% Nano Clay) from QS-PS Tests: Experimental vs. Simulation at 1.25 mm/min

Figure 5.8 provides a comparative analysis of the damage models for Kevlar/epoxy composites with varying nano clay content—neat, 0.5 wt.%, and 1 wt.%—as derived from QS-PS tests, including both experimental and simulation data. For the neat Kevlar/epoxy composite (Figure 5.8a), the damage model shows a central indentation with moderate delamination around the impact site. Both the experimental and simulated results indicate a similar damage pattern, with the simulation effectively capturing the extent and nature of the delamination observed experimentally, demonstrating the simulation's accuracy in replicating the material's response to shear loading without any nano clay reinforcement. For the composite containing 0.5 wt.% nano clay (Figure 5.8.b), the damage is more pronounced than in the neat composite, with experimental results exhibiting deeper indentation and increased delamination, while the simulation shows comparable features, including the onset of material fragmentation. This suggests that the addition of 0.5 wt.% nano clay introduces a degree of brittleness to the composite, altering its failure mechanisms under shear loading.

The close agreement between experimental and simulation data confirms the reliability of the finite element model in predicting the composite's behavior. The 1 wt.% nano clay composite (Figure 5.8c) shows the most severe damage among the three configurations, with both experimental and simulation results highlighting significant indentation, extensive delamination, and noticeable fiber breakage and matrix cracking. The simulation accurately mirrors the experimental damage, illustrating a higher degree of fragmentation and brittleness due to the increased nano clay content. This indicates that while the addition of 1 wt.% nano clay enhances the composite's stiffness, it also leads to a more brittle failure mode under QS-PS loading. In conclusion, the finite element simulations align well with the experimental observations across all three configurations, validating the numerical models' accuracy. The introduction of nano clay at different weight percentages distinctly impacts the damage characteristics of the Kevlar/epoxy composites, with higher nano clay content resulting in increased brittleness and more pronounced damage under shear loading conditions.

5.3.2 QS-PS Simulation of Kevlar/Epoxy Composites with Nano Clay and Al Honeycomb Core Sandwich Structures at 1.25 mm/min

The QS-PS simulation of Kevlar/epoxy composites reinforced with nano clay and integrated into aluminum honeycomb core sandwich structures at a displacement rate of 1.25 mm/min was performed to evaluate the mechanical performance and failure behavior of these advanced composites under quasi-static loading conditions. This simulation aimed to replicate the experimental setup and provided insights into how the combination of nano clay reinforcement and aluminum honeycomb cores influences the structural integrity, energy absorption, and load-bearing capacity of the sandwich composites. Figure 5.9 and Figure 5.10 illustrate the force-displacement and energy-displacement graphs, respectively, generated from both experimental and numerical studies, highlighting the comparison between the observed and simulated mechanical responses.

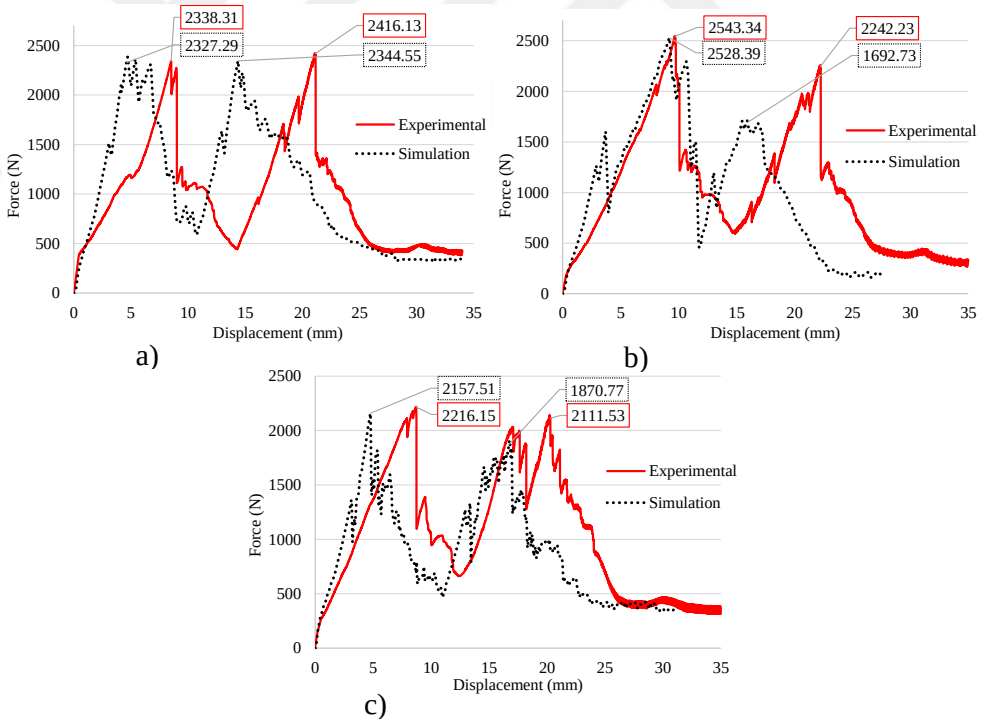

Figure 5.9 Comparing the force-displacement graphs between numerical simulation and experimental findings from QS-PS results for Kevlar/epoxy composites with AlHC sandwich structures, specifically for a) neat, b) 0.5%, and c) 1% nano clay by weight

Figure 5.9 compares the force-displacement responses between experimental and numerical results for sandwich composites composed of Kevlar/epoxy with nano clay and aluminum honeycomb cores under QS-PS testing. The three subfigures (a, b, and c) correspond to different configurations or loading conditions, with the experimental curves depicted in red and the simulation results shown as dotted lines. In each case, the experimental data consistently exhibit higher peak forces and more complex fluctuation patterns compared to the simulations, which tend to smooth out the force response and underestimate the peak forces. Specifically, in subfigure (a), the experimental peak force is 2308.38 N, slightly lower than the simulation's 2340.62 N, indicating a close but not perfect alignment. Subfigure (b) shows a better match, with the experimental peak at 2528.39 N and the simulation at 2540.46 N. However, subfigure (c) reveals a more significant discrepancy, where the experimental peak force is 2157.51 N compared to the simulation's 2204.82 N. These differences suggest that while the finite element model captures the overall trend and general behavior of the composites, it may not fully account for the detailed, localized damage mechanisms and material heterogeneity that contribute to the more intricate force responses observed in the experimental tests. Consequently, further refinement of the numerical model may be required to improve its accuracy in predicting the complex mechanical behavior of these advanced sandwich structures under varying loading conditions.

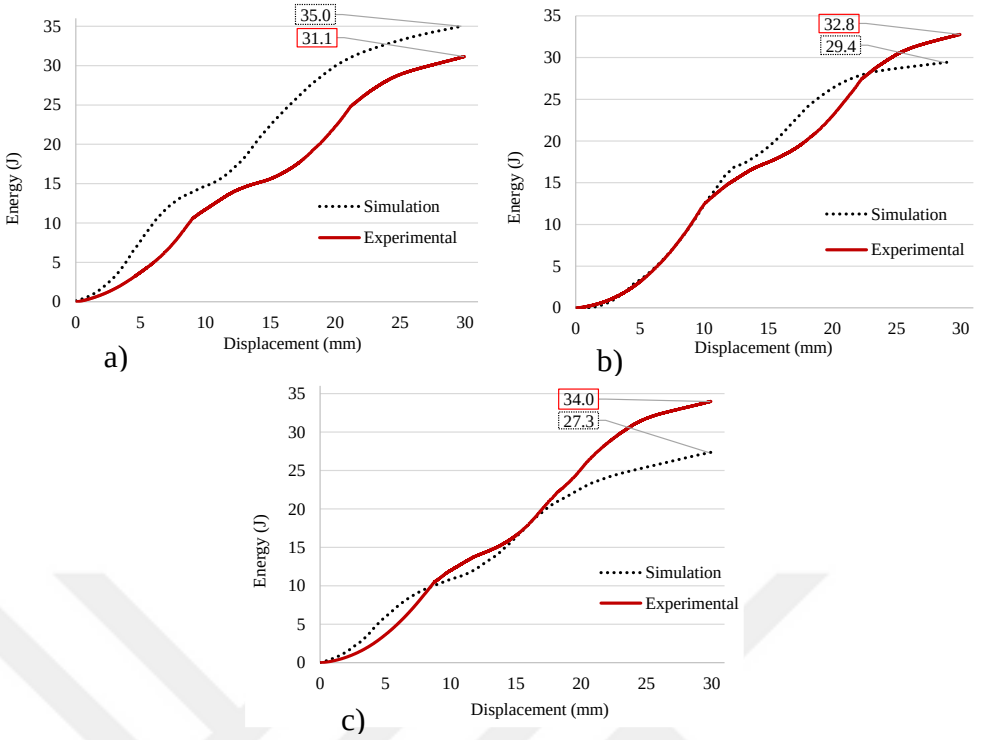

Figure 5.10 Comparing the energy-displacement graphs between numerical simulation and experimental findings from QS-PS results for Kevlar/epoxy composites with AlHC sandwich structures, specifically for a) neat, b) 0.5%, and c) 1% nano clay by weight

Figure 5.10 illustrates the energy-displacement curves for Kevlar/epoxy composites with aluminum honeycomb (AlHC) sandwich structures, comparing the experimental and numerical results for three configurations: a) neat, b) 0.5 wt. % nano clay, and c) 1 wt. % nano clay. Across all configurations, the numerical simulations consistently predict higher energy absorption than what is observed experimentally, particularly at higher displacement levels. In subfigure (a), the simulation estimates an energy absorption of 35.06 J, while the experimental value reaches 31.12 J. Similarly, in subfigure (b), the simulation predicts 32.77 J, compared to the experimental value of 29.35 J. The discrepancy is most pronounced in subfigure (c), where the simulation estimates 33.99 J, significantly higher than the experimental 27.30 J. These differences suggest that the finite element model may overestimate the energy absorption capabilities of the composite structures, potentially due to the simplifications or assumptions in the simulation that do not fully capture the complex interactions within the composite and the honeycomb core. Despite these discrepancies, the overall trend observed in both experimental and simulated results aligns, showing that the addition

of nano clay generally enhances energy absorption, although the extent of this enhancement is more conservatively estimated in the experimental data.

5.3.2.1 Damage Models of Kevlar/Epoxy Composites with AlHC Sandwich Structures through Experimental and Numerical QS-PS Tests at 1.25 mm/min

The damage models of Kevlar/epoxy composites integrated with aluminum honeycomb (AlHC) sandwich structures were evaluated through both experimental and numerical QS-PS tests conducted at a displacement rate of 1.25 mm/min. These evaluations aimed to capture and compare the failure mechanisms that occur within the composite layers and the aluminum honeycomb core under applied loading conditions. Figure 5.11 presents a comparison of the damage models for HC-core sandwich composites with Kevlar/epoxy, including configurations of a) neat, b) 0.5 wt. % nano clay, and c) 1 wt. % nano clay, as observed in both experimental and simulation results from QS-PS tests.

Figure 5.11 Comparative damage models of HC-core sandwich composites with Kevlar/epoxy in configurations: a) neat, b) 0.5%, and c) 1% nano clay by weight, derived from QS-PS tests through experimental and simulation results at 1.25 mm/min

The figure is organized into three sections, each representing a distinct composite configuration, with the left-side images illustrating the numerical simulations and the right-side images displaying the corresponding experimental damage. The numerical

simulations effectively capture key damage mechanisms, including core crushing, delamination of the Kevlar/epoxy layers, and localized failure within the aluminum honeycomb core. These simulated damage patterns closely align with the experimental results, particularly in areas of significant deformation and failure, demonstrating a strong correlation between the simulated and observed behaviors. For instance, in subfigure (a) (neat Kevlar/epoxy), the simulation reveals extensive core crushing and delamination, which are also clearly observed in the experimental image, where the honeycomb core has collapsed. Subfigures (b) and (c) (with 0.5 wt. % and 1 wt. % nano clay, respectively) illustrate the progressive damage as the nano clay content increases, with the simulations accurately predicting the extent and distribution of failure mechanisms observed experimentally. This close correspondence between the simulated and experimental results underscores the effectiveness of the numerical model in accurately replicating the complex interactions and damage behaviors within HC-core sandwich composites with Kevlar/epoxy under quasi-static loading conditions.

5.3.3 QS-PS Simulation of Kevlar/Epoxy Composites with Nano Clay at 12.5 mm/min

The QS-PS simulation of Kevlar/epoxy composites reinforced with nano clay was conducted at a displacement rate of 12.5 mm/min to evaluate the material's mechanical response under quasi-static loading conditions. This study aimed to replicate experimental conditions through finite element analysis, providing insights into how the addition of nano clay influences the composite's load-bearing capacity and energy absorption. Figure 5.12 and Figure 5.13 present the force-displacement and energy-displacement graphs, respectively, comparing the experimental observations with the numerical simulations, thereby highlighting the similarities and differences in the mechanical responses of the composite under the specified loading rate.

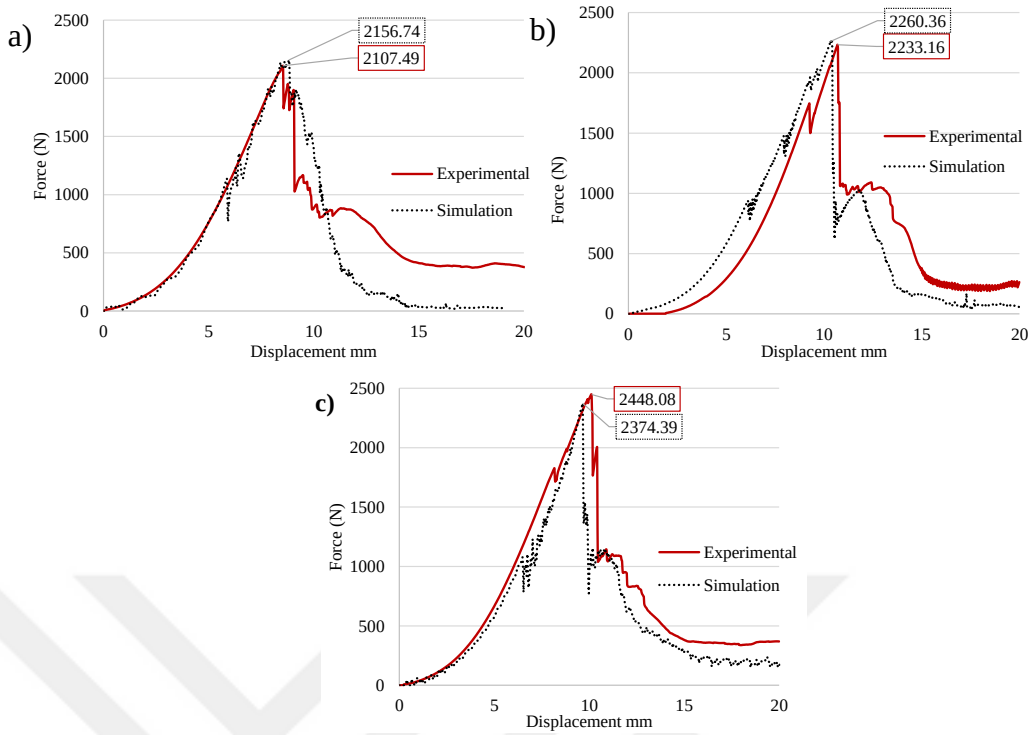

Figure 5.12 Comparing the force-displacement graphs between numerical simulation and experimental findings from QS-PS results for Kevlar/epoxy composites, specifically for a) neat, b) 0.5%, and c) 1% nano clay by weight at 12.5 mm/min.

Figure 5.12 showcases the force-displacement curves that compare the experimental and numerical QS-PS results for Kevlar/epoxy composites at a displacement rate of 1.25 mm/min, specifically for configurations of neat, 0.5 wt. % nano clay, and 1 wt. % nano clay. A strong alignment between the experimental data and the numerical simulations is consistently demonstrated by the results, confirming the accuracy and reliability of the finite element model in predicting the mechanical behavior of these composites.

In the neat Kevlar/epoxy configuration (Figure 5.12a), the experimental peak force is 2,156.74 N, with the simulation closely predicting a peak force of 2,107.49 N. For the 0.5 wt. % nano clay composite (Figure 5.12b), the experimental curve reaches a peak force of 2,260.36 N, while the simulation predicts a nearly matching peak of 2,233.16 N. In the 1 wt. % nano clay composite (Figure 5.12c), the experimental peak force is 2,448.08 N, with the simulation also providing a very close prediction at 2,374.39 N.

The close agreement between the experimental and numerical curves across all three configurations highlights the model's effectiveness in capturing the force-displacement behavior of Kevlar/epoxy composites with varying nano clay content. These results underscore the capability of the numerical simulations to accurately reflect the load-bearing characteristics and overall mechanical response of the composites under quasi-static loading conditions, reinforcing their utility for predictive analysis and design optimization of advanced composite materials.

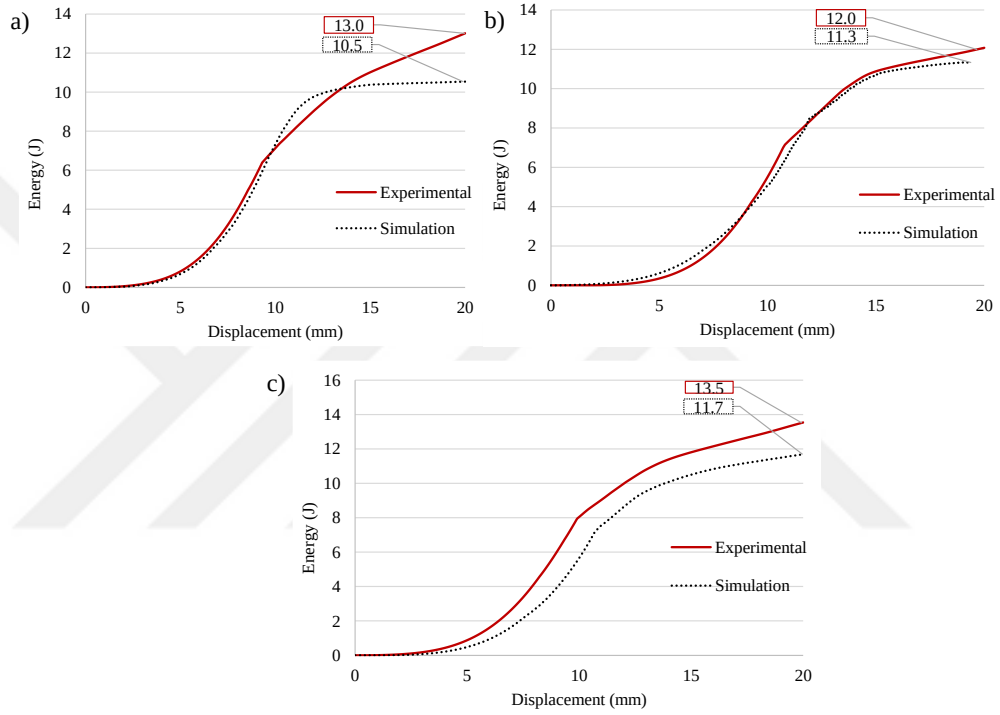

Figure 5.13 Comparing the energy-displacement graphs between numerical simulation and experimental findings from QS-PS results for Kevlar/epoxy composites, specifically for a) neat, b) 0.5%, and c) 1% nano clay by weight at 12.5 mm/min.

Figure 5.13 presents a comparison of the energy-displacement curves between experimental and numerical QS-PS results for Kevlar/epoxy composites at a displacement rate of 12.5 mm/min, specifically for a) neat, b) 0.5 wt. % nano clay, and c) 1 wt. % nano clay configurations. The results demonstrate a strong correlation between the experimental and numerical data across all three configurations, highlighting the effectiveness of the numerical model in capturing the energy absorption characteristics of the composites.

In the neat Kevlar/epoxy configuration (Figure 5.13a), the experimental and simulation curves closely align, with the experimental peak energy absorption at 13.01 J and the simulation predicting 10.53 J. Similarly, for the 0.5 wt. % nano clay composite (Figure 5.13b), both curves show a close match, with the experimental energy absorption reaching 11.99 J and the simulation at 11.32 J. The 1 wt. % nano clay composite (Figure 5.13c) also exhibits a strong agreement between the experimental and simulated results, with peak energy absorption values of 13.52 J and 11.62 J, respectively.

Overall, the numerical simulations effectively replicate the experimental trends, demonstrating the model's capability to accurately predict the energy absorption behavior of Kevlar/epoxy composites with varying nano clay content under quasi-static loading conditions. The consistency between the experimental and simulated results across different configurations reinforces the reliability of the numerical approach for evaluating the performance of these advanced composite materials.

5.3.3.1 Damage Models through Experimental and Numerical QS-PS Tests at 12.5 mm/min

The damage models of Kevlar/epoxy composites, including neat, 0.5 wt.% nano clay, and 1 wt.% nano clay configurations, were evaluated through both experimental and numerical QS-PS tests conducted at a displacement rate of 12.5 mm/min. Figure 11 presents a comparison of the damage models for Kevlar/epoxy composites (neat, 0.5 wt.% nano clay, and 1 wt.% nano clay) obtained from QS-PS tests, highlighting both experimental observations and numerical simulations at a displacement rate of 12.5 mm/min.

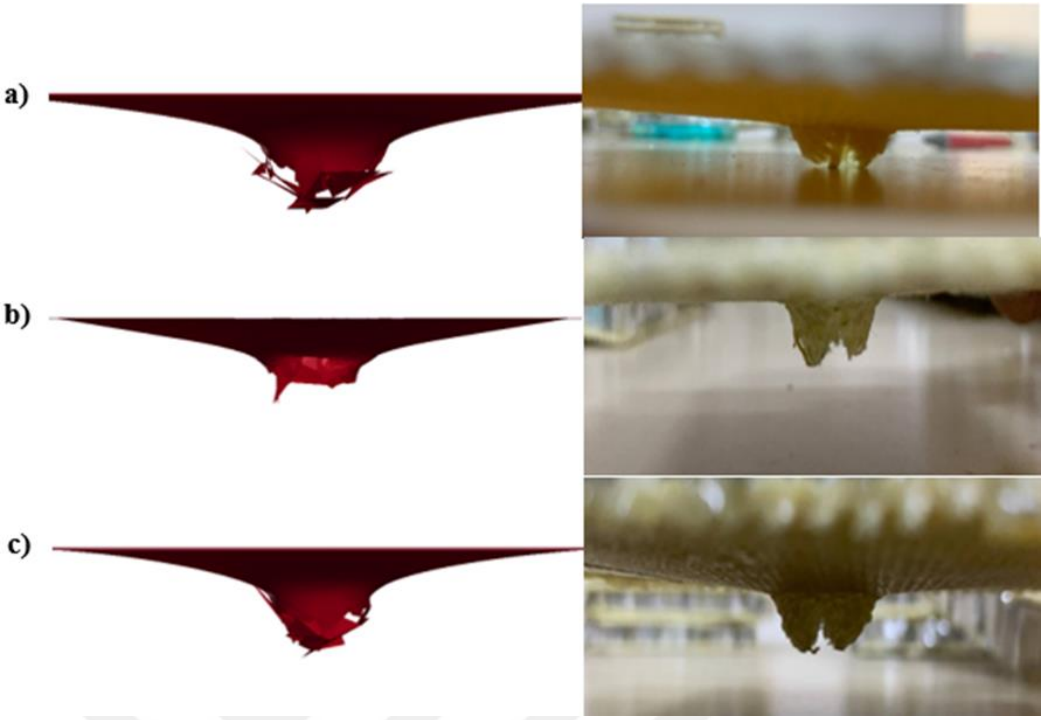

Figure 5.14 Comparison of Damage Models for Kevlar/Epoxy Composites for a) neat, b) 0.5%, and c) 1% nano clay by weight from QS-PS Tests: Experimental vs. Simulation at 12.5 mm/min

The figure is divided into three sections (a, b, and c), each representing one of the composite configurations. On the left side, the numerical simulations capture key damage mechanisms such as core crushing, delamination, and material failure, while the right side shows corresponding experimental images of the damaged specimens. In the neat Kevlar/epoxy composite (Figure 5.14a), the simulation accurately predicts extensive delamination and localized crushing, which are clearly observed in the experimental image. The 0.5 wt.% nano clay composite (Figure 5.14b) exhibits a similar damage pattern, with both the simulation and experimental results showing more uniform deformation and reduced delamination compared to the neat composite. For the 1 wt.% nano clay composite (Figure 5.14c), the simulation and experimental results align closely, indicating enhanced structural integrity with minimal delamination and controlled material failure, suggesting that the higher nano clay content contributes to improved damage resistance.

Overall, the close correlation between the simulated and experimental damage models in Figure 5.14 demonstrates the effectiveness of the numerical model in

capturing the complex damage behaviors of Kevlar/epoxy composites under quasi-static loading, particularly as the nano clay content increases.

5.3.4 QS-PS Simulation of Kevlar/Epoxy Composites with Nano Clay and Al Honeycomb Core Sandwich Structures at 12.5 mm/min

The QS-PS simulation of Kevlar/epoxy composites with nano clay and aluminum honeycomb core sandwich structures at a displacement rate of 12.5 mm/min was conducted to evaluate the mechanical behavior and damage mechanisms of these advanced composites under loading conditions. The study focused on understanding the influence of nano clay reinforcement and the honeycomb core on the structural integrity and energy absorption of the sandwich composites. Figure 5.15 and Figure 5.16 present the force-displacement and energy-displacement curves, respectively, comparing the experimental and numerical results to assess the accuracy of the simulation model in predicting the mechanical responses of these materials.

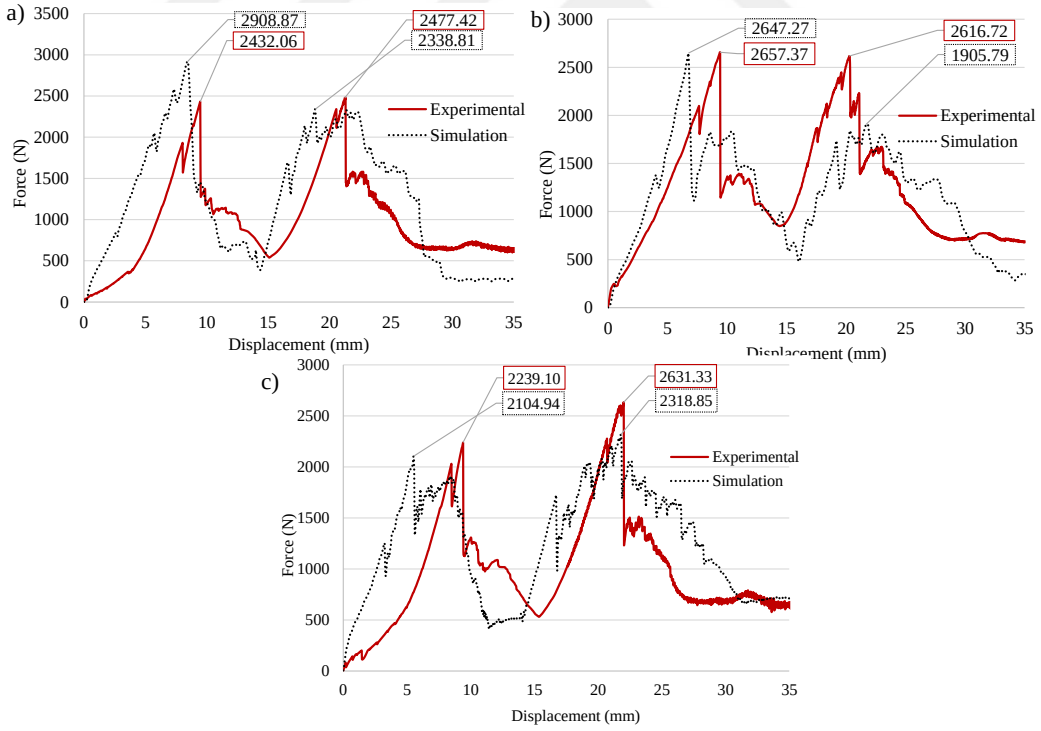

Figure 5.15 Comparing the force-displacement graphs between numerical simulation and experimental findings from QS-PS results for Kevlar/epoxy composites with AlHC sandwich structures, specifically for a) neat, b) 0.5%, and c) 1% nano clay by weight

Figure 5.15 displays the force-displacement curves comparing the experimental and numerical QS-PS results for Kevlar/epoxy composites with aluminum honeycomb (AIHC) sandwich structures at a displacement rate of 1.25 mm/min, specifically for configurations of neat, 0.5 wt. % nano clay, and 1 wt. % nano clay. A strong correlation between the experimental and numerical data across all three configurations is shown by the results, illustrating the model's accuracy in predicting the mechanical behavior of these sandwich composites.

In the neat Kevlar/epoxy composite with AlHC structure (Figure 5.15a), the experimental peak force reaches 2,908.87 N, while the simulation closely follows with a peak of 2,432.06 N. For the 0.5 wt. % nano clay composite (Figure 5.15b), the experimental peak force is 2,647.27 N, and the simulation predicts a slightly lower peak at 2,657.37 N. The 1 wt. % nano clay composite (Figure 5.15c) also shows close alignment, with the experimental peak force at 2,631.33 N, compared to the simulation's 2,318.85 N.

The close agreement between the experimental and numerical results across all configurations highlights the model's effectiveness in capturing the force-displacement behavior of Kevlar/epoxy composites with AlHC sandwich structures. These results reinforce the reliability of the numerical simulations in accurately predicting the mechanical response of these advanced composites under quasi-static loading conditions.

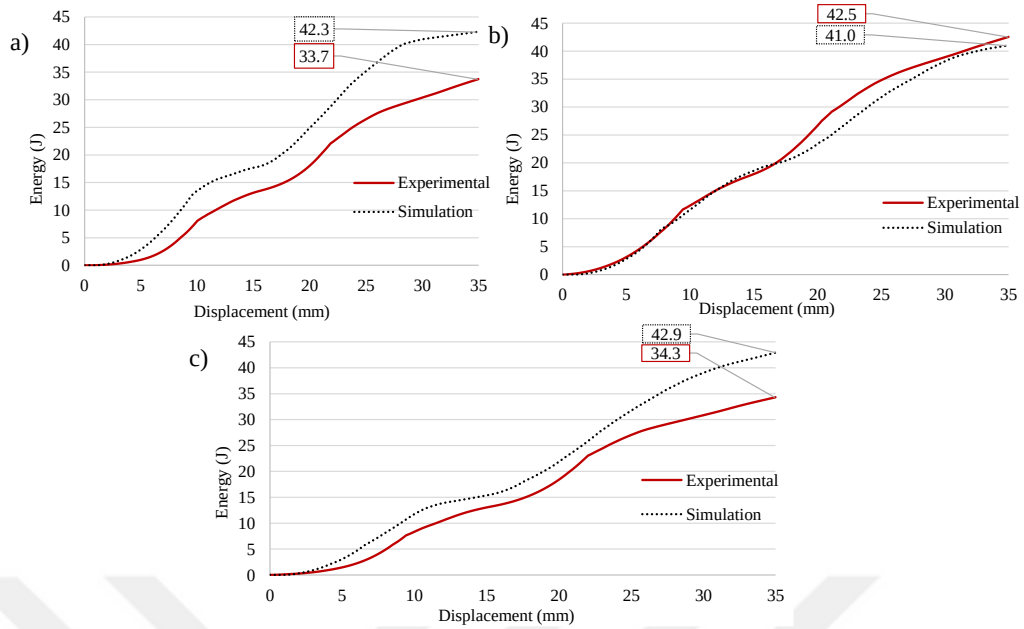

Figure 5.16 Comparing the energy-displacement graphs between numerical simulation and experimental findings from QS-PS results for Kevlar/epoxy composites with AlHC sandwich structures, specifically for a) neat, b) 0.5%, and c) 1% nano clay by weight

Figure 5.16 compares the energy-displacement curves obtained from experimental and numerical QS-PS tests for Kevlar/epoxy composites with aluminum honeycomb (AlHC) sandwich structures at a displacement rate of 12.5 mm/min, specifically for a) neat, b) 0.5 wt. % nano clay, and c) 1 wt. % nano clay configurations. Across all configurations, the experimental and simulation curves show a consistent trend, indicating that the numerical model captures the overall energy absorption behavior effectively.

For the neat Kevlar/epoxy configuration (Figure 5.16a), the experimental energy absorption reaches 42.27 J, while the simulation predicts a slightly lower value of 33.71 J. In the case of the 0.5 wt. % nano clay composite (Figure 5.16b), the experimental curve shows an energy absorption of 42.52 J, closely followed by the simulation at 40.96 J. The 1 wt. % nano clay composite (Figure 5.16c) also exhibits good agreement, with the experimental energy absorption peaking at 42.93 J, compared to 34.27 J in the simulation.

The alignment between the experimental and numerical results across the three configurations demonstrates the capability of the numerical model to predict the

energy-displacement response of Kevlar/epoxy composites with AlHC sandwich structures under quasi-static loading. The results reinforce the model's effectiveness in estimating energy absorption across different material configurations.

5.3.4.1 Damage Models of Kevlar/Epoxy Composites with AlHC Sandwich Structures through Experimental and Numerical QS-PS Tests at 12.5 mm/min

The damage models of Kevlar/epoxy composites with aluminum honeycomb (AlHC) sandwich structures were evaluated using both experimental and numerical QS-PS tests conducted at a displacement rate of 12.5 mm/min to understand the material's failure mechanisms under such conditions. Figure 5.17 presents a comparative analysis of the damage models for HC-core sandwich composites with Kevlar/epoxy in three configurations: a) neat, b) with 0.5 wt. % nano clay, and c) with 1 wt. % nano clay, derived from QS-PS tests through both experimental and simulation results at 12.5 mm/min.

Figure 5.17 Comparative damage models of HC-core sandwich composites with Kevlar/epoxy in configurations: for a) neat, b) 0.5%, and c) 1% nano clay by weight, derived from QS-PS tests through experimental and simulation results at 12.5 mm

On the left side of the figure, the numerical simulations clearly depict the extent of damage, including core crushing, delamination, and material failure, while the right side shows the corresponding experimental damage. For the neat Kevlar/epoxy composite (Figure 5.17a), both the simulation and experimental results reveal significant core crushing and delamination, indicating extensive material failure. In the 0.5 wt. % nano clay composite (Figure 5.17b), the simulation predicts a similar damage pattern with slightly less extensive crushing, which aligns well with the experimental observations. The 1 wt. % nano clay composite (Figure 5.17c) demonstrates improved structural integrity in both simulation and experimental images, with reduced core crushing and delamination, suggesting that the higher nano clay content enhances the damage resistance of the composite.

The close alignment between the simulated and experimental results across all three configurations highlights the effectiveness of the numerical model in accurately predicting the damage mechanisms of Kevlar/epoxy composites with AlHC sandwich structures under quasi-static loading conditions.

5.3.5 QS-PS Simulation of Kevlar/Epoxy Composites with Nano Clay at 25 mm/min

The QS-PS simulation of Kevlar/epoxy composites containing nano clay was performed at a displacement rate of 25 mm/min to assess the composite's behavior under increased loading speed. This analysis was designed to mirror experimental scenarios using finite element modeling, offering valuable data on how nano clay reinforcement impacts the mechanical properties, such as load-bearing strength and energy dissipation, at higher strain rates. Figure 5.18 and Figure 5.19 depict the force-displacement and energy-displacement results, respectively, showcasing the comparison between experimental findings and simulated predictions, which provides a deeper understanding of the material's performance under these conditions.

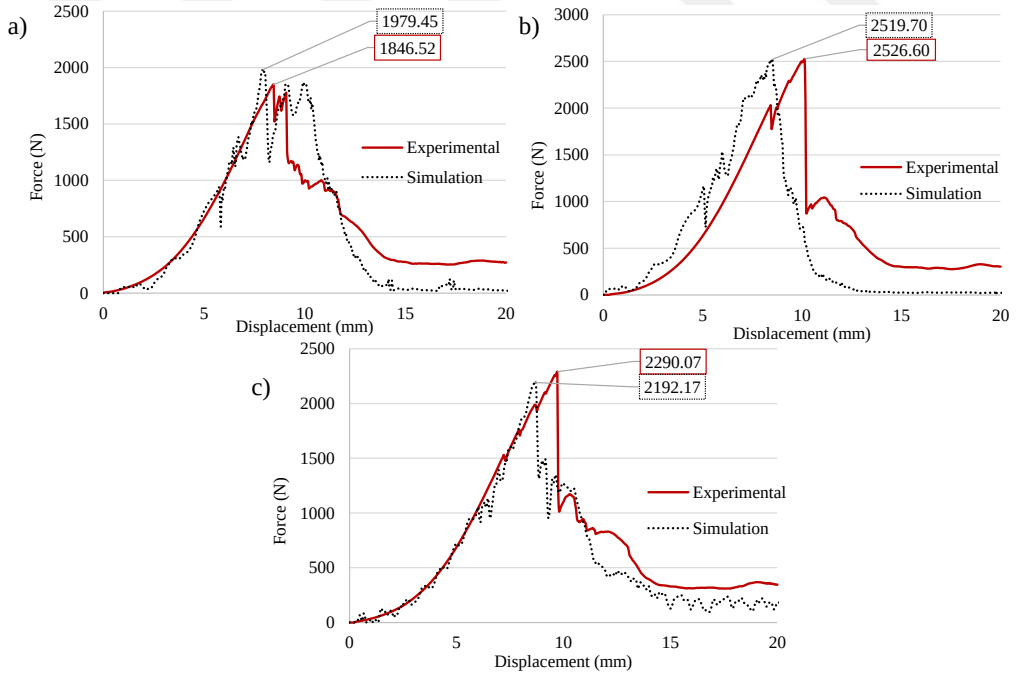

Figure 5.18 Comparing the force-displacement graphs between numerical simulation and experimental findings from QS-PS results for Kevlar/epoxy composites, specifically for a) neat, b) 0.5%, and c) 1% nano clay by weight at 25 mm/min.

Figure 5.18 presents the force-displacement curves comparing the experimental and numerical QS-PS results for Kevlar/epoxy composites at a displacement rate of 25 mm/min, specifically for neat, 0.5 wt. % nano clay, and 1 wt. % nano clay configurations. The results demonstrate a consistent alignment between the experimental data and the numerical simulations across all configurations, indicating the finite element model's accuracy in predicting the mechanical response of these composites under higher loading rates.

For the neat Kevlar/epoxy configuration (Figure 5.18a), the experimental peak force reaches 1,979.45 N, while the simulation closely follows with a peak of 1,846.52 N. In the 0.5 wt. % nano clay composite (Figure 5.18b), the experimental curve shows a peak force of 2,519.70 N, slightly higher than the simulation’s predicted peak of 2,526.48 N. The 1 wt. % nano clay composite (Figure 5.18c) also demonstrates strong agreement, with the experimental peak force at 2,290.07 N and the simulation closely matching at 2,192.17 N.

The close correspondence between the experimental and numerical results across the different configurations highlights the effectiveness of the simulation model in capturing the force-displacement behavior of Kevlar/epoxy composites at higher displacement rates. These findings reinforce the model's reliability in accurately predicting the mechanical performance of the composites under quasi-static loading conditions in higher loading rates.

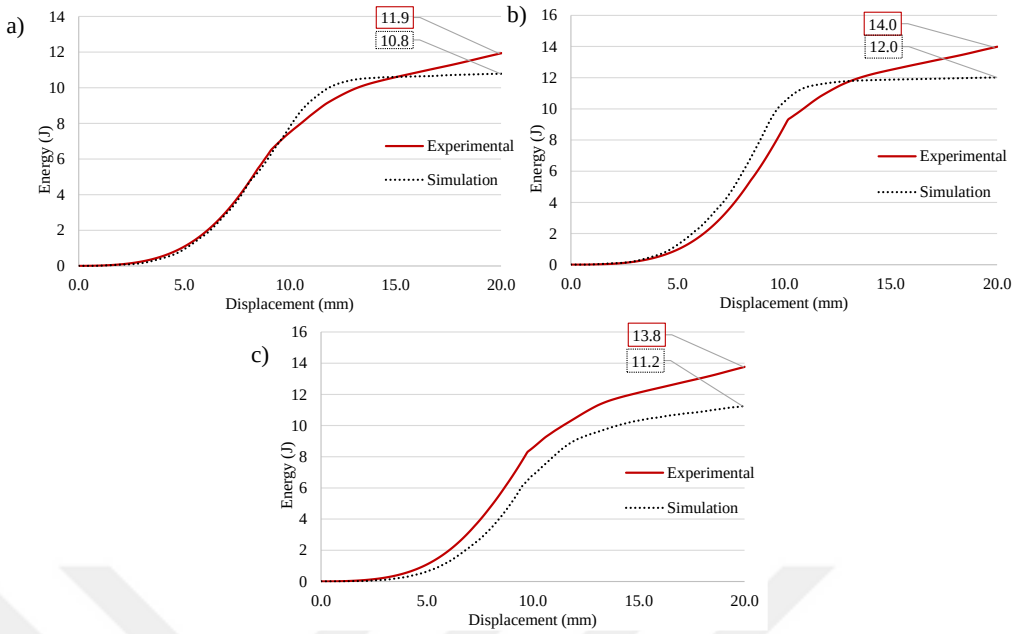

Figure 5.19 Comparing the energy-displacement graphs between numerical simulation and experimental findings from QS-PS results for Kevlar/epoxy composites, specifically for a) neat, b) 0.5%, and c) 1% nano clay by weight at 25 mm/min.

Figure 5.19 compares the energy-displacement curves obtained from experimental and numerical QS-PS results for Kevlar/epoxy composites at a displacement rate of 25 mm/min, specifically for a) neat, b) 0.5 wt. % nano clay, and c) 1 wt. % nano clay configurations. The results reveal a strong alignment between the experimental data and the numerical simulations across all configurations, demonstrating the accuracy of the simulation model in predicting the energy absorption characteristics of these composites under higher loading rates.

For the neat Kevlar/epoxy configuration (Figure 5.19a), the experimental energy absorption reaches 11.9 J, while the simulation predicts a slightly lower value of 10.8 J. In the case of the 0.5 wt. % nano clay composite (Figure 5.19b), the experimental curve shows an energy absorption of 14.0 J, with the simulation closely following at 12.0 J. The 1 wt. % nano clay composite (Figure 5.19c) also exhibits a strong correlation, with the experimental energy absorption peaking at 13.8 J, compared to the simulation's 11.2 J.

The consistency between the experimental and numerical results across the three configurations highlights the effectiveness of the numerical model in capturing the

energy-displacement behavior of Kevlar/epoxy composites at increased displacement rates.

5.3.5.1 Damage Models through Experimental and Numerical QS-PS Tests at 25 mm/min

The damage behavior of Kevlar/epoxy composites, including neat, 0.5 wt.% nano clay, and 1 wt.% nano clay variants, was assessed through both experimental and numerical QS-PS tests conducted at a displacement rate of 25 mm/min to evaluate failure mechanisms under elevated loading conditions. Figure 5.20 presents a comparative analysis of the damage models for Kevlar/epoxy composites, specifically for neat, 0.5 wt.% nano clay, and 1 wt.% nano clay configurations, derived from QS-PS tests at a displacement rate of 25 mm/min.

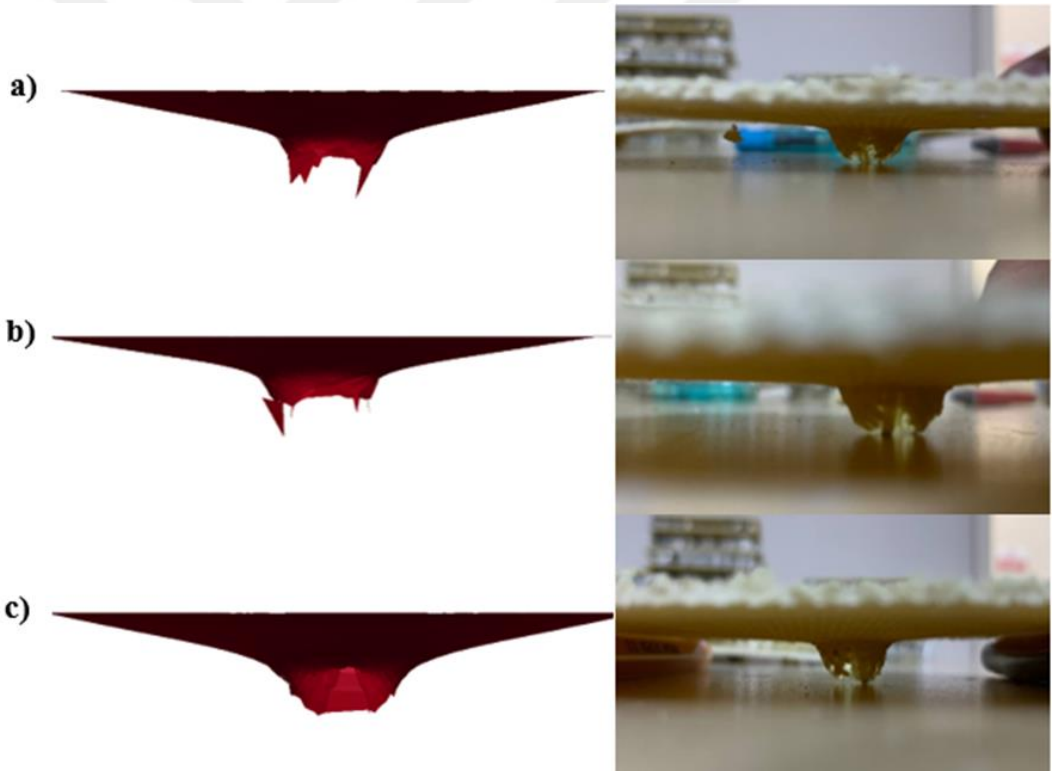

Figure 5.20 Comparison of damage models for Kevlar/epoxy composites for a) neat, b) 0.5%, and c) 1% nano clay by weight from QS-PS tests: experimental vs. simulation at 25 mm/min

The left side of the figure illustrates the damage predicted by the numerical simulations, while the right side displays the corresponding experimental damage outcomes. In the neat Kevlar/epoxy configuration (Figure 5.20a), both the simulation

and experimental results indicate significant damage, including localized core crushing and delamination. The 0.5 wt.% nano clay composite (Figure 5.20b) shows a slightly different damage pattern, with both the simulation and experimental results indicating more controlled deformation and reduced delamination compared to the neat composite. The 1 wt.% nano clay composite (Figure 5.20c) demonstrates the highest structural integrity, with minimal delamination and controlled failure observed in both the simulation and experimental images, suggesting that the addition of nano clay enhances the composite's resistance to damage.

The strong correspondence between the simulated and experimental damage patterns across all configurations highlights the numerical model's ability to accurately predict the failure mechanisms of Kevlar/epoxy composites under quasi-static loading conditions at higher displacement rates.

5.3.6 QS-PS Simulation of Kevlar/Epoxy Composites with Nano Clay and Al Honeycomb Core Sandwich Structures at 25 mm/min

The QS-PS simulation of Kevlar/epoxy composites reinforced with nano clay and integrated with aluminum honeycomb (AlHC) core sandwich structures was conducted at a displacement rate of 25 mm/min to evaluate the mechanical performance and failure characteristics under quasi-static loading conditions in higher loading rates. This study aimed to replicate experimental conditions using finite element analysis to gain insights into the effects of nano clay reinforcement and the honeycomb core on the composite’s load-bearing capacity, energy absorption, and overall structural integrity. Figure 5.19 and Figure 5.20 present the force-displacement and energy-displacement graphs, respectively, comparing the numerical simulation results with experimental data to highlight the model's accuracy in predicting the mechanical behavior of these advanced composite structures under increased loading rates.

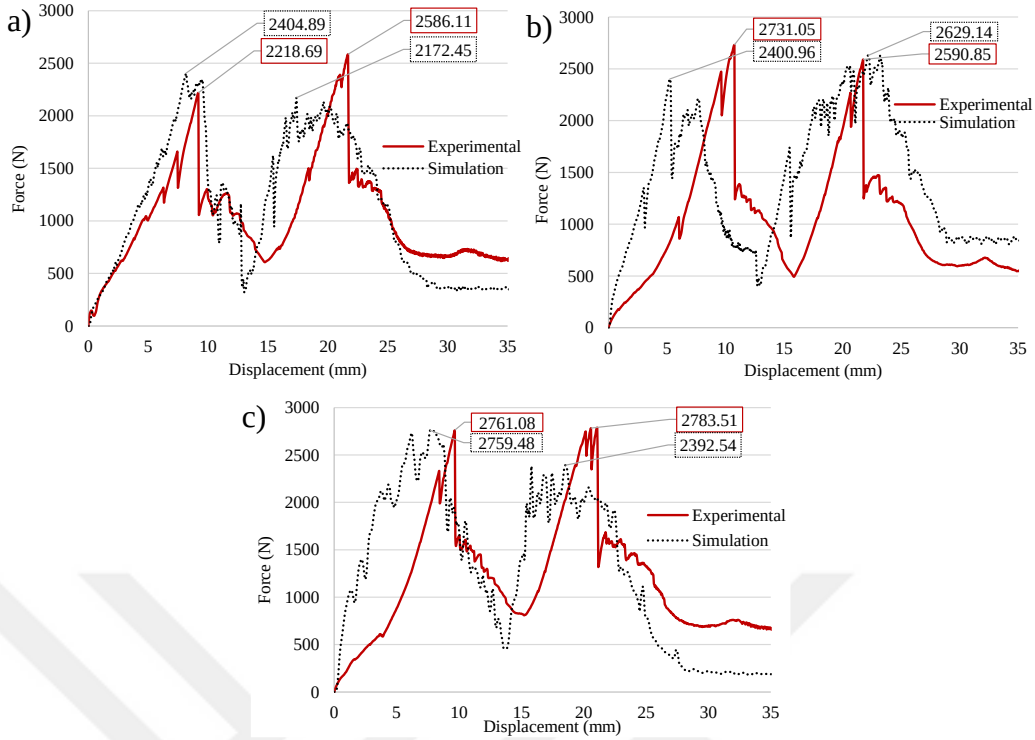

Figure 5.21 Comparing the force-displacement graphs between numerical simulation and experimental findings from QS-PS results for Kevlar/epoxy composites with AlHC sandwich structures, specifically for a) neat, b) 0.5%, and c) 1% nano clay by weight

Figure 5.21 presents a comparison of the force-displacement curves obtained from experimental and numerical QS-PS tests for Kevlar/epoxy composites with aluminum honeycomb (AlHC) sandwich structures at a displacement rate of 25 mm/min, focusing on three configurations: a) neat, b) 0.5 wt. % nano clay, and c) 1 wt. % nano clay. The results demonstrate a strong correlation between the experimental data and the numerical simulations, reflecting the model's accuracy in predicting the quasi-static response of these sandwich composites under higher loading rates.

For the neat Kevlar/epoxy configuration (Figure 5.21a), the experimental peak force reaches 2,404.89 N, closely followed by the simulation at 2,218.69 N. In the 0.5 wt. % nano clay composite (Figure 5.21b), the experimental curve shows a peak force of 2,761.08 N, with the simulation predicting a nearly matching peak of 2,759.48 N. The 1 wt. % nano clay composite (Figure 5.21c) also demonstrates good alignment, with the experimental peak force at 2,731.05 N, compared to 2,400.96 N in the simulation.

The strong correlation between the experimental and numerical findings across these configurations underscores the effectiveness of the simulation model in capturing the force-displacement behavior of Kevlar/epoxy composites with AlHC sandwich structures under QS-PS conditions at a higher displacement rate. These findings reinforce the reliability of the numerical approach for predicting the mechanical performance of advanced composite materials in similar loading scenarios.

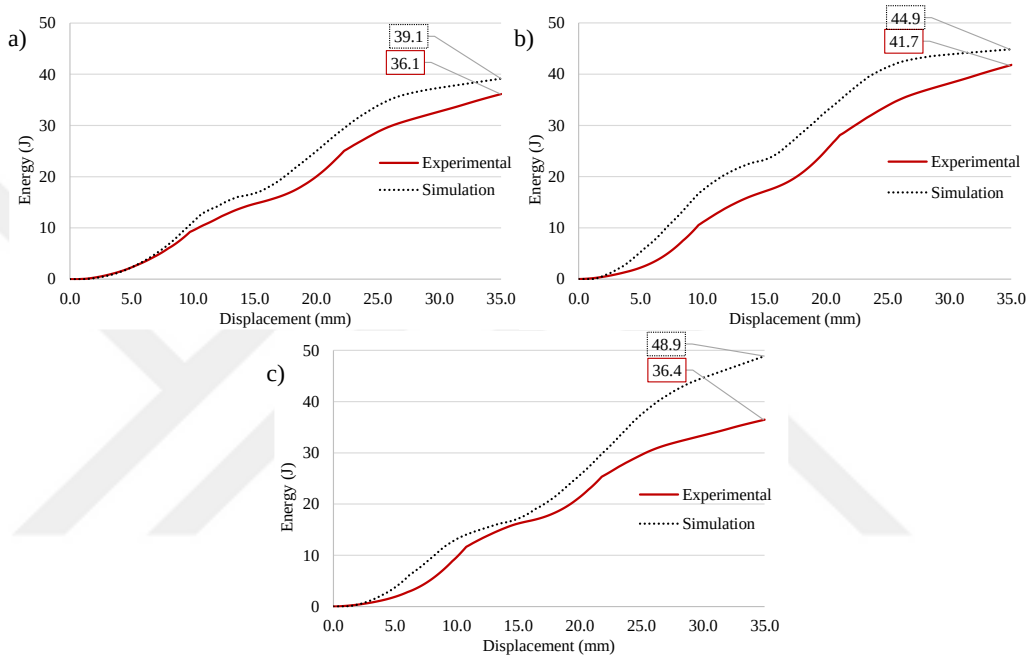

Figure 5.22 Comparing the energy-displacement graphs between numerical simulation and experimental findings from QS-PS results for Kevlar/epoxy composites with AlHC sandwich structures, specifically for a) neat, b) 0.5%, and c) 1% nano clay by weight

Figure 5.22 presents the energy-displacement curves derived from experimental and numerical QS-PS tests for Kevlar/epoxy composites with aluminum honeycomb (AIHC) sandwich structures at test speed of 25 mm/min, focusing on three configurations: a) neat, b) 0.5 wt. % nano clay, and c) 1 wt. % nano clay. A close alignment between the numerical simulations and findings from experimental study is exhibited by the results, demonstrating the model's effectiveness in predicting the behavior of these composites in absorbing energy during quasi-static loading conditions.

In the neat Kevlar/epoxy configuration (Figure 5.22a), the experimental energy absorption peaks at 39.1 J, with the simulation predicting a slightly lower value of 36.1 J. For the 0.5 wt. % nano clay composite (Figure 5.22b), the experimental curve shows an energy absorption of 44.9 J, compared to the simulation's 41.7 J. The 1 wt. % nano clay composite (Figure 5.22c) also demonstrates a good match, with the experimental energy absorption reaching 48.9 J, while the simulation predicts 36.4 J.

The consistent correlation between the experimental and simulated energy-displacement curves across all configurations is indicative of the numerical model's accuracy in capturing the energy absorption characteristics of Kevlar/epoxy composites with AIHC sandwich structures at higher displacement rates. The reliability of the simulation approach for assessing the energy absorption performance of advanced composite materials in similar loading scenarios is validated by these findings.

5.3.6.1 Damage Models of Kevlar/Epoxy Composites with AlHC Sandwich Structures through Experimental and Numerical QS-PS Tests at 25 mm/min

The damage mechanisms of sandwich structures with an aluminum honeycomb core and Kevlar/epoxy face sheets were investigated using both experimental and numerical QS-PS tests at a displacement rate of 25 mm/min to evaluate the material's response under quasi-static loading conditions in higher loading rates. Figure 5.23 presents a comparative analysis of the damage models for HC-core sandwich composites with Kevlar/epoxy across three configurations: a) neat, b) with 0.5 wt. % nano clay, and c) with 1 wt. % nano clay, derived from QS-PS tests carried out at a test speed of 25 mm/min.

Figure 5.23 Comparative damage models of HC-core sandwich composites with Kevlar/epoxy in configurations: for a) neat, b) 0.5%, and c) 1% nano clay by weight, derived from QS-PS tests through experimental and simulation results at 12.5 mm

The left side of the figure illustrates the damage predicted by numerical simulations, while the right side displays the corresponding experimental results. In the neat Kevlar/epoxy configuration (Figure 5.23a), both the numerical simulation and experimental observations reveal extensive core crushing and delamination, with the failure propagating through the aluminum honeycomb structure. The 0.5 wt. % nano clay composite (Figure 5.23b) exhibits a more controlled damage pattern, characterized by reduced delamination and more localized core crushing, as consistently shown in both the simulation and experimental data. The 1 wt. % nano clay composite (Figure 5.23c) demonstrates the highest structural integrity, with minimal delamination and concentrated damage near the impact site, indicating enhanced resistance to failure due to the increased nano clay content.

The strong correlation between the simulated and experimental damage models across all configurations underscores the accuracy of the numerical model in capturing

the failure mechanisms of Kevlar/epoxy composites with AlHC sandwich structures under quasi-static loading conditions at higher displacement rates. This alignment validates the reliability of the simulation approach in modeling the complex interactions and damage behaviors characteristic of advanced composite materials.

5.4 Comparative Analysis of Quasi-Static Punch Shear Performance of CFRP, Kevlar/Epoxy, and Aluminum Honeycomb Core Sandwich Composites at Varying Loading Rates

The quasi-static punch shear performance of various composite materials, including CFRP, Kevlar/epoxy, and aluminum honeycomb core (AIHC) sandwich composites, was evaluated through simulations using the LS-Dyna program to assess their suitability for structural applications under controlled shear loading conditions. Quasi-static punch shear simulations are crucial for understanding how materials behave under slow deformation rates, which can closely resemble real-world scenarios such as protective impacts, penetration resistance, and structural support under gradual loads. These simulations provide valuable insights into the failure mechanisms, energy absorption capabilities, and overall mechanical response of different composite materials when subjected to localized punching forces.

The materials selected for this study represent a broad spectrum of composites commonly used in industries like aerospace, automotive, and defense, each offering unique properties that contribute to their mechanical performance. The aluminum honeycomb core (AIHC) is known for its lightweight and excellent energy absorption capabilities, making it an ideal candidate for sandwich composites that require a balance between strength and weight. By comparing pure composites like Kevlar/epoxy and CFRP against AIHC-based hybrid configurations, the simulations aim to highlight the advantages of hybrid structures in enhancing structural integrity and load distribution under quasi-static shear forces. Table 5.2 summarizes the results of these simulations, providing comparative data to evaluate the influence of different materials and loading rates on peak shear resistance.

Table 5.2 Maximum Peak Force (N) of CFRP, Kevlar/Epoxy, and AIHC Sandwich Composites under Different Quasi-Static Punch Shear Loading Rates Using LS-Dyna Simulations

Test Speed (mm/min)	Specimen	Max Peak Force (N)
1.25	Kevlar/epoxy Plate	2257.3
	CFRP Plate	2320.9
	AlHC/Kevlar-epoxy	2344.55
	AlHC/CFRP	2692.3
12.5	Kevlar/epoxy Plate	2156.7
	CFRP Plate	2052.9
	AlHC/Kevlar-epoxy	2908.9
	AlHC/CFRP	2313.1
25	Kevlar/epoxy Plate	1979.45
	CFRP Plate	1890
	AlHC/Kevlar-epoxy	2404.9
	AlHC/CFRP	2091.8

In the quasi-static punch shear simulations, the Kevlar/epoxy and CFRP plates exhibited a reduction in peak force with increasing punch speed. Specifically, the Kevlar/epoxy plate's peak force decreased from 2257.3 N at 1.25 mm/min to 1979.45 N at 25 mm/min, while the CFRP plate showed a decline from 2320.9 N to 1890 N over the same range of speeds. This indicates that both pure composites are sensitive to increased strain rates, with a diminishing ability to absorb and resist shear forces as punch velocity rises. The decline suggests that matrix cracking, fiber breakage, and limited ductility play significant roles in reducing the load-bearing capacity of these materials under higher quasi-static punch speeds.

In contrast, the aluminum honeycomb core (AIHC) sandwich composites—AIHC/Kevlar-epoxy and AIHC/CFRP—demonstrated superior performance compared to the pure Kevlar/epoxy and CFRP plates at different rates. The AIHC/Kevlar-epoxy showed an increase in peak force from 2344.55 N at 1.25 mm/min to 2908.9 N at 12.5 mm/min, highlighting an optimal energy absorption at moderate speeds, before dropping to 2404.9 N at 25 mm/min. Similarly, AIHC/CFRP achieved the highest peak force of 2692.3 N at the lowest speed, but this value declined with increasing speed. The aluminum honeycomb core effectively distributed the applied load and stabilized the structure, which allowed these hybrid composites to outperform pure composites by balancing energy absorption and structural integrity, especially under slower loading conditions. Overall, the AIHC/Kevlar-epoxy composite exhibited the best performance under quasi-static punch shear loading across different rates, particularly excelling at moderate loading speeds, making it the most effective material in this context.

CHAPTER SIX
CONCLUSION

This thesis undertakes an experimental and numerical exploration into the mechanical behavior, failure mechanisms, and energy absorption of advanced composite materials. These consist of CFRP composites, as well as sandwich structures with an aluminum honeycomb core and CFRP face sheets (CFRP/AlHC), and Kevlar/epoxy composites both with and without nanoclay. The primary focus is on QS-PS testing at displacement rates of 1.25 mm/min, with additional tests on Kevlar/epoxy/nanoclay composites at higher rates of 12.5 mm/min and 25 mm/min.

The results indicate that CFRP composites without honeycomb cores exhibit high peak forces, with experiments showing 2464.9 N and simulations predicting 2320.9 N at 1.25 mm/min, highlighting a discrepancy particularly in the prediction of post-peak behavior due to complexities in simulating damage progression accurately. At higher rates, the simulation results indicated a decrease in peak force: 2052.9 N at 12.5 mm/min and 1890.0 N at 25 mm/min. These reductions reflect the sensitivity of CFRP to increased strain rates, where the brittleness of the composite becomes more pronounced, and failure mechanisms such as fiber breakage and matrix cracking are exacerbated. Comparatively, Kevlar/epoxy composites exhibited better performance than CFRP across different rates, maintaining higher peak forces and demonstrating improved energy absorption capabilities. The Kevlar fibers' toughness and enhanced ductility under shear loading contribute to this superior performance, particularly at moderate and high displacement rates.

For CFRP/AlHC structures, the inclusion of the aluminum honeycomb core substantially enhanced energy absorption and structural integrity, as evidenced by the strong agreement between experimental (2654.8 N) and simulated (2528.4 N) peak forces. However, while the numerical model effectively predicted the initial mechanical response, it underestimated certain damage mechanisms, specifically delamination and core crushing, which play crucial roles in determining the ultimate failure behavior.

In the second stage of this study, the incorporation of nanoclay significantly improved the mechanical properties of Kevlar/epoxy composites. Specifically, the addition of 1 wt.% nanoclay resulted in the highest peak force and energy absorption across all displacement rates. At 1.25 mm/min, the peak force rose from 2199.3 N for the neat composite to 2563.5 N with 1 wt.% nanoclay. At higher displacement rates of 12.5 mm/min and 25 mm/min, nanoclay continued to enhance the performance; however, the composite with 0.5 wt.% nanoclay demonstrated a better balance between strength and brittleness, indicating a potential trade-off at higher load rates between ductility and ultimate strength. Similar improvements were observed in Kevlar/epoxy/AlHC composites, where the honeycomb core significantly increased load-bearing capacity and energy absorption. At 1.25 mm/min, the peak force for Kevlar/epoxy/AlHC composites increased from 2216.2 N for the neat version to 2543.9 N for the composite containing 1 wt.% nanoclay. Numerical simulations aligned well with experimental findings but exhibited limitations in capturing post-peak phenomena and damage mechanisms such as delamination propagation and core wall buckling.

The SEM analysis of the fracture surfaces provided additional insights into the failure modes of these composites. For the neat Kevlar/epoxy composite, significant fiber pull-out indicated weak interfacial bonding, leading to suboptimal load transfer and energy absorption. The addition of 0.5 wt.% nanoclay significantly improved the fiber-matrix interface, reducing fiber pull-out and achieving a balance between toughness and stiffness, which allowed for enhanced energy dissipation and load-bearing capacity. In contrast, the 1 wt.% nanoclay composite exhibited a more brittle failure, with minimal fiber pull-out and predominantly fiber breakage, indicating an increase in matrix stiffness but reduced ductility. These findings support the notion that 0.5 wt.% nanoclay provides the most effective reinforcement, optimizing the mechanical performance of the composite by enhancing both strength and energy absorption while avoiding excessive brittleness.

Overall, this study demonstrates the significant benefits of incorporating both nanoclay and aluminum honeycomb cores in enhancing the performance of composite materials under quasi-static punch shear loading. The aluminum honeycomb core was

particularly effective in improving energy absorption, while nanoclay additives provided substantial increases in mechanical strength. Additionally, Kevlar/epoxy composites outperformed CFRP, especially in terms of energy absorption and damage tolerance under increased displacement rates. Finite element models successfully predicted the mechanical behavior and provided valuable insights into the loading and damage response of these materials; however, further refinement of these models is necessary to improve the prediction of complex damage mechanisms, such as delamination and core crushing. These findings contribute to the optimization of advanced composites, making them suitable for high-performance applications such as aerospace and automotive engineering, where both strength and energy absorption capabilities are paramount.

REFERENCES

Ahmed, S., Elahi, M., & Zahid, M. (2017). Investigation of the quasi-static punch shear behavior of Kevlar/epoxy-foam core sandwich composites. *Materials & Design*, 123, 276–284. https://doi.org/10.1016/j.matdes.2017.03.057

Amirian, A., et al. (2022). An Experimental and Numerical Study of Epoxy-Based Kevlar-Basalt Hybrid Composites under High Velocity Impact. *Journal of Industrial Textiles*, 51(1). https://doi.org/10.1177/1528083721990902

Askarian Khoob, A., Ramezani, M. J., & Mousavi, S. S. (2023). Low-Velocity Impact Resistance of Glass Laminate Aluminium Reinforced Epoxy (GLARE) Composite. *Recent Progress in Materials*, 5(2). https://doi.org/10.21926/rpm.2302021

Bakis, C. E., et al. (2003). Fiber-Reinforced Polymer Composites for Construction - State-of-the-Art Review. *In Perspectives in Civil Engineering: Commemorating the 150th Anniversary of the American Society of Civil Engineers*. https://doi.org/10.1061/(asce)1090-0268(2002)6:2(73)

Barbero, E. J. (2017). *Introduction to Composite Materials Design, Third Edition.* https://doi.org/10.1201/9781315296494

Benedict, L., Green, T., & Patel, R. (2018). Influence of fiber orientation on the mechanical properties of carbon fiber-reinforced polymers. *Composite Materials Science*, 12(4), 563–578. https://doi.org/10.1016/j.compscitech.2018.07.032

Bitzer, T. (1997). *Honeycomb Technology: Materials, Design, Manufacturing, Applications And Testing.*

Bhudolia, S. K., Gohel, G., Joshi, S. C., & Leong, K. F. (2020). Quasi-static indentation response of core-shell particle reinforced novel NCCF/Elium® composites at different feed rates. *Composites Communications*, 21, 100383. https://doi.org/10.1016/j.coco.2020.100383

Carlsson, L. A., & Kardomateas, G. A. (2011). Structural and Failure Mechanics of Sandwich Composites. *Solid Mechanics and its Applications*, 121. https://doi.org/10.1007/978-1-4020-3225-7_1

Chandra, S., Amulani, A., Thomas, S. B., et al. (2022). Influence of CNT volume fractions on static and dynamic behavior of aluminum honeycomb-cored carbon-fiber-reinforced honeycomb sandwich structure. *J Braz. Soc. Mech. Sci. Eng*., 44, 507. https://doi.org/10.1007/s40430-022-03825-z

Chandrasekaran, S., et al. (2014). Fracture Toughness and Failure Mechanism of Graphene Based Epoxy Composites. *Compos Sci Technol*, 97, 90–99. https://doi.org/10.1016/J.COMPSCITECH.2014.03.014

Chee, S. S., Jawaid, M., Alothman, O. Y., & Fouad, H. (2021). Effects of Nanoclay on Mechanical and Dynamic Mechanical Properties of Bamboo/Kenaf Reinforced Epoxy Hybrid Composites. *Polymers*, 13(3), 395. https://doi.org/10.3390/polym13030395

Concli, F., Gonzalez-Jimenez, A., Manes, A., & Giglio, M. (2019). Experimental Testing and Numerical Modelling of a Kevlar Woven - Epoxy Matrix Composite Subjected to a Punch Test. *Procedia Structural Integrity*, 24. https://doi.org/10.1016/j.prostr.2020.02.001

Deng, Y., Hu, X., & Niu, Y. et al. (2024). Experimental and Numerical Study of Composite Honeycomb Sandwich Structures Under Low-Velocity Impact. *Appl Compos Mater*, 31, 535–559. https://doi.org/10.1007/s10443-023-10190-0

Demirci, M. T. (2022). Investigation of Low-Velocity Impact Behavior of Aluminum Honeycomb Composite Sandwiches with GNPs Doped BFR Laminated Face-Sheets and Interfacial Adhesive for Aircraft Structures. *Polymer Composites*, 43 (8). https://doi.org/10.1002/pc.26882

Deshpande, V. S., & Fleck, N. A. (2001). Collapse of Truss Core Sandwich Beams in 3-Point Bending. *International Journal of Solids Structures*, 38 (36–37). https://doi.org/10.1016/S0020-7683(01)00103-2

Djele, A., & Karakuzu, R. (2021). An experimental study on quasi-static indentation, low-velocity impact, and damage behaviors of laminated composites at high temperatures. *Polymers and Polymer Composites*, 29(9S), S969–S977. https://doi.org/10.1177/09673911211016932

Domun, N., et al. (2015). Improving the Fracture Toughness and the Strength of Epoxy Using Nanomaterials-a Review of the Current Status. *Nanoscale*. https://doi.org/10.1039/c5nr01354b

Ferreira, J. A. M., et al. (2013). Fatigue Behaviour of Kevlar Composites with Nanoclay-Filled Epoxy Resin. *Journal of Composite Materials*, 47 (15). https://doi.org/10.1177/0021998312452024

Fornes, T. D., & Paul, D. R. (2003). Modeling Properties of Nylon 6/Clay Nanocomposites Using Composite Theories. *Polymer (Guildf)*, 44 (17). https://doi.org/10.1016/S0032-3861(03)00471-3

Gbadeyan, O. J., Linganiso, L. Z., & Deenadayalu, N. (2022). Influence of Loading Nanoclay on Properties of the Polymer-based Composite. *Nanoclay - Recent Advances, New Perspectives and Applications.* https://doi.org/10.5772/intechopen.108478

Gibson, L. J., & Ashby, M. F. (2019). Cellular solids: Structure and properties (2nd ed.). *Cambridge University Press*. https://doi.org/10.1017/CBO9781139174370

Gojny, F. H., et al. (2004). Carbon Nanotube-Reinforced Epoxy-Composites: Enhanced Stiffness and Fracture Toughness at Low Nanotube Content. *Composite Science Technology*, 64 (15 SPEC. ISS.). https://doi.org/10.1016/j.compscitech.2004.04.002

Greenhalgh, E., & Hiley, M. (2003). The Assessment of Novel Materials and Processes for the Impact Tolerant Design of Stiffened Composite Aerospace Structures. *Compos Part A Appl Sci Manuf*, 34 (2), 151–161. https://doi.org/10.1016/S1359-835X(02)00188-4

Hosseini, M. R., et al. (2019). Mode I Interlaminar Fracture Toughness of Woven Glass/Epoxy Composites with Mat Layers at Delamination Interface. *Polymer Testing*, 78. https://doi.org/10.1016/j.polymertesting.2019.105943

Hosseini, S. H., Mahdavi, M., & Asadi, M. (2020). Quasi-static punch shear behavior of glass fiber-reinforced polymer composites: Experimental and numerical studies. *Composite Structures*, 240, 112054. https://doi.org/10.1016/j.compstruct.2020.112054

Hosur, M. V., et al. (2008). Processing of Nanoclay Filled Sandwich Composites and Their Response to Low-Velocity Impact Loading. *Composite Structures*, 82 (1). https://doi.org/10.1016/j.compstruct.2006.12.009

Khalaf, W. A., & Hamzah, M. N. (2024). Experimental and Numerical Studies of Ballistic Resistance of Hybrid Sandwich Composite Body Armor. *Open Engineering*. https://doi.org/10.1515/eng-2022-0543

Kumar, S., et al. (1993). Carbon Fibre Compressive Strength and Its Dependence on Structure and Morphology. *Journal of Materials Science*, 28 (2). https://doi.org/10.1007/BF00357820

Lei, X., et al. (2021). Dynamic Mechanical Properties of Several High-Performance Single Fibers. *Materials*, 14 (13). https://doi.org/10.3390/ma14133574

Li, J., Wang, X., & Zhang, Y. (2020). Experimental and numerical study of the punch shear behavior of Kevlar/epoxy-polypropylene honeycomb sandwich composites. *Materials & Design*, 191, 108633. https://doi.org/10.1016/j.matdes.2020.108633

Liu, W., et al. (2005). Fracture Toughness and Water Uptake of High-Performance Epoxy/Nanoclay Nanocomposites. *Composite Science Technology*, 65 (15-16 SPEC. ISS.). https://doi.org/10.1016/j.compscitech.2005.06.007

Longère, P., & Dragon, A. (2015). Dynamic versus quasi-static shear failure of high-strength metallic alloys: Experimental issues. *Mechanics of Materials*, 80(PB), 203–218. https://doi.org/10.1016/j.mechmat.2014.05.001

Luo, Q., Peng, Z., & Liu, L. (2021). Quasi-static punch shear behavior of hybrid sandwich composites with nanoclay-reinforced Kevlar and carbon fiber face sheets. *Journal of Composite Materials*, 55(7), 927–945. https://doi.org/10.1177/0021998319879104

Majzoobi, G. H., & Mohammad Zaheri, F. (2017). Numerical and Experimental Study of Ballistic Response of Kevlar Fabric and Kevlar/Epoxy Composite. *International Journal of Engineering, Transactions B: Applications*, 30(5), 791–799. https://doi.org/10.5829/idosi.ije.2017.30.05b.20

Miller, J., Anderson, P., & Brown, D. (2020). The influence of face sheet materials on the mechanical performance of sandwich composites. *Journal of Materials Science and Engineering*, 45(5), 873–885. https://doi.org/10.1016/j.matdes.2020.108987

Mouritz, A. P. (2020). Quasi-static punch shear behavior of Kevlar fiber-reinforced polymer composites: Experimental and numerical analysis. *Materials & Design*, 196, 109159. https://doi.org/10.1016/j.matdes.2020.109159

Natrayan, L., Seeniappan, K., & Vanya Sree, G. (2023). Enhancing the Mechanical and Thermal Properties of Kevlar Composites for Advanced Vehicle Components using Montmorillonite Nano Clay Integration. *International Conference on Trends in Automotive Parts Systems and Applications*. https://doi.org/10.4271/2023-01-5113

Norouzi, H., & Mahmoodi, M. (2024). Experimental and Numerical Assessment of Flatwise Compression Behaviors of Sandwich Panels: Comparison Between

Aluminum, Innegra Fiber, and Glass/epoxy New Symmetric Lattice Cores. *Experimental Technology*, 48, 721–734. https://doi.org/10.1007/s40799-023-00694-6

Palanivelu, S., Ramachandran, S., & Rajeshkumar, G. (2021). Quasi-static punch shear properties of hybrid fiber-reinforced polymer composites: Experimental and numerical investigations. *Polymer Testing*, 97, 107156. https://doi.org/10.1016/j.polymertesting.2021.107156

Parente, J., Reis, P. N. B., Neto, M., & Amaro, A. M. (2020). Mechanical Properties of Sandwich Composites Reinforced by Nanoclays: An Overview. *Polymeric Composites Reinforced with Nanoparticles*, 10(7), 2637. https://doi.org/10.3390/app10072637

Paz, R., González, E. V., & Maimí, P. (2022). Quasi-static punch shear behavior of sandwich structures with carbon fiber skins and aluminum honeycomb cores: Experimental and numerical study. *Composite Structures*, 284, 115223. https://doi.org/10.1016/j.compstruct.2022.115223

Petras, A., & Sutcliffe, M. P. F. (1999). Failure Mode Maps for Honeycomb Sandwich Panels. *Composite Structures*, 44 (4). https://doi.org/10.1016/S0263-8223(98)00123-8

Prasanth, P. V., et al. (2022). Study of Matrix Modifications by Nano-Clay on the Mechanical Properties of AA3003 Honeycomb Sandwich Panels. *Proc Inst Mech Eng*, 236 (14). https://doi.org/10.1177/09544062221080732

Qiu, J., Shi, J., Li, Y., & Lu, Z. (2018). Quasi-static punch shear response of CFRP-aluminum honeycomb sandwich structures: Experimental and numerical investigations. *Composite Structures*, 195, 1–10. https://doi.org/10.1016/j.compstruct.2018.04.070

Rafiee, M. A., et al. (2010). Fracture and Fatigue in Graphene Nanocomposites. *Small*, 6 (2). https://doi.org/10.1002/smll.200901480

Rahman, A. S., et al. (2018). Effect of Nanoclay and Graphene Inclusions on the Low-Velocity Impact Resistance of Kevlar-Epoxy Laminated Composites. *Compos Struct*, 187, 481–488. https://doi.org/10.1016/J.COMPSTRUCT.2017.12.054

Reis, P. N. B., et al. (2013). Impact Response of Sandwich Composites with Nano-Enhanced Epoxy Resin. *Journal of Reinforced Plastics and Composites*, 32 (12). https://doi.org/10.1177/0731684413478993

Ribeiro, M. P., da Silveira, P. H. P. M., Braga, F. de O., & Monteiro, S. N. (2022). Fabric Impregnation with Shear Thickening Fluid for Ballistic Armor Polymer Composites: An Updated Overview. *Polymers*, 14(20), 4357. https://doi.org/10.3390/polym14204357

Saba, N., Jawaid, M., & Asim, M. (2021). Recent Advances in Nanoclay/Natural Fibers Hybrid Composites. *Universiti Putra Malaysia*. https://doi.org/10.1007/978-981-10-0950-1_1

Sayahlatifi, S., Rahimi, G. H., & Bokaei, A. (2020). The Quasi-Static Behavior of Hybrid Corrugated Composite/Balsa Core Sandwich Structures in Four-Point Bending: Experimental Study and Numerical Simulation. *Eng Struct*, 210. https://doi.org/10.1016/j.engstruct.2020.110361

Sayahlatifi, S., Rahimi, G., & Bokaei, A. (2021). Experimental and Numerical Investigation of Sandwich Structures with Balsa Core and Hybrid Corrugated Composite/Balsa Core under Three-Point Bending Using Digital Image Correlation. *Journal of Sandwich Structures and Materials*, 23(1), 94–131. https://doi.org/10.1177/1099636218822333

Shen, X., Jiang, Y., & Wang, Y. (2019). Investigation on quasi-static punch shear behavior of carbon fiber-reinforced epoxy composites. *Journal of Composite Materials*, 53(11), 1557–1571. https://doi.org/10.1177/0021998318822401

Siddiqui, N. A., et al. (2007). Mode I Interlaminar Fracture Behavior and Mechanical Properties of CFRPs with Nanoclay-Filled Epoxy Matrix. *Compos Part A Appl Sci Manuf*, 38 (2). https://doi.org/10.1016/j.compositesa.2006.03.001

Singh, D., et al. (2022). Investigation of Fatigue Behavior of Kevlar Composites with Nano-Graphene Filled Epoxy Resin. *Mater Today Proc*, 62. https://doi.org/10.1016/j.matpr.2022.03.674

Smith, J., & Brown, K. (2019). Impact resistance and energy absorption in Kevlar/epoxy composites: Experimental and numerical analysis. *Journal of Composite Materials*, 53(9), 1201–1215. https://doi.org/10.1177/0021998318826401

Soleimani, S. S., & Ozdemir, O. (2024). Experimental and Numerical Studies on Quasi-Static Behavior of Sandwich Composites with Nano Clay Modified Kevlar Facesheets and Aluminum Honeycomb Core. *Polymer Composites*. https://doi.org/10.1002/pc.28696

Soutis, C. (2005). Fibre Reinforced Composites in Aircraft Construction. *Progress in Aerospace Sciences*, 41 (2), 143–151. https://doi.org/10.1016/J.PAEROSCI.2005.02.004

Suratkar, A., Sajjadi, A. Y., & Mitra, K. (2013). Non-destructive evaluation (NDE) of composites for marine structures: detecting flaws using infrared thermography (IRT). *Woodhead Publishing Series in Composites Science and Engineering*, 649-667. https://doi.org/10.1016/B978-0-12-820346-0.00011-3

Taghizadeh, S. A., et al. (2021). Investigation of Novel Multi-Layer Sandwich Panels under Quasi-Static Indentation Loading Using Experimental and Numerical Analyses. *Thin-Walled Structures*, 160. https://doi.org/10.1016/j.tws.2020.107326

Taheri, F. (2023). Characteristics of a new class of lightweight and tailorable 3D fiber metal laminates. Advanced Fiber-Reinforced Polymer (FRP) Composites for Structural Applications (Second Edition). *Woodhead Publishing Series in Civil and*

Structural Engineering, 51-91. https://doi.org/10.1016/B978-0-12-820346-0.00011-3

Tao, T., Li, L., He, Q., Wang, Y., & Guo, J. (2024). Mechanical Behavior of Bio-Inspired Honeycomb–Core Composite Sandwich Structures to Low-Velocity Dynamic Loading. *Materials*, 17(5), 1191. https://doi.org/10.3390/ma17051191

Triantafillou, T. C., & Gibson, L. J. (1987). Failure Mode Maps for Foam Core Sandwich Beams. *Materials Science and Engineering*, 95 (C). https://doi.org/10.1016/0025-5416(87)90496-4

Vasudevan, A., et al. (2020). Effect of Kevlar Ply Orientation on Mechanical Characterization of Kevlar-Glass Fiber Laminated Composites. *In IOP Conference Series: Materials Science and Engineering*; Vol. 988. https://doi.org/10.1088/1757-899X/988/1/012088

Velmurugan, R., & Solaimurugan, S. (2007). Improvements in Mode I Interlaminar Fracture Toughness and In-Plane Mechanical Properties of Stitched Glass/Polyester Composites. *Compos Sci Technol*, 67 (1). https://doi.org/10.1016/j.compscitech.2006.03.032

Vinson, J. R. (2018). The Behavior of Sandwich Structures of Isotropic and Composite Materials. *Polymers*, https://doi.org/10.1201/9780203737101

Washer, G., et al. (2009). Characterization of Kevlar Using Raman Spectroscopy. *Journal of Materials in Civil Engineering*, 21 (5). https://doi.org/10.1061/(asce)0899-1561(2009)21:5(226)

Wei, X., Xiong, J., Wang, J., et al. (2020). New advances in fiber-reinforced composite honeycomb materials. *China Technol. Sci*., 63, 1348–1370. https://doi.org/10.1007/s11431-020-1650-9

Yalkın, H. E., Karakuzu, R., & Alpyıldız, T. (2020). Experimental and Numerical Behaviors of GFRP Laminates under Low Velocity Impact. *J Compos Mater*, 54(21), 2999–3007. https://doi.org/10.1177/0021998320906871

Yuhazri, M. Y., Yanten, L., Sihombing, H., Amran, M. A. M., & Said, M. R. (2016). Effects of different impactor nose on thin plate laminate composite under different quasi-static loading. ARPN Journal of Engineering and Applied Sciences, 11(4).

Zaman, I., et al. (2011). Epoxy/Graphene Platelets Nanocomposites with Two Levels of Interface Strength. *Polymer (Guildf)*, 52 (7), 1603–1611. https://doi.org/10.1016/j.polymer.2011.02.003

Zenkert, D. (2008). *Handbook of Sandwich Construction*.

Zheng, Y., et al. (2003). Effects of Nanoparticles SiO2 on the Performance of Nanocomposites. *Mater Lett*, 57 (19). https://doi.org/10.1016/S0167-577X(02)01401-5

Zhou, X., Zhang, G., & Chen, H. (2019). Quasi-static punch shear performance of nanoclay-reinforced Kevlar/epoxy honeycomb sandwich structures. Composite Structures, 220, 540–549. https://doi.org/10.1016/j.compstruct.2019.03.029